Temp.# 16303

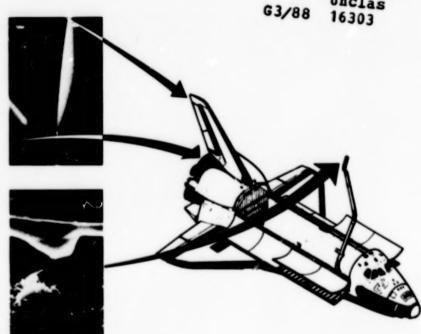
STAR 0 2 NOV 1 4 1985

NASA Conference Publication 2391

Second Workshop on Spacecraft Glow

(NASA-CP-2391) SECOND WORKSHOP ON SPACECRAFT GLOW (NASA) 294 P HC A13/HF A01 CSCL 03B

N86-13239 THRU N86-13269 Unclas



Proceedings of a workshop held at George C. Marshall Space Flight Center Huntsville, Alabama May 6-7, 1985

Second Workshop on Spacecraft Glow

J. H. Waite, Jr., and T. W. Moorehead NASA George C. Marshall Space Flight Center Marshall Space Flight Center, Alabama

Proceedings of a workshop sponsored by NASA George C. Marshall Space Flight Center, Huntsville, Alabama, and Universities Space Research Association, Washington, D.C., and held at Space Science Laboratory, George C. Marshall Space Flight Center Huntsville, Alabama May 6-7, 1985

National Aeronautics and Space Administration

Scientific and Technical Information Branch

1985

SUMMARY

The glows induced by the interaction of orbiting spacecraft with the atmosphere present a complex problem of interpretation whose solution requires a collaborative multidisciplinary approach embracing research in aeronomy, surface chemistry, plasma physics, fluid dynamics, and atomic and molecular spectroscopy. All these disciplines are represented in this collection of papers delivered at the Second Workshop on Spacecraft Glow. The workshop was held at the Space Science Laboratory of NASA's Marshall Space Flight Center in May 1985, and was partially sponsored by the Universities Space Research Association.

Observations of the space shuttle glows were summarized by Mende and Swenson. The spatial distributions of the ram glows on the vertical stabilizer are consistent with a distance of 20 cm in the case where the emitting species is released from an isotropic scattering surface. The glow spectrum has the appearance of a continuum. It peaks in intensity near 700 nm dropping below the detection limit at wavelengths shorter than 400 nm and longer than 800 nm. The fall-off at longer wavelengths is not firmly established because of possible effects of varying spacecraft window transmission. The $\cos^2\phi$ dependence on the angle of attack (ϕ) was discussed and some results on the duration of the enhancement of the ram glow following thruster firings were given. The glow intensity varies exponentially with altitude with a scale height approximating that of atomic oxygen. The glow did not change in intensity through the mission duration, suggesting that outgassing is not responsible. Mende concluded by arguing that the continuum is due to NO₂ produced by recombining O and NO.

An attempt to obtain glow spectra at higher resolution by Kendall et al. was described by Llewellyn.

A more detailed examination of the NO₂ hypothesis was presented by Swenson, Mende, and Clifton and further comments on it were made by Green, Marinelli, and Rawlins, by Kofsky and Barrett, and by Kendell et al. Mass spectrometric studies carried out on the Atmosphere Explorer satellites of the odd nitrogen chemistry and the formation of NO and NO₂ were described by Engebretson. He found that increasing the wall temperature greatly reduced the NO₂ formation. The observation of large amounts of NO₂ in the open source instruments was attributed to the entrance of ramming oxygen atoms through the orifice followed by a three-body recombination.

High-resolution spectra obtained from the ISO experiment on Spacelab 1 were presented by M. Torr and preliminary interpretations were offered by D. Torr, Khoyloo, and M. Torr and by Green, Marinelli, and Rawlins. Most of the N[†]₂ emission was attributed to the dayglow. A 14 kilorayleigh emission apparently emanating from the wake may arise from charge exchange collisions between the ramming oxygen ions and the enhanced N₂ bulge in front of the spacecraft surfaces producing N[‡]₂ ions that are swept into the wake by the spacecraft motion through the magnetic field. The N₂ Vegard-Kaplan bands between 160 and 190 nm were seen looking downward at low altitudes and the N[†]₂ Meinel bands also appeared strongly in some of the spectra. Anomalous vibrational distributions appear to be necessary to interpret the data. The identification of carbon compounds was discussed. A very bright visible continuum of non-atmospheric origin was found to underly the nightside spectra, and is possibly also present on the dayside. Detailed analysis is necessary to separate the spacecraft-induced glows from the atmospheric emissions.

Chakrabarti and Sasseen described observations of a 1 kilorayleigh glow in Lyman alpha at 600 km with an EUV instrument carried on a polar orbiting satellite. Its origin is as yet uncertain, but it is a potentially serious hazard to ultraviolet observations. Experiments to obtain glow data between 190 and 300 nm were presented by Spear, Ucker, and Tobiska and by Anderson. The latest results of a continuing analysis of Atmosphere Explorer glow data were reported by Dalgarno, Yee, and LeCompte. Their analysis of the data below 160 km indicates a spectrum differing from the high-altitude observations and an intensity apparently varying as the product of any pair of molecules N₂, O₂, and NO. In the following discussions, it was pointed out that near 160 km the mean free path in the ram direction may be of the same order as the baffle dimensions.

At high altitudes, the spectra, measured in band passes centered at 732 nm, 656 nm, 428 nm, and 3371 nm, are consistent with emission from vibrationally excited OH, supplemented by an additional source with a spectrum similar to that observed for the shuttle glows. The glow at 280 nm may be due to surface recombination of OH into the electronically excited $A^2\Sigma^+$ state.

The implications of these observations of the spacecraft glows and the Atmosphere Explorer glows for the Space Telescope mission were discussed by Clarke.

Several studies of the recombination, chemical reaction, and impact excitation mechanisms for producing the glow were reported. Papadopoulos surveyed his critical velocity theory and suggested that currents driven by the existence of sheaths in the vicinity of the vehicle can heat the ambient electrons to a degree that can excite a variety of vibrational and rotational emissions in the molecular component of the gas. He emphasized the similarity of the volume glow emission in the shuttle vicinity and the glow produced during thruster firings.

The presence of solid surfaces in orbit may provide the means of producing or enhancing glow in other ways. A spacecraft front surface at 250 km altitude, moving with its surface normal parallel to the direction of motion, is struck by atmospheric species at the rate of 10^{15} cm⁻² s⁻¹. Since the predominant species is atomic oxygen at this altitude, extensive oxidation of the surface may take place. Volatile products leaving the surface in an excited state may emit photons. The surface also acts to concentrate the emitted and ambient gas species by a pile-up effect as the spacecraft moves through the atmosphere at 8 km s⁻¹. Concentratioxn increases of a factor of about 50 above ambient have been calculated by Hueser, Brock, and Melfi and by Rantanen, Swanson, and D. Torr resulting in effective interaction mean free paths between free atmospheric species and surface-emitted species of a few tens of meters.

It is evident that in addition to the plasma processes, at least two other kinds of phenomena exist, one giving rise to the intense but spectrally diffuse red glow extending off surfaces with a characteristic length of $\sim\!20$ cm, and another probably associated with collisional excitation between the atmosphere and the ambient gas cloud which piles up on the front side of a satellite. This cloud may have an effective radius of tens of meters. The discussions of the first type of process by Kofsky and Barrett, Green et al., Kendall et al., and Swenson et al. emphasized the chemistry of the energized nitrogen-oxygen system. Mechanisms occur involving energetic oxygen and nitrogen which react on surfaces producing and desorbing an excited nitrogen oxide molecule which subsequently decays emitting a photon. Similar mechanisms have included desorbing of excited N2, CO, and other species.

Evidence supporting the second source of glows includes the observations of glows following thruster firings and the ISO spectrometer observations of Spacelab 1. The latter included line spectra of such species as O2, which may have been produced by reactive excitation of surface-emitted organic molecules with ambient atmospheric species. Such a scenario is supported by the ground-based infrared observations of Witteborn who has previously reported a glow extending beyond the shuttle by tens of meters. In this class of mechanism the surface is the source of the glow precursors. Reactive collisions between O atoms and organic molecules or radicals have a high probability of producing excited products. A paper by Gregory and Peters described the erosion of carbonaceous materials in orbit and provided a basis for estimating the source function of glow precursors. In addition to these two classes of processes, there may be a range of processes with intermediate decay lengths. An interesting extreme was described by Peters. The measurements of the shuttle red glow show maximum intensity at or near the shuttle tail fin surface, consistent with an intense emission from species absorbed on the surface. Peters suggested this may be simply caused by oxygen atoms collisionally excited into 1S and 1D states decaying while still in contact with the surface. Under such conditions, the usual atomic line emission would be broadened into bands of width qualitatively in agreement with the orbital measurements.

The chemical nature of the shuttle environment is a significant parameter. Neutral mass spectrometer data for several flights were presented by Miller and Carignan. Of particular value are measurements of the oxidation rate of different material surfaces in the shuttle environment. Leger and Visentine reported data from STS-5 and STS-8 which showed high reactivities of atomic oxygen with organic films, polymers, and many composites. The dependence of the glow intensity on different materials was reported by Mende and Swenson who also explored the effects of thruster firings.

Laboratory oxygen and nitrogen beam systems were discussed. While velocities of ~ 8 km s⁻¹ and fluxes of at least 10^{15} s⁻¹ are needed for a thorough study of glow and erosion, much useful work could be done at lower energies and fluxes. No system has yet reliably produced the energies and fluxes desired but active development programs are underway by Gregory, Green, Langer et al., Tolk et al., and Arnold and Peplinski.

Approximately 2 to 3 hours of the workshop were devoted to presentations of future plans for vehicle glow related studies. These plans ranged from concepts still in the proposal phase, to measurement sequences already approved for implementation on forthcoming missions (Mumma and Jennings, Fazic and Koch, and Leger and Visentine). The available data on surface glows are limited in spectral extent and in spectral resolution. Thus, fundamental information on these glows has yet to be acquired in the form of multi-spectral measurements of surfaces directed into the velocity vector. One category of future experiments dealt with this issue and included "improvised" experiments using existing mission hardware to do such things as measuring the glow of the surface of one instrument with another. Another dealt with more elaborate proposed cause-effect studies in which surfaces would not only be spectrally viewed, but would also be subjected to gas or charged particle beams.

The links between surface glows and the corrosion caused by the highly chemically active atomic oxygen environment are poorly understood, and a second category of future experiments focused on this topic, including both on-orbit studies and laboratory beam experiments.

Two points were brought out by these presentations and the related discussions. First, because the subject of vehicle optical environments is not the special concern of any one group and has no champion at NASA, attempts are being made to address the problem with non-optimized hardware and with hopes of only partial results. Second, while some progress could be made with instrumentation already included in future payloads, because shuttle glow is not the primary objective of these missions, it becomes a formidable task to obtain approval to use even nominal amounts of the mission resources for such studies.

Shuttle glow and an induced optical contamination surrounding vehicles in space is of concern to several disciplines, and it is in our interest to understand the nature of this optical environment and the limitations that it places on studies from space and the use of materials in space. In order to gain this understanding, a focused effort is needed, one that addresses the full extent of the problem. This workshop and the subsequent meetings of the steering committee will be used to develop a proposal for a NASA/Marshall Space Flight Center program to conduct such an effort.

A. Dalgarno

Program Committee:

Hunter Waite, Convener

John Clarke
Alex Dalgarno
Alex Dessler
John Gregory
Dennis Papadopoulos
Gary Swenson
Marsha Torr

TABLE OF CONTENTS

		Page
R	STU OBSERVATIONS	
	Vehicle Glow Measurements on the Space Shuttle	
	S. B. Mende and G. R. Swenson	1
	Space Shuttle Ram Glow: Implication of NO ₂ Recombination Continuum	
	G. R. Swenson, S. B. Mende, and S. Clifton	35
	AE and DE Mass Spectrometer Observations Relevant to the Shuttle Glow	
	M. J. Engebretson	46
	The Atmosphere Explorer and the Shuttle Glow	
	A. Dalgarno, J-H. Yee, and M. LeCompte	55
	Orbiter Glow Observations at High Spectral Resolution	
	D.J.W. Kendall, R. L. Gattinger, E. J. Llewellyn,	
	I. C. McDade, and S. B. Mende	63
	Neutral Mass Spectrometer Measurements in the Shuttle Bay Environment	
	E. Miller and G. Carignan	74
	Spectral Identification/Elimination of Molecular Species in Spacecraft Glow	
	B. D. Green, W. J. Marinelli, and W. T. Rawlins	82
	The UV-VIS Optical Environment of the Shuttle	
	M. R. Torr	98
	Enhanced N ₂ Emissions in the Shuttle Environment (Abstract only)	
	D. G. Torr, A. Khoyloo, and M. R. Torr	107
	Investigation of Vehicle Glow in the Far Ultraviolet	
	S. Chakrabarti and T. Sasseen	108
T	HEORETICAL CALCULATIONS	
	Spacecraft-Induced Plasma Energization and Its Role in Flow Phenomena	
	K. Papadopoulos and R. A. Smith	119
	Shuttle Vertical Fin Flowfield by the Direct Simulation Monte Carlo Method	
	J. E. Hueser, F. J. Brock, and L. T. Melfi	129

TABLE OF CONTENTS (Continued)

	Page
A Mechanism for the Local Concentration Enhancement of the Shuttle Atmosphere	
R. O. Rantanen, R. A. Swanson, and D. G. Torr	139
Surface-Catalyzed Recombination into Excited Electronic, Vibrational, Rotational, and Kinetic Energy States: A Review	
I. L. Kofsky and J. L. Barrett	149
Infrared Emission from Desorbed NO2 and NO	
I. L. Kofsky and J. L. Barrett	155
The NO-NO ₂ System at Laboratory Surfaces	
J. L. Barrett and I. L. Kofsky	165
A Model for Explaining Some Features of Shuttle Glow	
P. N. Peters	169
The Production of Glow Precursors by Oxidative Erosion of Spacecraft Surfaces	
J. C. Gregory and P. N. Peters	174
Activated Recombinative Desorption: A Potential Component in Mechanisms of Spacecraft Glow	
J. B. Cross	180
ABORATORY MEASUREMENTS	
Optical Radiation from the Interaction of Energetic Atoms, Ions, Electrons, and Photons with Surfaces	
N. H. Tolk, R. G. Albridge, R. F. Haglund, Jr., and M. H. Mendenhall	191
A Ground-Based Experimental Test Program to Duplicate and Study the Spacecraft Glow Phenomenon	
W. D. Langer, S. A. Cohen, D. M. Manos, D. H. McNeill, R. W. Motley, M. Ono, and S. Paul	202
Application of an Atomic Oxygen Beam Facility to the Investigation of Shuttle Glow Chemistry	
G. S. Arnold and D. R. Peplinski	212

TABLE OF CONTENTS (Concluded)

		Page
F	UTURE EXPERIMENTS	
	An Assessment of the Impact of Spacecraft Glow on the Hubble Telescope	
	J. T. Clarke	229
	Infrared Measurements of Spacecraft Glow Planned for Spacelab 2	
	G. G. Fazio and D. G. Koch	243
	Planned Investigation of Infrared Emissions Associated with the Induced Spacecraft Glow: A Shuttle Infrared Glow Experiment (SIRGE)	
	M. J. Mumma and D. E. Jennings	250
	Data Requirements for Verification of Ram Glow Chemistry	
	G. R. Swenson and S. B. Mende	260
	A Possible Experiment for the EOM 1-2 Mission (Abstract only)	
	M. R. Torr	269
	Space Shuttle Mechanistic Studies to Characterize Atomic Oxygen Interactions with Surfaces	
	L. J. Leger and J. T. Visentine	270
	The Shuttle Glow: A Program to Study the Ram-Induced Phenomena	
	H. R. Anderson	274
	Survey of Ultraviolet Shuttle Glow	
	K. A. Spear, G. J. Ucker, and K. Tobiska	277
A	GENDA	279
L	IST OF ATTENDERS	283

IN SITU OBSERVATIONS

PRECEDING PAGE BLANK NOT. FILMED

VEHICLE GLOW MEASUREMENTS ON THE SPACE SHUTTLE

S. B. Mende and G. R. Swenson

Lockheed Palo Alto Research Laboratory

Abstract. From the combined data set of glow observations on shuttle flight STS-3, STS-4, STS-5, STS-8, STS-9, 41-D, and 41-G some of the properties of the shuttle glow are discussed. Comparison of the STS-3 and STS-5 (240 and 305 km altitude, respectively) photographs shows that the intensity of the glow is about a factor of 3.5 brighter on the low-altitude (STS-3) flight. In an experiment to observe the dependence of the intensity on the ram angle, the angle of incidence between the spacecraft surface normal and the velocity vector, the Orbiter was purposely rotated about the x axis on the STS-5 mission. For a relatively large angle between the velocity vector and the surface normal there is an appreciable glow, provided the surface is not shadowed by some other spacecraft structure. As the angle becomes less the glow intensifies. Material samples were also exposed in the ram direction during nightside orbits and the glow surrounding the samples was photographed. The glow intensity varied depending on the nature of the sample surface. The thruster-induced light was also investigated in an experiment. Thrusters were initiated individually and the resulting luminosities were recorded by photographic and television techniques. These results show that the largest optical disturbance is created by the downward firing tail thrusters (-ve pitch) presumably because these thrusters fire towards the Orbiter wing which then thermalizes the exhaust gases by collisions. On the STS-8 mission when the altitude was 220 km the thruster-induced spacecraft glow was found to decay with a time constant which is 1/5th of the time constant obtained on STS-3. More recent data featured resolved spectrum and imagery of the glow with spectroscopic resolution of 31 Å FWHM between 4000 and 8000 Å. The spectrum of the glow on the shuttle tail pod could be clearly separated from spectrum of the reflected light from the Orbiter. From the measurements it is clear that the spectrum of the glow is a continuum in the passband of the instrument. Analyses have been performed which strongly suggest the emission originates from recombination continuum of NO2. The spectral shape of NO2 emission is highly variable with recombination process according to numerous laboratory studies. The spectral shape of the observed continuum may be the result of the recombination process involving surface-bonded NO and fast ram O atoms. If the recombined NO2 retains 10% of the kinetic energy of the ram OI, the thickness of the glow layer can be explained by the lifetime of NO(2B2) continuum. Previous satellite mass spectrometer measurements show that adequate NO,



is generated on spacecraft surfaces and that the recombining NO is produced by the reaction of atmospheric atomic N and O.

Introduction

The apparent vehicle glow of the space shuttle was detected during the flight of STS-3 [Banks et al., 1983]. Although the shuttle glow was not specifically predicted it has now been associated with other space-craft glow which was shown to surround free flier satellites such as the Atmospheric Explorer [Torr et al., 1977; Torr, 1983; Yee and Abreu, 1983]. Specific investigation of the shuttle glow was started on STS-4 when a transmission grating was mounted in front of a photogtraphic camera and several exposures were taken on-orbit to make preliminary spectral measurements of the spacecraft glow [Mende et al., 1983]. The space shuttle observations have also reported glows associated with thruster firings.

The physical process leading to the glow phenomenon is relatively poorly understood at present. Programs such as Space Telescope, IRT and other optical facilities can be planned and optimized around ram glow phenomena given an understanding of the physical process. These planning considerations can include operational restraints with respect to telescope ram during observations, orbit altitude, instrument baffle materials and coatings, and surface conditioning of the Orbiter (for

shuttle payloads).

The AE-E satellite was equipped with a Visual Airglow Experiment (VAE) which observed atomic and molecular features in the Earth's airglow layer. Backgrounds in the photometer filter channels were found to have a variability with ram angle. These data were reported by Yee and Abreu [1982, 1983] and displayed a detectable level of luminosity in the near UV channels of the instrument (3371 A) with increasing luminosity towards the red wavelengths (7320 X). The background in all filter channels, when plotted, described a bright ram source, increasing in brightness toward the red wavelengths. The analysis presented suggested the glow extended well away from the spacecraft alluding to the probability the emitter is metastable. OH Meinel bands were reported as being a likely candidate species for emission since the general red character and emission lifetime seemed to fit the evidence. The Yee and Abreu [1982] analysis had found a strong correlation between the ram emission intensity and altitude. The emission intensity closely followed the atomic oxygen scale height above 160 km altitude. Atomic oxygen then is the probable aeronomical constituent to be a chemical catalyst for whatever process is occurring. Slanger [1983] was among the first to report the OH hypothesis.

The DE-B spacecraft was equipped with a high resolution Fabry-Peroton Interferometer (FPI) [Hays et al., 1973]. In this instrument, a 7320 Å filter was utilized in series with the Fabry-Perot etalon. Abreu et al. [1983] reported on the background with ram effect associated with this channel. A ram glow was reported and the deduced etalon spectrum showed similarity with the OH spectrum observed in nightglow from the atmospheric limb. The available evidence from these two spacecraft seems to favor the OH hypothesis for the observed glows.

High resolution spectral measurements of the ISO spectrometer on Spacelab 1 show the presence of N_2 1PG bands [Torr and Torr, 1985]. There are also a number of other observed emission features which may be

IN WHAT I'M AND IN LOW TOTAL WAY

The Course of th

part of the natural aurora airglow background environment and therefore may not be be part of the shuttle glow. There are no associated imaging data with the ISO measurements and therefore the precise determination of the source of the emission could be difficult.

Green [1984] recently reviewed the ram glow data and theory for the shuttle environment. The review described the two classes of mechanisms, one being molecular emission from surface collisions and another due to the plasma critical velocity effect. In his discussions vibrationally excited CO, OH, or electronically excited N₂ were postulated as most likely candidates and were chemically plausible with the evidence at hand.

There is a proposed plasma process for glow production [Papadopoulos, 1983] which involves a two-stream instability between incoming ram and reflected ions. The ion instability sets up an electrostatic wave which in turn heats the ambient electrons. The energetic electrons can in turn excite in situ and ramming constituents. Pumping the electrons to 20+ eV will allow e + X reactions. The energy is sufficient to excite N₂ to 2nd positive, and possibly ionize to 1st negative. A lot of UV emissions could arise with this process whereas the chemical processes postulated are energetically limited to be red and infrared emitters. N₂ 1st negative (1,0) at 3914 Å and N₂ 2nd positive band at 3371 Å are spectral features expected for this physical process.

In this paper we shall review the measurements of the spacecraft glow which were carried out on the shuttle. Having discussed all the known measured properties of the glow we shall discuss a glow mechaninsm which at present seems to be the most plausible explanation of the observations.

The Dependence of the Glow Intensity on the Ram Angle

Examination of the early glow photographs from STS-3 showed that only those surfaces exhibited the glow phenomena which were in the direction of the velocity vector. In an experiment on the STS-5 mission it was verified that the glow intensity strongly depends on the attitude of the surface with respect to the velocity vector.

In the experiment during the first half of a night pass a full >360 degree roll was executed about the shuttle x axis while the orbital velocity vector was approximately in the shuttle y-z plane. The reader should note that the conventional shuttle coordinate system puts the x axis forward of the nose, the y axis out of the starboard wing, and the z axis straight down through the floor of the payload bay (e.g., see Figure 13). During the experiment photographs were taken of the tail section at 2-minute intervals to record the intensity of the glow on the shuttle tail surfaces. The resultant images are presented in Figure 1.

The roll experiment started just prior to the taking of the first picture at 16 hours and 33 minutes Mission Elapse Time (MET). The velocity vector at this time is out of the port and upward directions as shown by the arrow on Figure 1. Two minutes later at 16:35 the shuttle has rolled and the velocity vector is now essentially at about 35 degrees above the -y axis (port wing). This can be verified because one can see the shadowing caused by the engine pod on the port side. At

16:37 the velocity vector dipped below the horizontal (x-y plane) at about 50 degrees and there is only a faint glow remaining on the port side of the stabilizer. The pictures taken at 16:39 and 16:40 show no glow at all because the velocity vector is from the bottom up and all the surfaces to be photographed were shadowed.

On each photograph the approximate direction of the velocity vector is indicated. The direction of the velocity vector was first calculated from Orbiter data provided by the Johnson Space Center. The time code on each picture is only accurate within a minute and therefore the acurate value of the velocity vector for each photograph had to be interpolated from the position of the stars. By using a frame taken at 16:35 (Figure 1) we can establish the direction of the velocity vector fairly accurately from the shadowing of the engine pod. By comparison with a star atlas we could establish the rotation angle with respect to the rotation angle for each exposure in the star coordinata system. Since the velocity vector was essentially in the y-z plane the rotation of the stars gave a fairly accurate value for the angle of the velocity vector. Note that correction had to be made for the change of the direction of the velocity vector due to the orbital motion which amounts to approximately 4 degrees per minute.

The relative magnitude of the glow intensity could be obtained by microdensitometering of the original negative films. Tracings were made to measure the density of the glow luminosity on the tail section. This density was turned into equivalent exposure and the result are presented on Table 1.

TABLE 1. THE RELATIVE INTENSITY OF THE STS-5 STABILIZER GLOW

Time Code	Net relative exposure	Side	Angle of Velocity to surface normal	Cosine of angle
13:16:33	38	Port	80 deg.	0.17
13:16:35	89	Port	28 deg.	0.88
13:16:37	tail in shadow		-50 deg.	
13:16:37	tail in shadow		-97 deg.	
13:16:41	113	STBD	29 deg.	0.87

Unfortunately there are too few data points to draw very solid conclusions. However the numbers support the type of qualitative conclusions one was able to draw from the pictures. The intensity of the glow is not strictly proportional to the cosine of the angle and therefore not proportional to the flux of incoming atmospheric constituents. It appears that very large angles between the surface normal and the velocity vector provide substantial glow, for example, in frame 13:16:33 the angle is 80 degrees to the port side of the tail. When the angle decreases to 28 degrees the increase in glow is just a little over a factor of two. It would seem that the glow detected in the last frame (13:16:41) is anomalously too bright when compared to frame taken at 13:16:35. However the explanation is clear when we examine the actual photographs of Figure 1. The glow on the starboard side is viewed tangentially presenting a much narrower and therefore brighter profile than on the portside where the glow is visible over a larger region of the tail surface. If we were to integrate the glow over the larger region no doubt the overall intensity would be of the same order as the more tangential view of the starboard side for the same angle. The comparison between the two sides is clearly dependent on the detailed geometry of the problem and we have not pursued this in greater detail.

The conclusion that the glow intensity is not proportional to the cosine of the ram angle signifies that the glow is not directly proportional to the incoming flux of atmospheric particles showing that incoming particles at large ram angles are more likely to produce glow than particles at normal incidence.

The Dependence of Glow Intensity on Shuttle Altitude - Comparison of the STS-3 and STS-5 Glow Intensities

It has been rather difficult to use shuttle data to obtain a significant measurement of the altitude dependence of the glow intensity. Using a spacecraft which has an eccentric orbit such as the AE-C provides a much better data base [Yee and Abreu, 1983]. From the AE measurement Yee and Abreu [1983] found that in the altitude regime of the shuttle, the intensity of the spacecraft glow varied in the same manner as the atomic oxygen density. Since most shuttle flights were essentially in a circular orbit the measurements were restricted to comparisons between one flight to the next. The altitude of STS-3 was 240 km. On STS-5 (altitude of 305 km) the Hasselblad camera sequence was repeated in order to generate pictures for comparison with STS-3.

A relatively good comparison is provided in Figure 2 where we present an STS-3 and STS-5 photograph side by side. In these pictures the direction of the velocity vectors is similar. Both photographs were taken by the same type of camera and the same type of lens (F/3.5). Both negative originals were processed similarly, and a control exposure wedge was used to obtain the exposure density curve of each flight film. From comparison of the two photographs of Figure 2, one can see that the the glow generated density is roughly the same. This was confirmed by taking a microdensitometer trace of both images using the original negatives. However the exposure duration for the STS-3 and STS-5 photographs were 10 and 100 seconds, respectively. This would suggest a brightness ratio of the order of 10. In reality however the films exhibit reciprocity failure, and the equivalent exposure is not directly proportional to the exposure time. Using data supplied by the Johnson Space Center we could correct for the film reciprocity failure and obtain the real ratio of the glow intensities. In summary, the best estimate of the intensity ratio between the STS-3 and STS-5 glow is about 3.5. This ratio for glow intensities for altitudes of 240 and 300 km is fairly well in agreement with the trend shown by Yee and Abreu [1983] and therefore in farily good agreement with the scale height variation of an atomic constituent such as 0 or N.

The Intensity of the Glow as a Function of the Distance from the Surface of the Spacecraft

From the early pictures depicting the space shuttle Orbiter it was evident that the glow appears to be standing off from the ram surfaces. The analysis of one of these early pictures [Yee and Dalgarno, 1983] shows that the standoff distance is of the order of a few centimeters from the surface. There is generally a consensus that the excited molecule is formed on the spacecraft surface and it leaves the surface

with some exit velocity. Thus the standoff distance is a characteristic parameter of the lifetime of the emitting species which is leaving the

surface and emitting the glow photons.

In November/December 1983 during the Spacelab 1 mission the standoff distance of the glow was investigated. Mission Specialist Dr. O. K. Garriott took several image-intensified photographs of the tail section. Some of these images were digitized and analyzed in detail. The view of the tail from the Spacelab I module provides a suitable observing geometry for a close-up view of the tail. The images from this observation point give a much more detailed view of the tail and the glow on the tail. The appearance of the width of the glow layer appears to be somewhat irregular from this view. However appropriate modeling calculations were carried out using the geometry shown in Figure 3. In this calculation the shadowing of other Orbiter parts and the appropriate perspective effects were both included to show that the basic law or exponential decay with distance holds. The resulting observed curve is shown on Figure 4. An appropriate exponential curve with an exponential characteristic standoff distance of 20 cm was superimposed on the curve. Thus the characteristic standoff distance associated with the tail, which can be assumed to be a flat plate, is about 20 cm. If the exit velocity of the emitting species were known, then it would be possible to calculate the lifetime of the emission.

On the STS-5 mission a glow experiment was carried out to monitor the intensity of the glow in front of a number of material samples. The intensity of the glow as a function of the material samples will be discussed later. At this point we shall discuss the question of the possible dependence of the standoff distance on the nature of the material surface. For this experiment material samples were used to cover the remote manipulating system (RMS) arm (see Figure 11). The samples were in the form of tapes which were bonded to the arm. Image intensifer photography of the arm enabled our studying the dependence of

the standoff distance with the sample of the materials.

The RMS arm is a cylindrical object with a diameter of 15 inches. In the view on the photographs the ram glow appears directly above the arm since the ram vector is from straight up (-Z) direction. Microdensitometer tracings were obtained to show the decay of the glow with distance from the arm. On Figure 5 two curves are shown. The top curve is the microdensitometer tracing associated with the glow in front of the chemglaze sample. The bottom curve represents the glow in front of the Kapton sample. The baseline brightness is the intensity representing the night sky and on the tracing left corresponds to the top of the image and right to the bottom. The RMS region is indicated being 15 inches in diameter. Note that the region of the chemglaze sample is closer to the observer and therefore the dimensions are slightly larger. The curves represent the uncorrected film density of the image. The linear distance from the arm where the intensity falls to one-half of its value is measured in each case and is indicated on the figure.

Although there is a large difference in the intensity between the two material samples the distance associated with the decay of the glow remains the same. The true intensity ratio between the glow in front of the two samples is about 3. As we have discussed previously the standoff distance is a characteristic of the lifetime of the emitting species. From our measurement it appears quite clear that the standoff distance in front of the two different material samples is the same; thus, the lifetime of the emitting species is presumably also the same.

The Spectra of the Glow

During the STS-4 mission the spectrum of the glow was recorded by an unaided Hasselblad camera using the objective grating [Mende et al., 1983]. Based on a single photograph it was derived that the spectrum of the glow consisted of a relatively diffuse spectrum primarily at the red-infrared end of the visible spectrum. Although it was hard to obtain quantitative information from this glow spectrum it seemed to be most intense in the region between 6300 Å and the window cutoff at 8000 Å. Because of the lack of sensitivity of the unaided F/3.5 camera and the unfavorable direction of the velocity vector, long exposure duration (400 seconds) was required.

On STS-5 the intensified camera permitted the taking of short exposure grating spectra. Unfortunately the STS-5 spectral results are not spectacular because the direction of the velocity vector was unfavorable during the time the grating exposures were taken. An additional problem was the presence of the Earth near the field-of-view producing a strong

unwanted background.

The first truly succeesful objective grating glow spectrum was obtained on STS-8 in September 1983. One of the objectives of this experiment was to obtain a good signal-to-noise ratio objective spectrum of the tail glow. The velocity vector was aligned with the Orbiter y axis (this direction is in the direction of the starboard wing). Five exposures were taken with the grating in position and the lens set at F/2.8. The durations of the five exposures were 8, 4, 1, 1/4, and 1/15 second, respectively. The 1-second duration exposure is reproduced in Figure 6. The glow illuminated the starboard side of the tail and the starboard engine pod. These can be observed most clearly in the right side of the picture where the zero order image is located. The horizontal streaks on the photographs are the first-order images or spectra of stars. Some stars have both their zero-order point images and their first-order spectral streak images in the picture. The large diffuse image a little left of the center is the first-order or spectral image of the glow. Approximate wavelength scale was superimposed on the frame.

From Figure 6 it is qualitatively evident that the shuttle glow is spectrally diffuse. It is also clear that there is very little glow in the wavelength range of 4300 to about 5000 Å. In the range above 5000 Å the glow becomes more intense falling off towards the higher end presumably due to the falling response of the image intensifier photocathode [Mende, 1983].

In the spectral image of Figure 6 there is an apparent line emission. This is evident because of the presence of a well-defined image of the tail in first order. Since it is a well-defined image its wavelength can be derived fairly accurately. Within the accuracy of the measurements the wavelength of this feature was found to be 7600+50 Å. This suggests that the observed emission is scattered airglow in the 02 atmospheric airglow band at 7619. There is other evidence that this feature is not part of the spacecraft glow. Close examination of the figure will reveal that the first-order image is equally bright on both sides of the tail while the glow in the zero-order image is very much brighter on the starboard side. Only extended scattered light sources could provide equal luminosity on both sides of the tail. Our previous

results [Mende, 1983] already shows that the 7619 A component of the airglow is the most intense airglow component reaching several hundred kilorayleighs in the limb view.

In view of the state of knowledge it was essential to obtain spectral data with improved resolution and with simultaneous documentation of the spatial extent of the glow source region. For mission 41-D a special glow spectrometer was constructed. The instrument has three operating modes. The three modes are schematically illustrated in Figure 7. The top illustration shows the instrument with the grating and slit out of the optical path. In this mode the intensifier camera works in a straight through imaging mode with a real image formed at the plane of the slit by the objective lens. A permanent targeting slit is superimposed on the image to provide a fiducial for aiming the system. The image is then collimated by the collimating lens and refocused on the image intensifier photocathode by the camera objective lens. The image intensifier has a light amplification gain of 50,000. The output phosphor of the image intensifier tube is re-imaged on the film or in the viewfinder of the 35-mm single lens reflex camera attached to the system. The observer looking through the viewfinder will see the targeting slit superimposed on the image. In this mode the astronaut is able to point the instrument and accurately document the position of the spectral slit on the image. The second mode shows the spectrometer with the grating in the optical path. In this mode the grating produces an objective spectrum. In addition to the image which was produced in the previous mode another image, the first-order image, also appears. The distance between the two images is proportional to the wavelength of the light forming the image. This type of slitless objective grating was used for previous glow investigations by Mende et al. [1983], Mende [1983], Mende et al. [1984].

The third mode represents the high resolution spectrographic mode. In this mode the slit covers are also placed into the optical train. They cover up the image except the narrow slit formed by two parallel bars of the targeting slit. In this mode the system is equivalent to a transmission grating spectrometer with grating rulings of 300 lines per mm. Three identical lenses were used all three were F/1.4 f=50 mm. The slit width was 0.0508 mm.

The theoretical resolution $d\lambda$ of the spectrometer with a 300 line per mm grating can be estimated as:

 $d\lambda = 1/3000 * \sin (0.0508/50)$ (cm) $d\lambda = 34 \%$

The reference photographic image of the shuttle tail and engine pods is shown on Figure 8 taken on September 4, 1984, at 17 34 50. In this image the targeting slit was superimposed on the tail section, the engine pod, and a bulkhead in the payload bay. The slit crosses some other areas on the Orbiter skin which are also somewhat luminous. The sources of the light on the Orbiter are the glow, reflected airglow, or starlight.

The corresponding spectrum taken with the grating and slit in the optical train is shown on Figure 7 (17:36:01). From the comparison of Figures 6 and 7 spectrum of the glow and the Orbiter surfaces may be identified. Starting from the top of the photograph, the top region is the spectrum of the bulkhead. This shows two distinct lines. From the

preflight calibration of the wavelength dispersion these lines are clearly identified as atomic 0 at 5577 Å and the $O_2(0,0)$ band at 7620 Å. It may be seen that while 5577 is a narrow spectral line showing up as a thin line, the $O_2(0,0)$ band is quite wide representing the larger wavelength extent of the $O_2(0,0)$ band. This demonstrates that the observed luminosity on the Orbiter is mainly due to scattering of the Earth's airglow.

Microdensitometer tracings of this glow were obtained and the calibrated intensity response of the film was applied to the measured film density and plotted in Figure 10 (bottom curve). The curve was corrected for device responsivity by using the preflight calibration data obtained from a light source of know emissivity as a function of wavelength and is also shown in Figure 10 (top curve). The corrected curve represents a normalized intensity of the source emission.

The measured spectral responsivity of the spacecraft glow on STS 41-D shown in Figure 10 is very similar to the result found on STS-8 [Mende et al., 1984b], both of which show a peak near 7000 Å. Our approach of using the spectral slit in this instrument eliminates the contamination of earlier results by the scattered airglow and leaves no doubt about the absence of any distinct spectral features in the spectrum of the spacecraft glow.

The experiment data show quite conclusively that the spacecraft glow has a continuum spectra within the spectral resolution of the instrument. It shows that the glow is not simple atomic or molecular band spectra. Considerations of the thickness of the glow layer around the spacecraft and associated lifetimes of the excited states exclude the possibility of a many-component molecular spectra produced by a wide variety of emitting materials. Thus we need to look for a single component which has a complex continuum spectra. Emission continuum is rare in molecular systems. The most abundant elements in the ramming atmosphere are OI and N2 and the simplest combination of these constituents producing a continuum is NO2. Heppner and Meredith [1958] reported seeing an NO continuum in a rocket wake. The suggestion that spacecraft glow could be caused by NO and O recombination was made by by Torr et al. [1977] in connection with the emisssions observed on the Atmosphere Explorer (AE) satellite. However this suggestion was discarded in favor of other mechanisms because the observed glow spectrum did not totally agree with laboratory spectrum.

The measured spectrum of the spacecraft glow on STS 41-D shown in Figure 10 portrays the same features as those reported on STS-8. A peak is obtained around 7100 Å with a gradual fall off towards both the short and longer wavelengths. The approach of using the spectral slit eliminates the contamination of earlier results from scattered airglow and leaves no doubt about the absence of any distinct spectral features in the spectrum of the spacecraft glow.

In a recent report of Torr and Torr [1985], a high resolution spectrum of the glow taken by the Spacelab I ISO instrument was published. The ISO spectrum was taken while the Orbiter and atmosphere were in full sunlight, and the instrument was looking directly into the ram. Since many features of this spectrum were attributable to natural airglow and vehicle glow in front of and within the instrument it might be very fruitful to compare the two spectra. Since the resolution of the ISO instrument is 6 Å it would be desirable perhaps to convolute the ISO spectrum with a 35 Å slit width prior to comparison. Nevertheless even

without such a convolution it seems evident that the two spectra are somewhat dissimilar.

Glow Intensity Dependence on the Spacecraft Surface

The dependence of the glow intensity on the nature of the spacecraft surface was investigated on STS-5 and 41-D missions. In the STS-5 experiment the Orbiter velocity was aligned parallel to the Orbiter-z axis (this direction is vertically up in the Orbiter bay). The material samples were photographed with the intensifier camera without the grating. First samples mounted on the remote manipulator system (RMS) arm were photographed with varied exposure times. The material samples on the RMS arm were mounted in the form of 4-inch-wide tapes. The layout of the tapes was selected to maximize the "limb glow" over the curvature of the cylindrical arm. The layout is illustrated photographically in Figure 11 a. This picture was taken prior to flight. The samples are in the following sequence: kapton, aluminum, black chemglaze, aluminum, and kapton. The samples were repeated in order to avoid the possible ambiguity caused by the slightly different geometry of the different view angles of the samples.

Kapton was chosen because of its known high weight loss property in shuttle orbital environment, aluminum was chosen because of its known stability, and black chemglaze (carbon filled, urethane based, matt black light absorbing paint) because of its application in low light level detecting devices [see image intensified photograph (Figure 11b) of the RMS arm with the material samples]. The glow above the chemglaze is stronger than the glow above the other materials. Aluminum glows the least. The kapton samples and their associated glow are indistinguishable from the covering material of the arm. This photograph is the first solid evidence that the spacecraft ram glow depends on the

material surface properties of the spacecraft.

This experiment was essentially repeated on the 41-D mission with nine different material samples. Unfortunately mission 41-D flight was combined with another mission and the replanned mission did not fly at the desired altitude of 220 km. Instead the altitude for 41-D was close to 300 km which reduced the signal-to-noise ratio in the experiment to barely detectable levels. The camera was in the spectrometer configuration and was aimed so that the slit was perfectly parallel with the arm. Due to the weakness of the image, the glow within the slit could not be analyzed. To obtain the best data we used the region between the slit and the arm. Since the glow was very faint, the comparison proved to be very difficult.

Microdensitometer tracings parallel with the arm were obtained. The first tracing shown in Figure 12 included the region of the glow which is between the black bar of the targeting slit and the arm. Another densitometer tracing was taken of the night sky just above the slits. This night sky tracing was used as a basis for correction because of a

non-uniform response in the system.

Figure 12 shows the uncorrected microdensitometer tracings, the position identification of each material sample, and a horizontal bar representing averaged glow intensity above the sample. The intensity above the sample was corrected for the apparent non-uniformity derived from the night sky trace. The correction resulted in an increase of the glow intensities above the material samples on the left side of the

image. The corrected values were represented by the upper horizontal bars. It is interesting to note our corrections are consistent with visual observations of the flight crew. During the performance of the experiment the crew reported that the samples furthest to the left of the image were glowing the most intensely.

Based on the data obtained from the 41-D experiment (Figure 12) the materials samples were ranked from 1 to 9 in order of their glow producing properties from minimum to maximum, respectively.

One was assigned to polyethylene and nine to the apparantly brightest glowing Z302 overcoated with Si. However the marginality of the signal-to-noise ratio makes it difficult to draw strong conclusions.

It has been well established that the spacecraft glow is generated by emission from metastable molecules which had been excited on the surface of the of the spacecraft. There are several possibilities regarding the source of the metastable molecules. These molecules could be resident on the surface as contaminants. In that case, however, one would expect the glow intensity greatly variable depending on the length of the on orbit exposure or the temperature of the surface. No such evidence has been reported so far. One would also expect adjacent surface samples to be contaminated equally; therefore no surface material specific glow intensity would be expected. Another source of the molecules could be the bulk surface material. This contradicts the evidence discussed by Mende et al. [1984] where it was reported that on STS-8 the intensity of the glow in front of the kapton sample was much less than in front of the chemglaze sample and the depletion rate of kapton was much higher than that of the chemglaze. We can draw similar conclusions from the 41-D experiment. For example the chemically stable MgF2 sample exhibits intense glow characteristics. Polyethylene seems to produce the least glow. All these results point to the fact that in the glow production the surface accommodation property of the sample is important and not the chemical stability of the bulk material. Thus it can be deduced that the surface acts as a catalyst. The source of the metastable molecules producing the glow must be the environment itself.

Thruster Firings and Associated Glow

It was discovered on the early shuttle flights that the firing of a shuttle thruster creates a great deal of observable light [Banks et al., 1983]. This effect was thought to be the result of the unburned fuel combining with the ambient atomic O. It was also observed that in addition to this spontaneous light emission after a thruster firing, there is also a marked enhancemment of the spacecraft ram glow. To investigate the effects of the various thrusters an experiment was performed on the STS-8 mission. In this experiment the camera was opened for 2 seconds. During the exposure a selected thruster was fired for a minimum single impulse by manual operation of a crew member. There are six vernier thrusters on the Orbiter (Figure 13); some of them can be operated singly while others are usually operated in pairs. Four different combination of thruster firings were performed and the results photographed. A 2-second duration background exposure was also taken between each thruster firing to assure that all thruster effects disappeared prior to the next firing. The results are shown in Figure 14 in the form of a collage of the photographic images. The top left picture represents the background image with no thruster firings.

Since the camera was in the objective grating configuration and the Orbiter attitude was such that the velocity vector is from the direction of the starboard wing, this picture is identical to Figure 6. Note that the only thruster which has a noticeable effect on the picture background is the downward firing tail thrusters. The following explanation can be provided. The downward tail thruster is directed towards the wing. The gases emitted by the other thrusters leave the vicinity of the Orbiter with their emission velocity, however, the downward tail thrusters throw their output on the wing where the gases thermalize and will take up the velocity of the spacecraft. This luminous cloud will travel with the spacecraft.

The time development of the thruster firings can be best studied by means of the Orbiter closed-circuit TV cameras. A thruster firing event documented by the orbiter TV cameras on video tape are included in Figure 15. To aid in the timing of the event a time counter which ran in seconds and one-hundredth seconds was superimposed on the frames. The status of this time counter provided a unique identification of the TV frame. The first image at time is a background frame at :53:32. The second and third images show the thrusters while in operation. The following frames show the decay of the glow on the engine pods which persists well after the thrusters had been shut off. The TV sequence (Figure 15) was taken on mission STS-8 at an altitude of 220 km.

Figure 16 shows the thruster-induced glow intensity as a function of time. This was obtained by integrating the video signal from all pixels inside of a rectangular area which includes the glow on the port side engine pods. This integrated signal was plotted by a chart recorder. Note that the video signal may include a number of relatively unknown parameters such as the signal non-linearities and the time response characteristics of the television system. Nevertheless the effects of these parameters on our conclusoins are believed to be negligible. Two observations were plotted in Figure 16. The top one is from the low-altitude portion of STS-8 at 220 km altitude and the bottom is from STS-3 [Banks et al., 1983] at 240 km altitude. The decay is considerably longer for the low-altitude case.

Discussion

Understanding of the spacecraft glow is important because it may shed light on unanticipated upper atmospheric chemical and physical processes and the spacecraft glow has also its practical significance as a contaminant to light-sensitive instrumentation.

The spectral results of mission 41-D are not altogether new. From previous measurements STS-4, STS-5, and STS-8 we have come to realize that the spacecraft glow had a continuum spectra and was devoid of significant lines. The present results are confirming these findings and have yielded high enough signal-to-noise ratios to permit quantitative interpretation of the emissivity as a function of wavelength. Preliminarily we can say that the spectra of the glow shows relatively little emission intensities below 500 nm and above this the emissions reached a peak between 600 and 700 nm. Without more quantitative densitometry it is hard to interpret the data any further. The basic shape of the spectral content is of course no surprise when we look at the color photos with the orange-red images of the spacecraft glow.

Perhaps it is even more significant to mention that there are no distinct spectral features in the spectrum. From the observation of the reflected airglow light at 557.7 nm and 762.2 nm we can see that the instrumentation is fairly sensitive to distinct line emissions, had they been present.

We have examined many of the properties of the shuttle glow. It is now our task to examine the theoretical ideas which are consistent with

the above findings.

From our new observations of the continuum emission from the shuttle and from the realization that the NO recombination spectrum is largely variable depending on the reaction conditions and the catalyst, we strongly suggest that the shuttle glow is produced by NO, recombination continuum. It has been suggested by Green [1984] that N2 molecules having a collisional energy of 9.3 +2 eV are capable of dissociating on the surface (dissociation energy is 9.8 eV). In the simplest picture the reaction N+O=NO(B2) takes place on the surface where the ambient OI(3P) originates from the atmosphere. Reeves et al. [1960] found this to occur in laboratory experiments when NI and OI were mixed. They found that the NO(B2) was formed and the associated beta band emission was observed in their wall catalysis experiment with N and O atoms. If a significant portion of the formed NO remains in contact with the wall, then the NO would be exposed to the ramming OI. Reaction of NO with raming OI would create NO, which would be removed from the surface in the process. It is well known that the 3-body recombination is efficient for NO and OI, i.e., NO + OI + (M) -NO, +(M).

The spectrum shown in Figure 10 has many simularities to that published by Fontijn et al. [1964]. In Figure 17, the spectrum is replotted and compared with the Fontijn et al. measurement. The Fontijn et al. measurement of NO₂ continuum was produced when NO was mixed with OI where the OI was produced with a microwave discharge. Their published spectrum was acquired by viewing end-on into a 2-cm-diameter by 20-cm-long vessel. Paulsen et al. [1970] performed an experiment which also measured the NO₂ continuum in recombination as well as that continuum produced with thermal emission with gas temperature between 900 K and 1335 K. In their experiment, they found the peak of the recombination continuum at 6400 Å also but found some discrepancy at red wavelengths between their spectrum and that of Fontijn et al. The Paulsen et al. spectrum is also plotted in Figure 17. It is clear that the laboratory spectrum is not within the error of the measured spectrum

produced here.

Recombination spectrum also can be very different in shape dependent on the recombinant species. NO+03 produces a spectral peak near 1.2 microns [Greaves and Garvin, 1959]. With excited 03, the recombination shifts to the blue proportionally with the internal vitration state of 03 [Braun et al., 1974]. Recombination with 0, [Kenner and Ogryzlo, 1984] produces a recombination continuum which peaks near 8000 Å. The continuum populated thermal distribution peaks >1 micron [Paulsen et al., 1970]. The recombination of raming OI atoms with a surface monolayer of NO has not been studied in the laboratory. Golomb and Brown [1975] found laboratory dence for thermal effects on the spectral shape of the OI recombination spectrum at low temperature (200-350 K range). They found a translate the blue portion of the continuum to decrease with increasing aperature. They also found the peak of their spectrum at 6800 Å which is the same as that measured on the shuttle. The effect

of the ram velocity may be responsible for considerable alteration of the observed spacecraft spectrum. An equivalent temperature for ramming OI is ~100,000 K.

NO2 has a complex vibrational structure which has been widely studied in recombination experiments. Upper state mixing of NO2 can occur, likely between the 2B1 and 2B2 states. The complex upper state population has been described by Neuberger and Duncan [1954], Douglas [1966], Paulsen et al. [1970], and Gangi and Burnelle [1971]. Very short lifetimes in the blue and red have been only reported in thermal production of the continuum [Paulsen et al., 1970]. It has been assumed here that the upper state of NO2 in recombination with OI(3P) has a representative lifetime as found in fluorescence and the values found by Schwartz and Johnston [1969] are valid.

The NO₂ continuum is a superposition of many states. The resultant average lifetime of NO₂ in fluorescence is ~80 microseconds at 5500 Å and decreases in the blue to ~60 microseconds at 4000 Å according to Schwartz and Johnston [1969]. It was previously reported by Yee and Dalgarno [1983] that the effective e-folding distance in the glow from the surface is ~20 cm. This has been reverified as discussed here for several STS-9 glow images. If the emission is represented by the red-green wavelengths of emission, the average lifetime would be ~70 microseconds. If we assume x = t*v [Yee and Dalgarno, 1983], where x = 20 cm, we would infer that the exit velocity from the surface would be ~2.5 km/sec (<1/3 the ram velocity) if NO₂ were the emitter. This corresponds to an effective exit temperature of 10,000 K. This is ~25% the ram energy of OI yet considerably higher than the expected surface temperature of near 300 K. In the process of producing the NO₂ then, total thermal accommodation of the OI does not occur.

Most of our photography took advantage of the oblique viewing of the shuttle surfaces to maximize the intensity. A preliminary estimate of the STS-8 glow intensity would suggest between 10 and 100 kilorayleighs for these oblique views. For viewing the glow in a direction normal to the shuttle surfaces, we estimate the intensity to be in the 1 to 10 kilorayleighs category. Assuming that it is of the order of 5 kilorayleighs, then the total number of radiating particles is 5 x 109 per cm⁻² of the surface area.

The oxygen density was estimated to be $2.3 \times 10^9 \text{ cm}^{-3}$ for the STS-8 flight (Hedin, private communication, 1983). The spacecraft velocity of 7.3 km/sec yields a total 0 flux of $1.7 \times 10^{15} \text{ cm}^{-2}$. Accordingly if the glow is caused by the 0 flux incident on the spacecraft, then approximately one in 10^6 0 particles causes the emission of a glow photon.

It is interesting to examine the efficiency of the NO₂ production and compare it to the total light output. The atomic N density is of the order of 10⁷ per cm³ at shuttle altitude. From the mass spectrometer observations of Engebretson and Mauersberger [1979], a large fraction of this N will combine with the wall and form NO in a surface-absorbed state. There are about 2 orders of magnitude more O atoms available for the NO production. Assuming that the rate of NO production, r_{NO}, is determined by the N flux,

$$r_{NO} = N_N \cdot v \cdot \epsilon_{NO} \sim 8 \times 10^{12} \epsilon_{NO}$$

where N_N is the density of atomic nitrogen, v is the velocity of the Orbiter, and ε_{NO} is the efficiency for producing NO per surface impact of N. The portion of the spectrum between 4000 Å and 8000 Å of Orbiter glow from the

stabilizer corresponds to ~5 kilorayleighs of surface normal intensity. In other words, the observed photon yield to atomic nitrogen flux is ~25%.

According to Engebretson and Mauersberger [1979], the efficiencies for producing NO and NO₂ are high. Since each recombinant NO₂ emits in the recombination process, there appears to be adequate NO₂ production to feed the glow process.

TABLE 2. THE MATERIAL SAMPLES AND THE GLOW INTENSITY IN ARBITRARY UNITS

Material	Ranking
Mgf2	8
2306	6
Z302 Overcoated with Si	9
Z302	7
Polyethylene	1
401-C10	2
Carbon Cloth	4
Chemical Conversion Film	5
Anodized Al	3

Acknowledgments. The authors wish to express their gratitude to personnel of the Marshall and Johnson Space Flight Centers for their support of the experiments. Special mention should be made of Mr. K. S. Clifton and Dr. R. Gause at Marshall Space Flight Center. Encouragement and help is acknowledged from Dr. P. M. Banks of Stanford University and Dr. L. Leger and Dr. O. K. Garriott of the Johnson Space Center. Helpful discussions are acknowledged with Dr. Irving Kofsky of PhotoMetrics, Inc. These series of experiments would not have been possible without the active collaboration and enthusiastic participation of the astronaut flight crews on the various missions. This research was supported by NASA through the Space Telescope program and under the Atmospheric Emissions Photometric Imager Program NAS8-32579 and by a Lockheed Independent Research Program.

References

Abreu, V. J., W. R. Skinner, P. B. Hays, and J. H. Yee, Optical effects of spacecraft-environment interaction: Spectrometric observations by the DE-B satellite, AIAA-83-2657-CP, Shuttle Environment and Operations Meeting, Washington, D.C., 1983.

Banks, P. M., P. R. Williamson, and W. J. Raitt, Space Shuttle glow observa-

tions, Geophys. Res. Lett., 10, L118, 1983.

Braun, W., M. J. Kurylo, A. Kaldor, and R. Wayne, Infrared laser enhanced reactions: Spectral distribution of the NO₂ chemiluminescence produced in the reaction of vibrationally excited O3 with NO, J. Chem. Phys., 61, 461, 1974.

Douglas, A. E., Radiative lifetimes of molecular states, J. Chem. Phys., 45, 1007, 1966.

Engebretson, M. J., and K. Mauersberger, The impact of gas-surface interactions on mass spectrometric measurements of atomic nitrogen, J. Geophys. Res., 84, 839, 1979.

Fontijn, A., C. B. Meyer, and H. I. Schiff, Absolute quantum yield measurements of the NO-O reaction and its use as a standard for chemiluminescent reactions, J. Chem. Phys., 40, 64, 1964.

Gangi, R. A., and L. Burnelle, Electronic structure and electronic spectrum of nitrogen dioxide. III. Spectral interpretation, J. Chem. Phys., 55, 851, 1971.

Greaves, J. C., and D. Garvin, Chemically induced molecular excitation: Excitation spectrum of the nitric oxide-ozone system, J. Chem. Phys., 30, 348, 1959.

Green, B. D., Atomic recombination into exicted molecular-A possible mechanism for shuttle glow, Geophys. Res. Lett., 11, 576, 1984.

Golomb, D., and J. H. Brown, The temperature dependence of the NO-O chemiluminous recombination. The RMC mechanism, J. Chem. Phys., 63, 5246, 1975.

Hays, P. B., G. Carignan, B. C. Kennedy, G. G. Shephert, and J. C. G. Walker, The Visible Airglow Experiment on Atmosphere Explorer, Radio Sci., 8, 369, 1973.

Heppner, J. P., and L. H. Meredith, Nightglow emission altitudes from rocket measurements, J. Geophys. Res., 63, 51, 1958.

Kenner, R. D., and E. A. Ogryzlo, Orange chemiluminescence from NO2, J. Chem. Phys., 80, 1, 1984.

Mannella, G., and P. Harteck, Surface-catalyzed excitations in the oxygen system, J. Chem. Phys., 34, 2177, 1961.

Mende, S. B., Vehicle glow, AIAA-83-2067-CP, Shuttle Environment and Operations Meeting, Washington D.C., 1983.

Mende, S. B., Experimental measurement of Shuttle Glow, AIAA-84-0550, presented at AIAA 2nd Aerospace Sciences Meeting, Reno, January

Mende, S. B., O. K. Garriott, and P. M. Banks, Observations of optical emissions on STS-4, Geophys. Res. Lett., 10, 122, 1983.

Mende, S. B., P. M. Banks, and D. A. Klingelsmith, III, Observation of orbiting vehicle induced luminosities on the STS-8 mission, Geophys. Res. Lett., 11, 527, 1984.

Neuberger, D., and A. B. F. Duncan, Fluorescence of nitrogen dioxide, J. Chem. Phys., 22, 1693, 1954.

Paulsen, D. E., W. F. Sheridan, and R. E. Huffman, Thermal and recombination emission of NO2, J. Chem. Phys., 53, 647, 1970. Schwartz, S. E., and H. S. Johnston, Kinetics of nitrogen dioxide

fluorescence, J. Chem. Phys., 51, 1286, 1969.
Reeves, R. R., G. Mannella, and P. Harteck, Formation of excited NO and No by wall catalysis, J. Chem. Phys., 32, 946, 1960.

Slanger, T. G., Conjectures on the origin of the surface glow of space vehicles, Geophys. Res. Lett., 10, 130, 1983.

Torr, M. R., P. B. Hays, B. C. Kennedy, and J. C. G. Walker Intercalibration of airglow observations with the Atmosphere Explorer satellites, Planet. Space Sci., 25, 173, 1977.

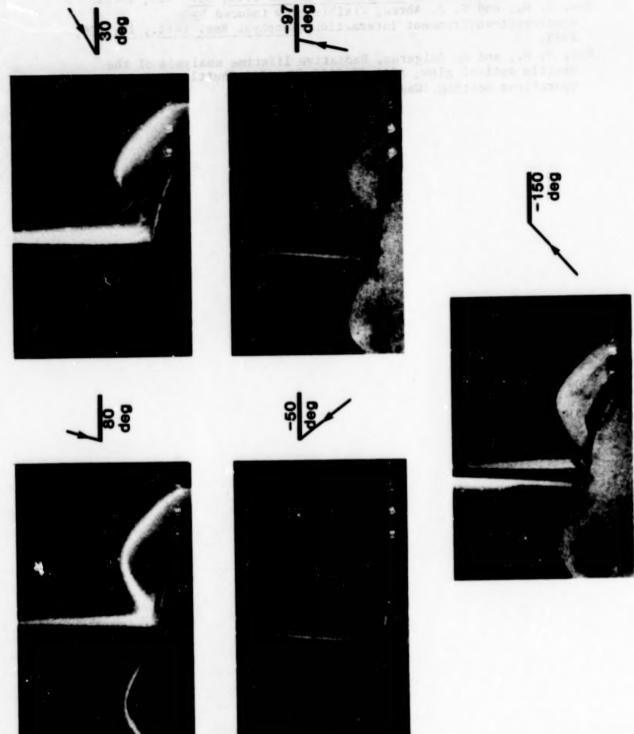
Torr, M. R., Optical emissions induced by spacecraft-atmospheric interactions, Geophys. Res. Lett., 10, 114, 1983.

Torr, M. R., and D. G. Torr, A prelimianry spectroscopic assessment of the Spacelab 1/Shuttle optical environment, J. Geophys. Res., 90, 1683, 1985.

- Yee, J. H., and V. J. Abreu, Optical contamination on the Atmosphere
- Explorer-E satellite, Proceedings of the SPIE, 338, 120, 1982.

 Yee, J. H., and V. J. Abreu, Visible glow induced by spacecraft-environment interaction, Geophys. Res. Lett., 10, 126, 1983.
- Yee, J. H., and A. Dalgarno, Radiative lifetime analysis of the Shuttle optical glow, AIAA-83-2660-CP, AIAA Shuttle Environment and Operations Meeting, Washington D.C., 1983.

ORIGINAL PAGE IS OF POOR QUALITY



The glow as appears on different parts of the Orbiter as the Orbiter rotates around the x axis. F18. 1.

ORIGINAL PAGE IS OF POOR QUALITY



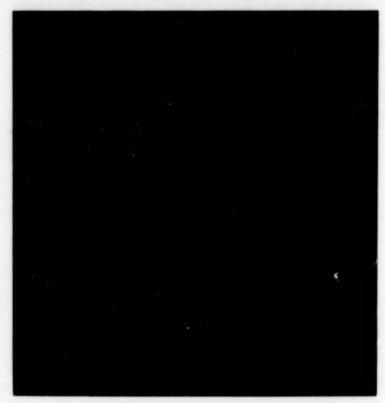


Fig. 2. Unaided Hasselblad photographs on STS-3 and STS-5.
The exposure times are 10 and 100 seconds, respectively.
The velocity vector is more or less from the same direction for each.

GLOW VIEWING GEOMETRY

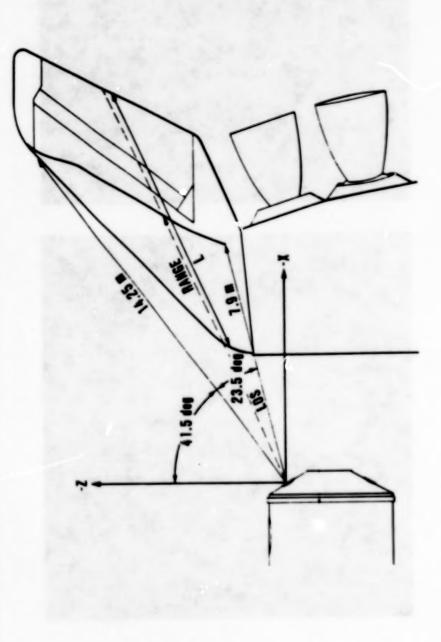


Fig. 3. The viewing geometry of the tail from the Spacelab 1 module on STS-9.

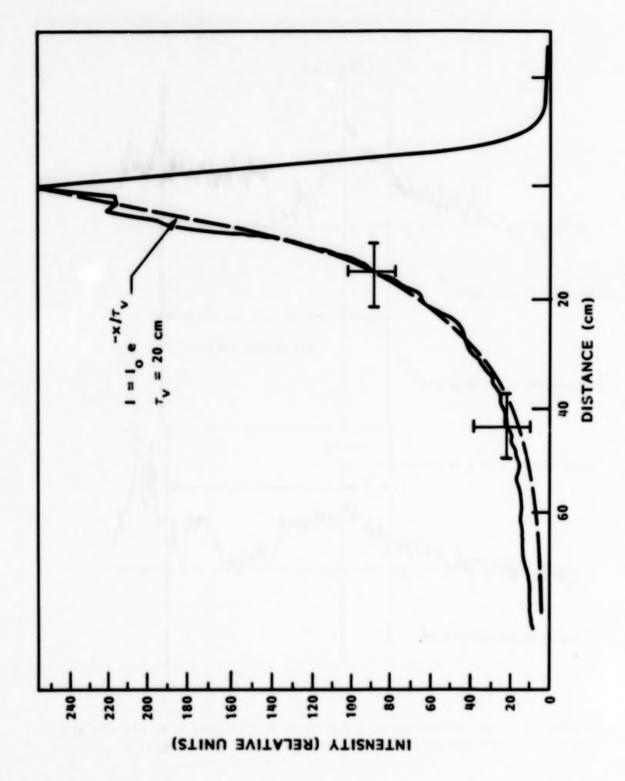


Fig. 4. Glow intensity as a function of the distance from the tail.

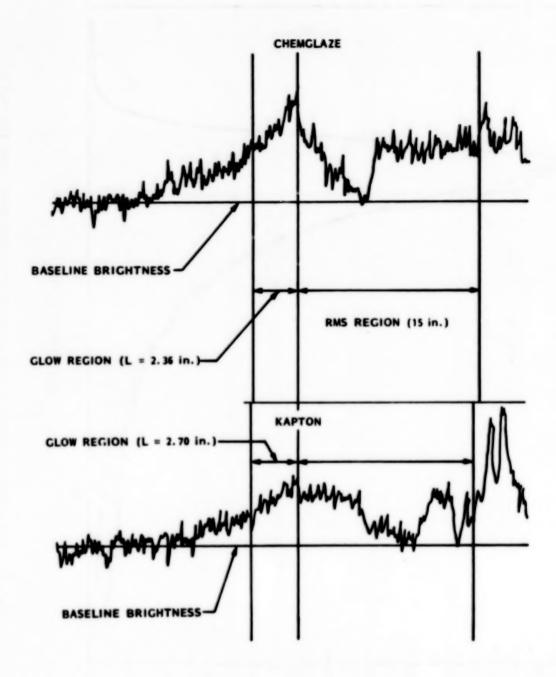


Fig. 5. Glow intensity as a function of distance from the RMS arm for two material samples, chemglaze and kapton.



Fig. 6. Objective spectrum of the shuttle glow from STS-8.

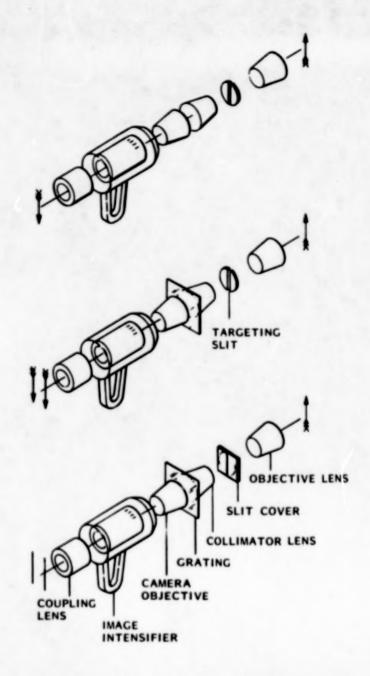
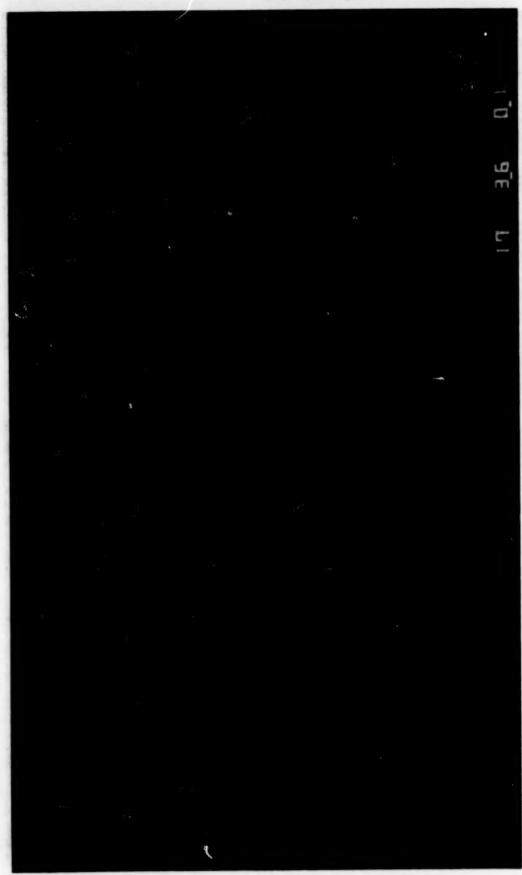


Fig. 7. Image intensified slit spectrograph for shuttle glow observations. Top is shown with straight through imaging configuration. Middle is shown in objective grating configuration. Bottom is shown in spectrometer configuration.

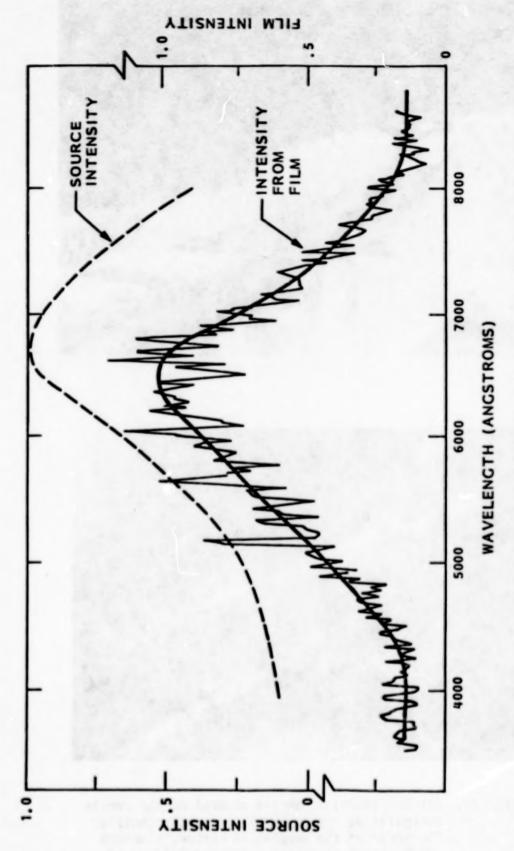
ORIGINAL PAGE IS OF POOR QUALITY



Straight through imaging looking at the shuttle tail, port engine pod, and bulkhead. Photograph taken at 17:34:50. F1g. 8.



Continuum spectra is produced By comparison with Figure 3 the objects can be identified. Orbiter skin produces line spectra of scattered airglow. Continuum spectra is produce by vehicle glow. Same image as Figure 3 except that grating and slit has been included. F1g. 9.



(Top) Corrected spectrum of spacecraft glow where the instrument response has been tracing has been corrected for the calibrated D-Log-E response of the film. The noise character in the data is primarily due to ion scintillations in the image applied to the curve drawn through the data shown in the bottom of the figure. (Bottom) Six line average tracing of spacecraft glow identified in Figure 2. intensifier which have accumulated in the image over the 30-second exposure. F1g. 10.

ORIGINAL PAGE IS OF POOR QUALITY

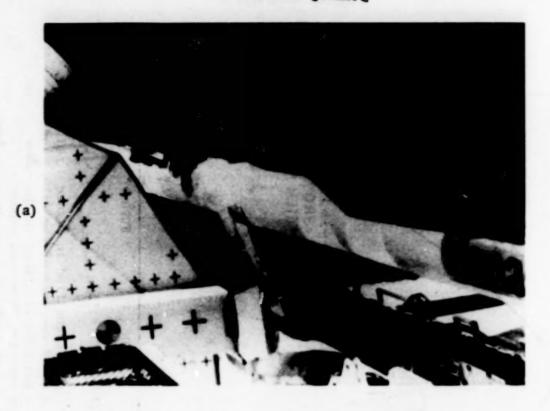




Fig. 11. (a) The material samples mounted on the remote manipulating system (RMS) arm on the shuttle. The order of the samples is kapton, aluminum oxide, black chemglaze, aluminum oxide, and kapton. (b) Material samples glowing in the ramming atmosphere.

RELATIVE GLOW INTENSITIES

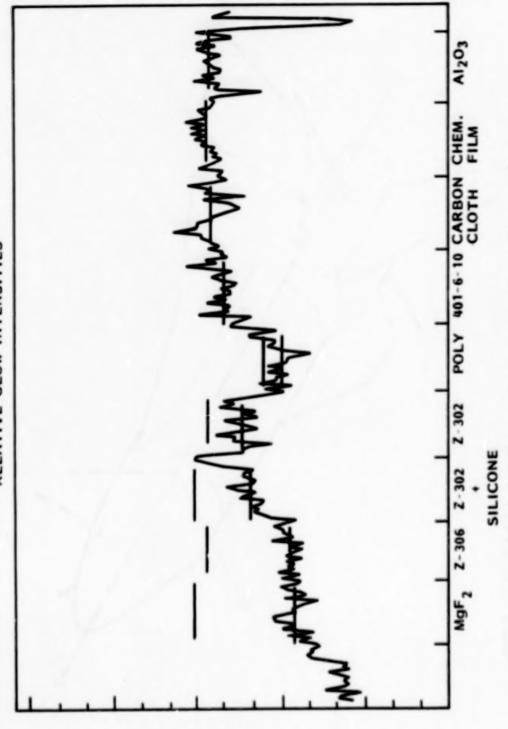


Fig. 12. Microdensitometer tracings of the nine glow samples on mission 41-D.

=3

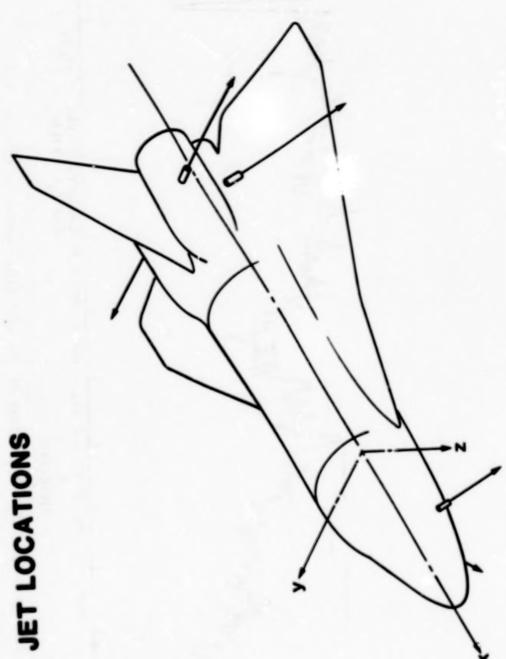
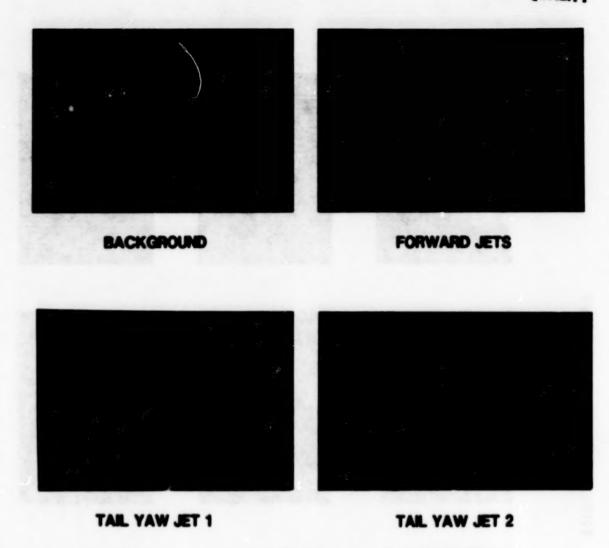
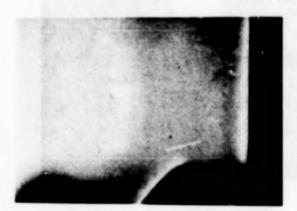


Fig. 13. A schematic sketch of the location of the thrusters on the Orbiter.

THRUSTER FIRINGS

ORIGINAL PAGE IS OF POOR QUALITY

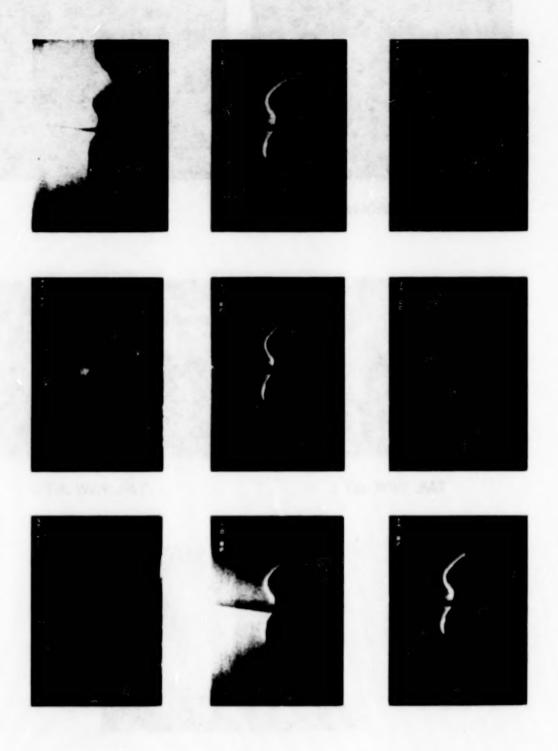




TAIL DOWNWARD JETS

Fig. 14. The effect of firing thrusters during the exposures. Top left, no thrusters fired.

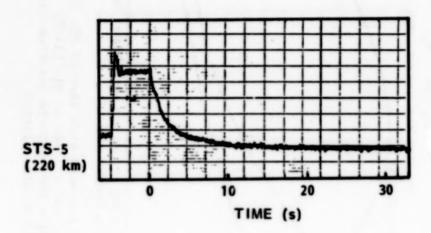
ORIGINAL PAGE IS OF POOR QUALITY



Collage of television monitor photographs of the thruster firing as recorded by the Orbiter bulkhead closed-circuit television cameras. Time counter in seconds and hundredths of seconds. Note that glow on engine pods is enhanced after jet firing. Fig. 15.

THRUSTER FIRING DECAY

ORIGINAL PAGE IS OF POOR QUALITY



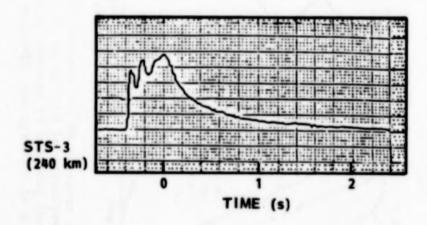
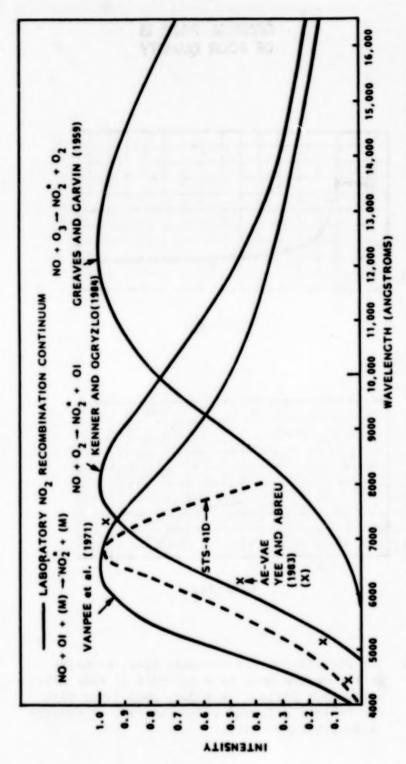


Fig. 16. The function of the thruster glow intensity on the engine pods as a function of time after a thruster firing. The data were taken with the Orbiter bulkhead video cameras. Intensity is in arbitary units.



The spectrum of the spacecraft glow compared with that of the laboratory experiments of Fontijn et al. [1964] and Paulsen et al. [1970]. A spectral blend produced by spectrally e-folding the measured spectrum with lifetime data of Schwartz and Johnston [1969] is also plotted. F18. 17.

SPACE SHUTTLE RAM GLOW: IMPLICATION OF NO RECOMBINATION CONTINUUM

Gary Swenson and Steve Mende

Lockheed Palo Alto Research Laboratory

Stu Clifton

Space Science Laboratory NASA Marshall Space Flight Center

Abstract. The ram glow data gathered to date from imaging experiments on space shuttle suggest the glow is a continuum (within 34 A resolution); the continuum shape is such that the peak is near 7000 X decreasing to the blue and red, and the average molecular travel leading to emission after leaving the surface is 20 cm (assuming isotropic scattering from the surface). Emission continuum is rare in molecular systems but the measured spectrum does resemble the laboratory spectrum of NO, (B,) recombination continuum. The thickness of the observed emission is consistent with the NO2 hypothesis given an exit velocity of ~2.5 km/sec (1.3 eV) which leaves ~3.7 eV of ramming OI energy available for unbonding the recombined NO, from the surface. The NO, is formed in a 3-body recombination of OI + NO + [M] = NO, + [M], where OI originates from the atmosphere and NO is chemically formed on the surface from atmospheric NI and OI. The spacecraft surface then acts as the [M] for the reaction. Evidence exists from orbital mass spectrometer data that the NO and NO, chemistry described in this process does occur on surfaces of spectrometer orifices in orbit. Surface temperature effects are likely a factor in the NO sticking efficiency and, therefore, glow intensities.

Background

The AE-E satellite was equipped with a Visual Airglow Experiment (VAE) which observed atomic and molecular features in the Earth's airglow layer. Backgrounds in the photometer filter channels were found to have a variability with ram angle. This recognition of a ram background in the AE instrument was first cited by Torr et al. [1977]. These data were reported by Yee and Abreu [1982, 1983]. The data displayed a detectable level of luminosity in the near UV channels of the instrument (3371 Å), with increasing luminosity towards the red wavelengths (7320 X). The background in all filter channels, when plotted, described a bright ram source, increasing in brightness toward the red wavelengths. The analysis presented suggested the glow extended well away from the spacecraft alluding to the probability that the emitter is a metastable. OH Meinel bands were reported as being a likely candidate species for emission, since the general red character and emission lifetime seemed to fit the evidence. The Yee and Abreu [1982] analysis had found a strong correlation between the ram emission intensity and altitude. The emission intensity closely followed the atomic oxygen scale height above 160 km altitude. Atomic oxygen then is

N86-13241

the probable aeronomical constituent to be a chemical catalyst for whatever process is occurring. Slanger [1983] was among the first to report the OH hypothesis. Langhoff et al. [1983] discussed the simplification of OH to the infrared glow spectrum implied by OH

chemistry possibilities.

The DE-B spacecraft was equipped with a high resolution Fabry-Perot Interferometer (FPI). In this instrument, a 7320 Å filter was utilized in series with the Fabry-Perot etalon. Abreu et al. [1983] reported on the background with ram effect associated with this channel. A ram glow was reported and the deduced etalon spectrum showed similarity with the OH spectrum observed in nightglow from the atmospheric limb. The available evidence from these two spacecraft seems to favor the OH hypothesis for the observed glows.

Glow observations have been reported by a number of investigators from shuttle missions STS -3, -5, -8 and -9. Banks et al. [1983] reported glow from Orbiter television and still camera pictures around aft spacecraft surfaces while documenting glows associated with an electron accelerator experiment on STS-3. Mende [1983] and Mende et al. [1983,1984a,b]have documented ram glows associated with STS -5, -8, and 9 using an intensified camera. On the later missions (STS-8 and -9), objective grating imagery of spacecraft glow from the vertical stabilizer depicted a red stuctureless glow [Mende et al., 1984b]. The special resolution is on the order of 150 Å. On the STS-8 mission it was observed that glows from surface samples including aluminum, kapton, and black chemglaze (a polyurethane black paint typically used in low light level detection instrument baffles) were not equally bright. The surface characteristic and/or the material makeup clearly was shown to affect the glow brightness.

High spectral measurements of the ISO spectrometer on Spacelab 1 show the presence of a red dominated glow [Torr and Torr, 1984]. There are a number of observed emission features which may be part of the natural aurora airglow background environment and therefore may not be part of

the shuttle glow.

There is a proposed plasma process for glow production [Papadopoulos, 1983] which involves a two-stream instability between incoming ram and reflected ions. The ion instability sets up an electrostatic wave, which in turn heats the ambient electrons. The pumped-up electrons can in turn excite in situ and ramming constituents. Pumping the electrons to 20+ eV will allow e + X reactions. The energy is sufficient to excite N₂ to 2nd positive, and possibly ionize to 1st negative. A lot of UV emissions could arise with this process whereas the chemical processes postulated are energetically limited to be red and infrared emitters. N₂ first negative (1,0) at 3914 X and N₂ 2nd positive band at 3371 X are spectral features expected for this physical process. Detailed calculations have been made by Kofsky and Barrett [1983] regarding the ion instabilities and likely excitation emissions.

Green [1984] recently reviewed the ram glow data and theory for the shuttle environment. The review described the two classes of mechanisms, one being molecular emission from surface collisions and another due to the plasma critical velocity effect. In his discussions, vibrationally excited CO, OH or electronically excited N₂ were postulated as most likely candidates and chemically plausible with the evicence at hand.

More recently, shuttle glow spectrum was reported from STS 41-D with 34 A resolution by Mende et al. [1984c] and Swenson et al. [1985]. These data show the shuttle ram glow to be an emission continuum within the instrument resolution.

The current evidence strongly suggests the glow associated with the ramming atmosphere is a result of NO₂ in recombination [Swenson et al., 1985]. The natural atmosphere is reacting with the 8 km/sec vehicle to produce the phenomenon. The purpose of this presentation is to review the evidence and our current interpretation of the physical processes leading to the glow.

NO, Recombination Chemistry

The picture of spacecraft glow that has evolved includes the optical observations from the space shuttle and Explorer series satellites. we have recently assembled a theory that's consistent with the observations of the shuttle glow spectrum. the theory basically involves the fact that NO forms and sticks on orbiting surfaces (more efficiently on cold ones). NO will react very quickly in 3-body recombination with OI to form NO2. The surface monolayer of NO is exposed to fast atmospheric OI on ram spacecraft surfaces. Since NO2 forms with ramming OI, the 5 ev OI also contains enough energy to unbond the formed NO2 from the surface. NO2 leaving the surface at 2.3 km/sec can account for the observed e-fold in the stand-off luminous glow from the space shuttle. The bottom part of Figure 1 shows the OI interacting with surface sticking NO to form NO2. The excited NO2 which exits the surface gives the red glow.

Wall catalytic formation of NO was observed by Reeves et al. [1960] with laboratory experiments involving NI and OI. Their experiments showed that N(S) + O(P) = NO(B π) forms on the wall and the NO gas phase is formed followed by emission, i.e., NO(B π) = NO(X π) + h ν (beta bands). In their experiments, emission from the excited gas product coming off the wall was observed.

Spectrum of Shuttle Glow

An experiment was operated on several space shuttle missions to provide spatial and spectral distributions of the ram glow associated with the space shuttle Orbiter. The most recent data featured resolved spectrum and imagery of the glow with spectroscopic resolution of 34 Å FWHM between 4000 Å and 8000 Å [Swenson et al., 1985]. The spectrum of the glow on the shuttle tail pod could be clearly separated from reflected light from the Orbiter. The spectrum was taken at 290 km altitude from the ram surface. The spectrum noise was dominated by the ion scintillation in the image intensifier which produces a grain over the entire image of the 30-sec exposure.

In Figure 2, the spectrum from STS 41-D is plotted and compared with laboratory spectrum of Fontijn et al. [1964] and Paulson et al. [1970]. The laboratory spectrum was produced from 3-body recombination of NO+OI+(M) = NO₂+(M). Continuum emission is not common in molecular systems. NO₂ certainly has the ingredients of composition from the ambient source to be the candidate emitter. The spectrum isn't a perfect fit to the laboratory spectrum by any means, but we attribute this to the temperature at which the spacecraft reaction is taking place as opposed to the laboratory experiments. The laboratory spectrum is typically formed with a recombinant temperature of ~300 K whereas the 5 eV ramming OI characterizes a 60,000 K effective recombinant temperature.

It is well established that NO2 can take on a number of spectral

shapes dependent on the recombinant species and the available internal energy of the recombinant such as found with 03 (see Figure 3). Figure 3 shows the laboratory recomination spectrum for NO2 for 3-body curve as well as the spectrum for 2-body recombination with NO and 03 where the 03 is vibrationally excited to different states. The laboratory spectra, again, are all-low temperature spectra. For comparison, we have shown the measured STS 41-D spectrum, which we contend is spectrally different as a result of the ramming OI energy. Golomb and Brown [1975] found laboratory evidence for thermal effects on the spectral shape of the OI recombination spectrum at low temperature (200-350 K) range. They found the intensity of the blue portion of the continuum to decrease with increasing temperature.

Mass Spectrometer Evidence

What evidence do we have that NO forms and sticks on orbiting surfaces in the thermosphere? The best evidence is that reported by the mass spectrometer investigations and what has been observed in NI, NO, and NO2. Engebretson and Mauersberger [1979] described in detail the response of NO with respect to thermal and orbital parameters for their instrument on AE-C satellite. It's been known since mass spectrometers first flew that most of the atmospheric NI entering the mass spectrometer orifice converts to NO with wall collisions and in fact, a large percentage of the NI signal is deduced from the NO (mass 30) signal in the instruments (see Engebretson and Mauersberger, [1979] and the references cited therein). It's been well established in laboratory experiments that the NI and OI wall reaction form the gas phase NO. Engebretson and Mauersberger [1979] then reported a most interesting phenomenon. They reported that NO was absorbed on the spectrometer walls (with efficiencies higher at low wall temperatures). The top part of the chemistry shown in Figure 1 reflects what has been observed in the mass spectrometer orifice. They observed the gas phase NO, and from temperature and altitude geometry, they deduced that a significant amount of NO was sticking to the wall. The UV emission from surface catalyzed NO in the gas phase has been observed in the laboratory and should be observable on an orbiting ram surface with the proper instrument [Reeves et al., 1960]. Only the NO beta bands are observed in the laboratory (temperatures ~300 K) surface-catalyzed excitation type experiments. What will happen on the spacecraft surface with OI at 5 eV producing the NO is uncertain.

What about the link between the top (NO) chemistry and the bottom (NO₂) chemistry depicted in Figure 1? Engebretson and Mauersberger also noted NO₂ formed in the orifice (most efficienctly at low wall temperatures). In fact, Engebretson (private communication) indicates that this NO₂ is observed in the open ion source configuration of the type used with AE-C but is not as prevalent in closed ion source instruments. This implies that without a source of energetic OI, the NO+OI = NO₂ (gas phase) chemistry does not take place or that wall collision chemistry acts to destroy the NO₂ after it does form.

Surface temperature has been found to be a very important parameter in the effective surface sticking efficiency and NO₂ formation rate in the studies performed by Engebretson and Mauersberger [1979]. The colder surfaces are more efficient for NO to stick, and therefore we could expect a more intense NO₂ emission but lesser NO beta band emission

since it is the gas phase NO which emits the beta bands. The warmer surfaces then would tend to emit less NO_2 (red) emission, but more NO (blue beta band) emission.

Source Continuity Considerations

Does the source availability account for the luminosity observed in the red glow? At 250 km we observe "6 kilorayleighs of visible glow when viewing normal to a ram surface (interpreted from e-folding considerations of spacecraft tile surface glows). in other words, "6.109 photons/cm² sec are observed. The atomic nitrogen population of "107 [Engebretson et al., 1980] with a spacecraft velocity of 8.105 cm/sec yields a nitrogen flux of 8.1012 to the surface. The efficiency of producing an NO₂ recombination photon would necessarily be "1%. This is not unreasonable in NI,OI chemistry. Engebretson and Mauersberger [1979] reported a wall loss probability of NI at >10% per wall collision. If we assume that loss always results in an NO production, an NO monolayer sticking to the surface would be very quickly replaced after an NO molecule is lost from the surface due to ramming OI.

Lifetime and Energy Considerations

What about lifetime and e-folding considerations in the observed luminosity? The lifetime of NO, in flourescence is ~70 microseconds according to Schwartz and Johnston [1969]. It was previously reported by Yee and Dalgarno [1983] that the effective e-folding distance an average molecule travels prior to emission is ~20 cm. (This has been reverified on several STS-9 images at Lockheed.) If we assume x = t*v [Yee and Dalgarno, 1983], where x = 20 cm, we would infer that the exit velocity from the surface would be ~2.5 km/sec if NO2 were the emitter. This corresponds to an effective exit temperature of 10,000 K (1.28 eV). This is ~25% the ram energy of QI; considerably higher than the expected surface temperature of near 300 K. In the process of producing the NO₂ then, total thermal accommodation of the OI does not occur. In summary, the lifetime and energy considerations are reasonable with NO, being the emitter. That leaves ~3.7 eV of the initial ramming OI for unbonding the NO, from the surface. We expect from the experimental observations of NO and NO₂ variations observed between surface temperatures of 300° K and 400° K by Engebretson and Mauersberger [1979] that the surface bond energy for NO is very small.

Other Considerations and Summary

The mass spectrometer orifice modulation of a surface monolayer of NO fits with the glow observations in principle. If NO can form on an instrument surface, it can also form on other surfaces including the spacecraft skin. It is well understood that the surfaces of the mass spectrometer orifice and that of the shuttle surface are very different. To date, we only have spectrum of the shuttle glow since glows of other emitting material samples have been from small areas at high altitudes and consequently weak to the observing instruments [Mende et al., 1984a,c]. The observed surface samples have been a mixture of insulator

and conductor type materials, from all of which a glow emanates. When observing the stand-off glows from these small samples, we do note the e-folding distance is about the same as it is on the Orbiter skin. This suggests to us that the glow is originating from the same chemistry as we observe on the Orbiter. It is this link that lends further credibility to the link between the chemistry observed in the mass spectrometer orifice [Engebretson and Mauersberger, 1979] and that postulated as shuttle ram surface chemistry here [Swenson et al., 1985].

Some further comments regarding the spacecraft glow are warranted.

1. Conjecture has been that a "dirty" space shuttle is responsible for the glow and that because it is dirty, that type of vehicle is not good for remote studies. We notice that whether data are taken on day 1 or day 9 of a space shuttle mission, the glow intensity seems to be about the same. On the contrary then, the phenomenon is a natural one characteristic of all spacecraft. The edge-on view of between 2 and 12 meters of stabilizer and ohms pod surface presents a lot of area to produce glow for cabin or Spacelab module instruments such as the handheld imager. The subtleties of surface temperature and surface type certainly influence the glow intensity. Our theory supports ram glow as a natural phenomenon and by nailing down the physical process, we can extend models to other spacecraft.

2. Not all materials glow to the same degree. However, when observing the stand-off distance of other materials, we note that the e-folding distance of intensity from the surface is about the same for all. This supports the same chemistry cited in Figure 1 as likely happening on all surfaces, but the NO sticking efficiency may be important in glow production. Material type is a key to minimizing

the effect.

3. The glow originating from AE-C, we believe, results from the same chemistry we have cited as being responsible for the glow on the space shuttle. The confusion in comparison, especially from the difference in intensity as a function of angle from the ram direction, very likely relates to the fact that a large portion of the AE-C glow was originating from the instrument baffle as well as from the surrounding spacecraft surface. The baffle glow was not included in the original analysis.

There are certainly some puzzles reported in the literature that do not fit our hypothesis. Torr and Torr [1984] report N2 lst Pos spectrum in apparent ram data in a shuttle-based spectrometer. It is possible that their measurement is contaminated by dayglow or some other natural phenomenon since the experiment was operated during a daylit orbit. It cannot be dismissed however that they possibly observed a baffle or extended ram glow. The Dynamics Explorer B data in the Fabry-Perot channel suggests structure in a narrow region of spectrum of that satellite [Abreu et al., 1983]. Some of the structure was consistent with OH emission spectrum and some was not. The ram glow we attribute to NO₂ in recombination is the near surface glow which e-folds 15-20 cm from the surface.

References

Abreu, V. J., W. R. Skinner, P. B. Hays, and J. H. Yee, Optical effect of spacecraft-environment interaction: Spectrometric observations by DE-B satellite, AIAA-83-CP838, AIAA Shuttle Environment and Operations Meeting, 178, 1983.

Banks, P. M., P. R. Williamson, and W. J. Raitt, Space shuttle glow observations, Geophys. Res. Lett., 10, 118, 1983.

Engebretson, M. J., and K. Mauersberger, The impact of gas-surface interactions on mass spectrometric measurements of atomic nitrogen, J. Geophys. Res., 84, 839, 1979.

Engebretson, M. J., J. A. Defreese, and K. Mauersberger, Diurnal, seasonal, and nighttime variations of atomic nitrogen in the equatorial thermosphere, J. Geophys. Res., 85, 2165, 1980.

Fontijn, A., C. B. Heyer, and H. I. Schiff, Absolute quantum yield measurements of the NO-O reaction and its use as a standard for chemiluminescent reactions, J. Chem. Phys., 40, 64, 1964.

Golomb, D., and J. H. Brown, The temperature dependence of the NO-O chemiluminous recombination, J. Chem. Phys., 63, 5246, 1975.

Greaves, J. C., and D. Garvin, Chemically induced molecular excitation: Excitation spectrum of the nitric oxide-ozone system, J. Chem. Phys., 30, 348, 1959.

Green, B. D., Atomic recombination into excited molecular-A possible mechanism for shuttle glow, Geophys. Res. Lett., 11, 576, 1984.

Kenner, R. D., and E. A. Ogryzlo, Orange chemiluminescence from NO2, J. Chem. Phys., 80, 1, 1984.

Kofsky, I.L., and J. L. Barrett, Optical emissions resulting from plasma interactions near windward directed spacecraft surfaces, AIAA-83-CP838, AIAA Shuttle Environment and Operations Meeting, 198, 1983.

Langhoff, S. R., R. L. Jaffee, J. H. Yee, and A. Dalgarno, The surface glow of the Atmospheric Explorer C and E Satellites, Geophys. Res. Lett., 10, 896, 1983.

Mende, S. B., Measurement of vehicle glow on the space shuttle, AIAA-83-CP838, AIAA Shuttle Environment and Operations Meeting, 79,

Mende, S. B., O. K. Garriott, and P. M. Banks, Observations of optical emissions on STS-4, Geophys. Res. Lett., 10, 122, 1983.

Mende, S. B., P. M. Banks, and D. A. Klingelsmith, III, Observation of orbiting vehicle induced luminosities on the STS-8 mission, Geophys. Res. Lett., 11, 527, 1984a.

Mende, S. B., G. R. Swenson, and K. S. Clifton, Preliminary results of the Atmospheric Emissions Photometric Imaging Experiment (AEPI) on Spacelab 1, Science, 225, 191, 1984b.

Mende, S. B., G. R. Swenson, K. S. Clifton, R. Gause, L. Leger, and O. K. Garriott, Space vehicle glow measurements on STS 41D, Submitted to J. Spacecraft and Rockets, 1984c.

Papadopoulos, K., On the shuttle glow, SAI Report 84-147-WA, 1983.

Paulsen, D. E., W. F. Sheridan, and R. E. Huffman, Thermal and recombination emission of NO2, J. Chem. Phys., 53, 647, 1970.
Reeves, R. R., G. Manella, and P. Harteck, Formation of excited NO and

No by wall catalysis, J. Chem. Phys., 32, 946, 1960.

Schwartz, S. E., and H. S. Johnston, Kinetics of nitrogen dioxide fluorescence, J. Chem. Phys., 51, 1286, 1969.

Slanger, T. G., Conjectures on the origin of the surface glow of space vehicles, Geophys. Res. Lett., 10, 130, 1983.

Swenson, G. R., S. B. Mende, and K. S. Clifton, Ram vehicle glow spectrum: Implication of NO2 recombination continuum, Geophys. Res. Lett., 12, 97, 1985.

Torr, M. R., P. B. Hays, B. C. Kennedy and J. C. G. Walker, Intercalibration of airglow observations with the Atmospheric Explorer Satellites, Planet. Space Sci., 25, 173, 1977.

Torr, M. R., and D. G. Torr, Atmospheric spectral imaging, Science, 225,

Vanpee, M., K. D. Hill, and W. R. Kineyko, AIAA J. (Am. Inst. Aeronaut. Astronaut.), 9, 135, 1971.

Yee, J. H., and A. Dalgarno, Radiative lifetime analysis of the spacecraft optical glows, AIAA-83-CP838, AIAA Shuttle Environment and Operations Meeting, 191, 1983.

Yee, J. H., and V. J. Abreu, Optical contamination on the Atmospheric Explorer-E satellite, Proceedings of the SPIE, 338, 120, 1982.

Yee, J. H., and V. J. Abreu, Visible glow induced by spacecraft-environment interaction, Geophys. Res. Lett., 10, 126, 1983.

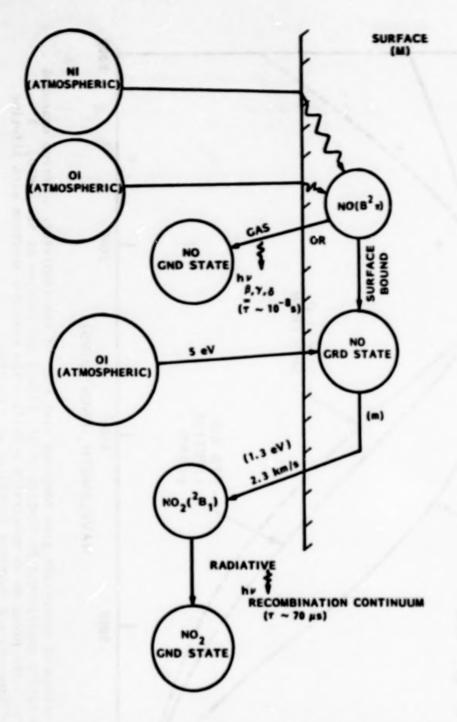
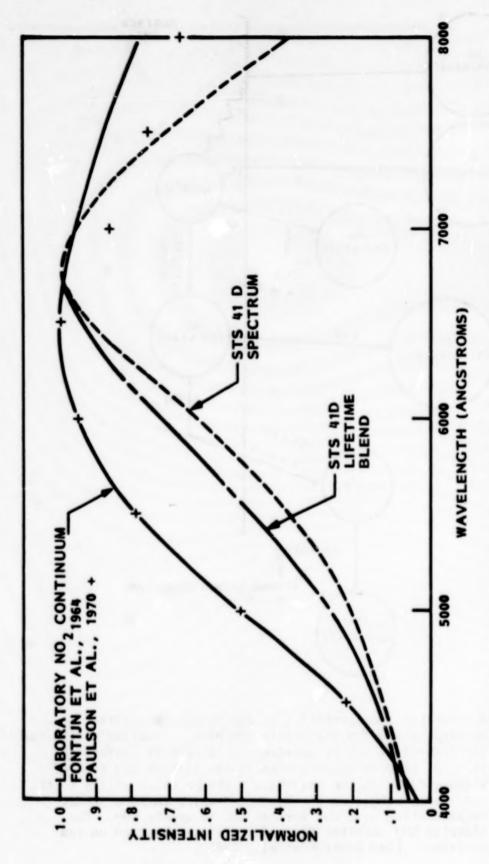
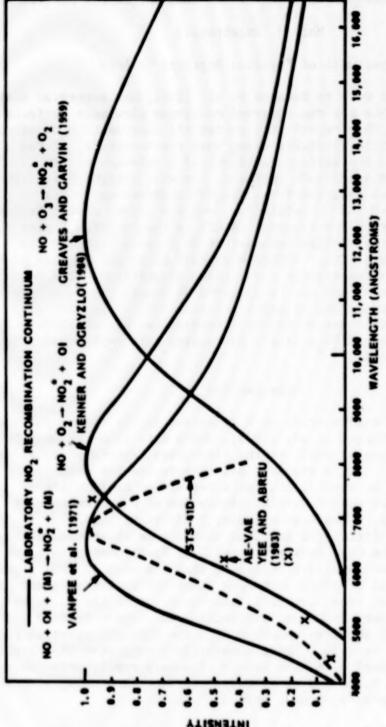


Fig. 1. A schematic representation of the chemistry believed to be responsible for spacecraft ram glow. Starting at the top, the ramming OI and NI intercept a spacecraft surface and form NO, some of which sticks to the surface and some of which escapes in the gas phase. The NO which sticks to the surface is subjected to ramming OI which forms a 3-body recombination with the surface [M] to create NO2. The escaping NO2 radiates the red continuum observed on ram surfaces. [See Swenson et al., 1985.]



The spectrum of spacecraft glow compared with that of the laboratory spectrum measured in laboratory experiments by Fontijn et al. [1964] and Paulsen et al. [1970]. A spectral blend produced by spectrally e-folding the measured spectrum with lifetime data of Schwartz and Johnston [1969] is also plotted.



The NO₂ recombination spectrum for 3-body recombination [Vanpee et al., 1971], and for 2-body recombination with upper state 03 [Kenner and Ogryzlo, 1984], as well as vibrationally excited 03 [Greaves and Garvin, 1959]. The STS 41-D plotted [Yee and Abreu, 1983]. It is noted that the laboratory spectrum of spectrum is plotted as a dashed curve and the Atmosphere Explorer data are recombination can take on a large range of spectral shape dependent on the state of the recombinant constituents.

AE AND DE MASS SPECTROMETER OBSERVATIONS RELEVANT TO THE SHUTTLE GLOW

Mark J. Engebretson

Department of Physics, Augsburg College

Abstract. Recent work by Swenson et al. [1985] has suggested that NO, may be responsible for the observed continuum glow near surfaces of the space shuttle. This report will review the observations of atomic nitrogen (N) at shuttle altitudes using mass spectrometers, giving special attention to the surface reactions of N relevant to the production of NO, on spacecraft surfaces. We will present data from two semi-open source mass spectrometers, the OSS instruments on the Atmosphere Explorer-C and -D satellites, and the closed source Neutral Atmospheric Composition Spectrometer (NACS) on the Dynamics Explorer-2 satellite, to show the similar behavior of NO in each case and the contrasting behavior of NO. Although signals of NO and NO, are highly dependent on surface temperature and surface composition, it appears that direct exposure of ion source surfaces to rammed gas is a necessary condition for the production of large amounts of NO2. We will also present evidence that elevated surface temperatures can significantly reduce the production of NO,, likely by causing more rapid desorption of NO from these surfaces.

Introduction

The first comprehensive study of N densities in the thermosphere was presented by Mauersberger et al. [1975], using data from the Open Source Neutral Mass Spectrometer (OSS) on the Atmosphere Explorer-C satellite [Nier et al., 1973]. It is standard practice to use the mass spectrometer signal of mass 32 (0,) as a measure of ambient atomic oxygen because of ion source surface adsorption of O and subsequent recombination into 0, (see, for example, Hedin et al., 1973). A similar process was discovered to occur in the case of atomic nitrogen: observations from the Open Source Neutral Mass Spectrometer (OSS) on the Atmosphere Explorer-C satellite indicated that the mass 30 (NO) signal and the direct signal of atomic nitrogen (mass 14) exhibited identical variations with local time, latitude, and season, once the relatively large source background of NO was subtracted out. Approximately 95% of the N atoms detected appeared as NO or NO,, the dominant spectral peak of which is also at mass 30. These observations suggested that highly reactive N atoms entering the ion source of a mass spectrometer were likely to adsorb on metal surfaces and/or to react chemically with the dominant adsorbed species, atomic oxygen.

A recent study of data from the Neutral Atmospheric Composition Spectrometer (NACS) on the Dynamics Explorer-2 satellite [Carignan et al., 1981] has confirmed that with this instrument also the mass spectrometer signal of NO provides a quantitative measure of thermospheric N densities [Engebretson and Nelson, 1985].

Temperature Dependence

As part of the analysis of NO signals it was found that the level of background NO in the mass spectrometer ion source could be correlated with the temperature of the ion source walls. When data were taken on successive orbits, the background level of mass 30 decreased significantly after the first orbit, reaching stable levels on the third and subsequent orbits, but reverting to earlier levels after one or more orbits of experiment inactivity.

Shown in Figures 1 and 2 are logarithmic plots of source densities of mass 30 (NO), 40 (Ar), 14 (a product of electron bomberdment of N₂), and 4 (He) as a function of time for two spinning orbits, 1630 and 1632, run November 21, 1981. The NACS instrument was off during orbit 1629, but on during successive perigee passes during orbits 1630-1633. Note that at the beginning of orbit 1630 the mass 30 background was nearly 8 x 10 cm⁻³, while on orbit 1632 it was a factor of 10 lower at comparable altitudes. All other signals shown appear to be nearly identical on both orbits.

This contrast between "cold" and "warm" orbits, with ion source surface temperatures of approximately 300 K and 450 K, respectively, is characteristic of data from each of the satellite mass spectrometers studied here. Table 1 shows representative data for masses 30 and 46 from elliptical orbit passes of AE-C and DE-2 for such "cold" and "warm" orbits. In each case there are significantly lower signals of masses 30 and 46 on the downleg of these orbits when ion source surfaces are warmed up. Near the end of each pass, however, there is considerably less variation between "cold" and "warm" passes, consistent with the closer agreement in surface temperature near the end of each pass.

It is also clear in Table 1 that the abundance of NO₂ on the downleg of an orbit is dependent on temperature effects. Data from both AE-C and DE-2 instruments indicate that NO₂ signals are even more sensitive than NO signals to variations in surface temperature. Figures 3 and 4 show data from the OSS mass spectrometer on AE-C for two orbits specially programmed for a study of the variation of NO and NO₂ with surface temperature history. During this period in late 1975 the AE-C satellite was operated only one day a week, for two full circular orbit passes at 310 km altitude. Orbit 8530 was run after the usual 30-min OSS warmup. Orbit 8536 was preceded by a 4-hour warmup, thus simulating operations during two previous perigee passes in elliptical orbit operations.

The sharp early morning rise characteristic of thermospheric N densities is evident in Figure 3, a plot of net mass 30 signals from orbit 8536, but is obscured in the data from the beginning of orbit 8530 (Figure 4). Comparison of the two figures indicates that NO₂ accounts for most of the excess mass 30 signal observed on orbit 8530 (NO₂ produces 2.7 times as much signal at mass 30 as at mass 46). It is also important to note that although the ratio of NO₂ to NO appears to drop throughout orbit 8530, indicating the gradual desorption of an adsorbed species, the spin modulation evident on both orbits suggests that much of the NO₂ observed must be attributed to a relatively fast production process.

Ram Effects

The method of using mass 30 signals to measure thermospheric N worked successfully with other satellite mass spectrometers as well. Signals of masses 30 and 14 on the AE-D OSS instrument also were proportional, and the use of a gold-plated ion source on the AE-D instrument appeared to reduce considerably the dependence of the net NO signal on surface temperature effects. The NACS instrument on DE-2 also used a gold-plated ion source, but the closed source design of this instrument prohibited direct access of any molecules or atoms to the ionization chamber, hence excluding any direct measurements of N atoms.

A comparison of NO and NO, observations from the AE-C, AE-D, and DE-2 mass spectrometers is presented in Table 2. The ion source surfaces of the AE-C instrument are made of nichrome, while those of the AE-D and DE-2 instruments are gold plated. The AE-C and -D ion sources are of an open source design, with ram acceptance angles of 30 and 12 degrees, respectively, while the DE-2 ion source is closed, necessitating typically 100 wall collisions and complete thermal accommodation of all gas molecules before they will be analyzed by the mass spectrometer. Table 2 shows that the open source instruments produce large amounts of NO, with the fraction increasing as the satellite proceeds toward higher altitudes. The AE-D data at 700 km indicate nearly 100% of the mass 30 signal is due to NO. Although the DE-2 NACS instrument also uses a gold-plated source, the DE-2 data indicate the reverse effect: the fraction of NO, decreases to less than 3% as the satellite passes toward higher altitude. We attribute this striking difference to the closed source geometry of the DE-2 instrument, and infer that the thermal accommodation of the ramming gas (much of which is thermospheric 0) significantly reduces the probability of converting adsorbed NO into NO2.

Further analysis of the surface chemical processes reported here is contained in papers by Engebretson and Mauersberger [1979] for the Open Source Neutral Mass Spectrometer (OSS) instruments on the Atmosphere Explorer satellites, and Engebretson and Nelson [1985] for the Neutral Atmospheric Composition Spectrometer (NACS) instrument on the Dynamics Explorer-2 satellite.

Summary of Observations

Data from three satellite mass spectrometers have shown that odd nitrogen molecules are formed in abundance on the surfaces of mass spectrometer ion sources as a result of the impact of thermospheric 0 and N atoms. The adsorption and desorption of NO and NO, from these surfaces appears to vary considerably with surface temperature. Heating of ion source surfaces appears to significantly reduce the concentration of these species, especially NO,. Comparison of data from open and closed source instruments with gold-plated surfaces indicates that adsorbed NO is much more likely to be converted to NO, by ramming 0 atoms than by less energetic (thermalized) 0 atoms.

Implications for Shuttle Glow

The large mass spectrometer background and small spin modulation we

have observed suggest that NO and NO will likely form long-lasting monolayers on various satellite and/or shuttle surface materials. Production of NO is likely to be greatly enhanced on cold surfaces exposed to ramming thermospheric gas. Although our experience is clearly limited to two metallic surfaces, we consider it likely that the simple gas-surface reactions reported here will take place on other spacecraft surfaces as well. The optical observations and modeling of Swenson et al. [1985] and the mass spectrometric observations reported here make NO a likely candidate for the source of the glow observed near the ram-oriented surfaces of various spacecraft.

It is intriguing to consider the use of a mass spectrometer to verify the presence of NO and NO, on surfaces other than those within the mass spectrometer's ion source. Although the large signal of odd nitrogen from mass spectrometer ion source surfaces makes this a difficult task, a beam inlet system, which is essentially an extension of the open source geometry used in the Atmosphere Explorer satellite mass spectrometers, may provide a feasible way to complement existing optical detection systems.

Acknowledgments. This research was supported by the Dynamics Explorer Guest Investigator Program through NASA Grant NAG 5-349 to Augsburg College.

References

Carignan, G. R., B. P. Block, J. C. Maurer, A. E. Hedin, C. A. Reber, and N. W. Spencer, The neutral mass spectrometer on Dynamics Explorer B, Space Sci. Instrum., 5, 429-441, 1981.

Engebretson, M. J., and K. Mauersberger, The impact of gas-surface interactions on mass spectrometric measurements of atomic nitrogen, J. Geophys. Res., 84, 839-844, 1979.

Engebretson, M. J., and J. T. Nelson, Atomic nitrogen densities near the polar cusp, Journal of Geophysical Research, in press, 1985.

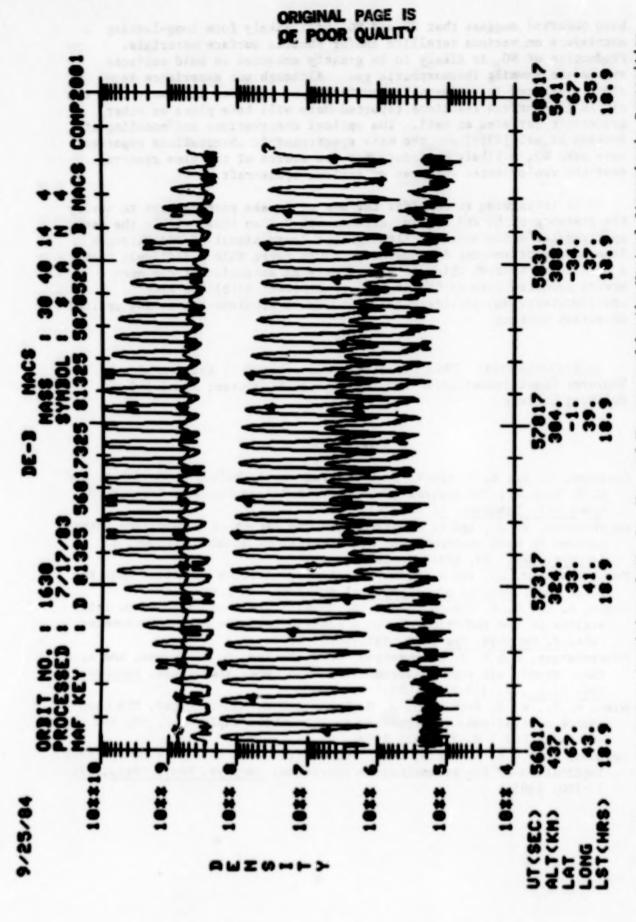
Hedin, A. E., B. B. Hinton, and G. A. Schmitt, Role of gas-surface interactions in the reduction of Ogo 6 neutral particle mass spectrometer data, J. Geophys. Res., 78, 4651-4668, 1973.

Mauersberger, K., M. J. Engebretson, W. E. Potter, D. C. Kayser, and A. O. Nier, Atomic nitrogen measurements in the upper atmosphere, Geophys. Res. Lett., 2, 337-340, 1975.

Nier, A. O., W. E. Potter, D. R. Hickman, and K. Mauersberger, The opensource neutral-mass spectrometer on Atmosphere Explorer-C, -D, and -E. Padio Sci., 8, 271-281, 1973.

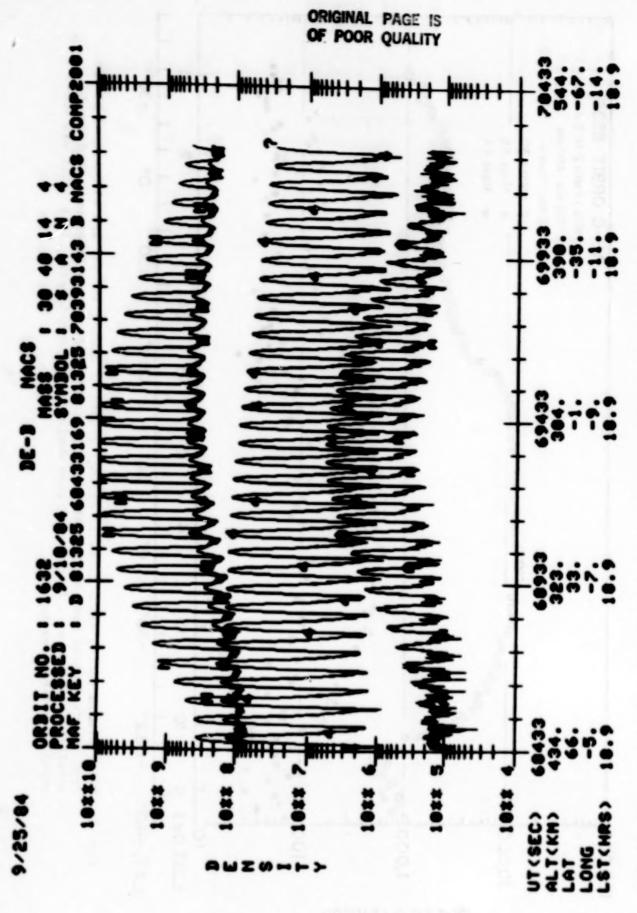
-E, Radio Sci., 8, 271-281, 1973.

Swenson, G. R., S. B. Mende, and K. S. Clifton, Ram vehicle glow spectrum: Implication of NO₂ recombination continuum, Geophys. Res., Lett., 12, 97-100, 1985.



49

Fig. 1. Ion source number densities of NO, Ar, N2, and He measured by the Neutral Atmospheric Composition Spectrometer (NACS) on orbit 1630 of the Dynamics Explorer-2 satellite, plotted as a function of The NACS instrument was off during the previous orbit. universal time (UT).



Ion source number densities of NO, Ar, N2, and He for orbit 1632 of DE-2, as in Figure 1. The NACS instrument was on for two successive perigee passes prior to this orbit. Fig. 2.

Net (forward facing minus backward facing) counts of masses 30, 44, and 46 measured by the satellite, plotted as a function of time during a full orbit pass. This orbit was pre-Open Source Neutral Mass Spectrometer (OSS) on orbit 8536 of the Atmosphere Explorer-C ceded by a 4-hour warmup. Fig. 3.

L.S.T. (hr.)

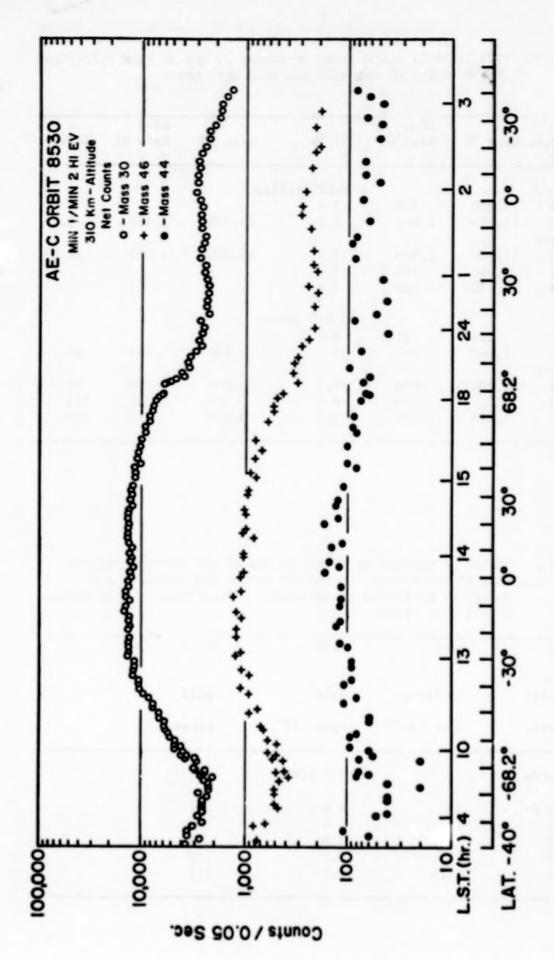
- 4

80

Counts / 0.05 Sec.

000'000

0000



Net counts of masses 30, 44, and 46 for orbit 8530 of AE-C, as in Figure 3. This orbit was preceded by a standard 30-min warmup.

TABLE 1. TYPICAL ORBIT COUNT RATES OF MASSES 30 AND 46 FROM ELLIPTICAL DESPUN ORBITS OF THE AE-C AND DE-2 SATELLITES

The state of the s

Altitud	e Mass 30	AE-C Nass 46	30/46	Mass 30	DE-2 Mass 46	30/46
		. 1	"COLD" or	bits	73	70
500	1,800	500	3.6			
300	17,500	2,000	8.8	29,200	3,130	9.3
Perigee						
300	17,000	1,000	17.0	12,900	1,200	10.8
500	2,850	310	9.2			
700	1,450	260	5.6			
			"WARM" or	bits		
500	320	36	8.9			
300	7.800	430	18.1	9,900	161	61.7
Perigee						
300	12,400	670	18.5	13,800	330	41.3
500	2,000	230	8.7	3,500	30	115
700	1,060	200	5.3	2,050	15	137

TABLE 2. RATIOS OF SIGNALS OF MASSES 30 AND 46 FOR THREE SATELLITE MASS SPECTROMETERS. INTENSITY RATIOS ARE DETERMINED AT THE GIVEN ALTITUDES ON THE UPLEG OF ELLIPTICAL ORBITS UNDER SUNLIT CONDITIONS.

	AE-C	AE-D	DE-2	
Source material	nichrome	gold	gold	
Geometry	open (30°)	open (12°)	closed	
Altitude		(30) / N(46)	9	
300 km	18	4.6	41	
400	13	3.6	56	
500	8.7	3.6	92	
600	6.6	3.5	120	
700	5.3	2.7	137	

THE ATMOSPHERE EXPLORER AND THE SHUTTLE GLOW

A. Dalgarno, J-H. Yee, and M. LeCompte

Harvard-Smithsonian Center for Astrophysics

Abstract. Recent analyses of the Atmosphere Explorer data are discussed in which it is demonstrated that the satellite glows have two components, one at high altitudes which is consistent with excitation in single collisions of atmospheric oxygen atoms with the vehicle surface and the other at low altitudes which is consistent with double collisions of nitrogen molecules. Contrary to an earlier suggestion, the low-altitude data are not consistent with single collisions of oxygen molecules.

The separation of the two components strengthens the conclusion that the high-altitude glow arises from vibrationally excited OH molecules produced by a formation mechanism that is different from that leading to the normal atmospheric OH airglow. The spectrum is consistent with association of oxygen and hydrogen atoms at sites on the surface into the vibrational levels of OH. The low-altitude glow is consistent with the Green mechanism but there are difficulties with it.

The shuttle glows are different and have the spectral appearance of emission from NO2. The characteristics of the shuttle glows and the satellite glows will be constructed and a tentative resolution of the differences in the Atmosphere Explorer and shuttle glows will be offered.

Discussion

Much detailed information about the glows resulting from the interaction of spacecraft with the atmospheric environment has been acquired from studies of the data provided by the Visible Airglow Experiment onboard the Atmosphere Explorer satellites [Hays et al., 1973]. Figure 1 illustrates the glow intensity at 732 nm as a function of altitude [Yee and Abreu 1982, 1983]. Above 160 km the intensity is directly proportional to the ambient number density [0] of atomic oxygen. Yee and Abreu [1982, 1983] suggested that the glow was produced by oxygencontaining metastable molecules released from the surface after energetic collisions with oxygen atoms and they drew attention to laboratory studies of OH, NO and NO₂ surface luminosities. The shuttle glow intensity appears to increase with diminishing altitude and may also be proportional to [0] [Banks et al., 1983; Mende et al., 1983, 1984a,b, 1985].

Yee and Abreu [1982, 1983] analyzed the variation of the glow intensity with the angle of attack and obtained a distribution $\cos^3\phi$ with some emission persisting to an angle of 120°. In laboratory studies of the dissociative absorption probability, the variation with ϕ depends upon the interacting species and the nature of the surface. A variation as $\cos^3\phi$ happens to be consistent with a one-dimensional barrier model of desorption which has received experimental support from studies of the interaction of the light molecule H₂ with Cu surfaces

N86-13243

[Balooch et al., 1974]. For the heavier molecule N_2 on a W(110) surface, in contrast, the dissociative absorption probability depends only weakly on angle [Auerbach et al., 1984] as apparently does the shuttle glow intensity [Mende et al., 1984a,b].

The efficiency with which the glow is produced on the AE satellites for each collision of an oxygen atom was found to increase during the satellite lifetimes indicating that surface processing was occurring [Yee et al., 1984]. The shuttle does not remain in orbit long enough for time-dependent effects on the luminosity to be detectable though direct shuttle-based measurements have demonstrated a substantial erosion of various materials and the glow intensity depends upon the surface material [Mende et al., 1984b, 1985].

The observation of a glow at angles greater than 90° on the AE satellites was attributed to the surface release of excited molecules with a finite radiative lifetime [Yee and Abreu, 1982, 1983]. The distribution with \$\phi\$ is consistent with a decay length of 10 m. Because the analysis did not take account of the Maxwellian velocity distribution of the impacting atoms, the derived value of 10 m should be regarded strictly as an upper limit. The corresponding radiative lifetime probably lies between 10 ms and 1 ms.

The shuttle glow can be analyzed more directly in that the glow is seen to be spatially extended. A careful analysis of the photographs of the glow yielded a decay length of 20 cm and suggested that the mechanisms of the AE and shuttle glows are different [Yee and Dalgarno, 1983, 1985].

The measured intensity ratio of the AE glow in the band passes centered at 732 nm and 656 nm is 2.15 between 170 and 175 km and 2.25 between 140 and 145 km [Yee and Abreu, 1982, 1983; Langhoff et al., 1983], close to the OH intensity ratio observed in the night airglow. Together with the inferred radiative lifetime, the similarity of the intensity ratios led Slanger [1983] to suggest vibrationally-excited OH as the molecule responsible for the AE luminosity. Further data obtained over a wavelength range extending to 280 nm [Yee and Abreu, 1983] gave a spectrum which differs from that of the airglow but Langhoff et al. [1983] showed that the OH identification could be retained by postulating OH formation through a surface association mechanism that populates all the vibrational levels at nearly uniform rate. Their model reproduced satisfactorily the shorter wavelength data but it yielded a 732 nm/656 nm intensity ratio between 5.6 and 7.4. They suggested tentatively that the discrepancy with the measured ratio of 2.15 was due to the uncertainties in the line positions of transitions originating in the high vibrational levels for which no laboratory data exist.

Additional support for the OH identification was obtained from measurements with a Fabry-Perot interferometer onboard the Dynamics Explorer DE-B satellite [Abreu et al., 1985]. Two lines were detected whose positions, corrected for the Doppler shift arising from the moving satellite, coincide with lines of OH. A third line was detected which could also be due to OH. Although persuasive, we note that the lines also coincide in position within the accuracy of the measurements with three lines of the first positive system of N2.

The spectrum of the shuttle glow [Mende et al., 1983, 1984a,b 1985] is different from the AE glow. It appears to be without structure and is very similar to the NO2 recombination continuum [Swenson et al.,

1985]. Emission from NO₂ has been the subject of many laboratory studies [Fontijn et al., 1964; Paulsen et al., 1970; Kenner and Ogryzlo, 1984; Kuwabara et al., 1984]. Swenson et al. [1985] suggested that NO, produced by the ramming N₂ and O, remains on the surface where it reacts further with the ambient oxygen atoms. A more efficient mechanism may utilize the ambient NO molecules and N atoms and N₂O may be formed as well as NO₂. The excited NO₂ molecules have a lifetime of about 80 µs at 500 nm [Schwartz and Johnston, 1969]. To be consistent with the derived spatial extent of 20 cm [Yee and Dalgarno, 1983], the NO₂ must be released with a velocity of 2.5 km s⁻¹ corresponding to a kinetic energy of about 1.4 eV.

An alternative theory of the spacecraft glow has been advanced by Papadopoulos [1984]. According to it, energetic electrons are produced by a plasma interaction and the glow is caused by electron impact excitation. The plasma phenomenon determines the spatial extent of the glow. We have extended an earlier study by Kofsky [1984] of the expected spectrum. As Kofsky [1984] pointed out, the most intense emissions appear in the ultraviolet, a region not yet observed on the space shuttle. Weaker emissions occur in the visible and infrared but the behavior of the spectrum below 600 nm is quite different from both the shuttle and the AE spectra.

The plasma mechanism leads to a glow intensity which increases with the ambient electron density. The AE glow has been analyzed. No correlation was found between its intensity and the electron density [Yee et al., 1984].

Below 160 km, the intensity of the AE glow is no longer proportional to [0] and the spectrum is different [Yee and Abreu, 1982, 1983]. Slanger [1983] remarked that the enhancement in the glow intensity above that obtained by extrapolating the contribution from atomic oxygen was directly proportional to the number density [0₂] of ambient molecular oxygen, but a more detailed study by Yee et al. [1985] of a larger data base concludes instead that the glow intensity can be represented by the expression

$$I_{\lambda} = k_0(\lambda)[0] + k_{N_2}(\lambda)[N_2]^2$$
 (1)

where $[N_2]$ is the number density of ambient molecular nitrogen. The variation as the square of $[N_2]$ could be alternatively a variation as the product of any pair of the molecules N_2 , O_2 and NO which have similar scale heights in the altitude range of the observations. A variation as $[N_2]^2$ indicates a mechanism involving the successive collisions of two molecules and is consistent with the mechanism suggested by Green [1984] for the shuttle glow. However if it is to make a significant contribution to the shuttle glow, its efficiency must be several orders of magnitude greater on the shuttle than the values derived for the AE satellites. A possible objection to the Green mechanism is the success of the ion mass spectrometric measurements of atomic nitrogen [Engebretson and Mauersberger, 1979] on the AE satellites which argues that little dissociation of N_2 occurred. If N_2 is not dissociated by impact with the surface, the shuttle glow mechanism may be modified by invoking ambient N or NO in place of the dissociated N_2 .

Table 1, reproduced from Yee et al. [1985], gives the derived relative intensities from the process involving 0 and from the process

involving N_2 . The N_2 mechanism gives rise to a spectrum decreasing rapidly in intensity at the shorter wavelengths, and its increasing importance at low altitudes is responsible for the steeper glow spectrum below 160 km. At longer wavelengths, the spectrum bears some similarity to the spectrum measured on the Spacelab 1/shuttle mission degraded to match the resolution of the AE photometer [Torr and Torr, 1985]. The spectrum resulting from the Green mechanism is not available and it is unclear how well it might reproduce the observations.

The discrepancy between the model value of the 732 nm/656 nm intensity ratio and the value corresponding to the oxygen mechanism, shown in Table 1, is substantial. It can be removed by postulating an additional source of emission in the spectral region between 600 and 700 nm.

A plausible candidate is the shuttle glow mechanism.

A microdensitometer trace of the objective grating spectrum of the glow on the tail of the shuttle STS-8 gave an intensity per unit wavelength near 700 nm of about 450 R/A corresponding to a total glow intensity of 1MR [Mende et al., 1984a]. The shuttle glow intensity is enhanced by the oblique geometry of the observations. Corrected to a direction normal to the shuttle surface, we estimate an intensity between 10 and 20 R/A. For the AE satellite the intensity is reduced further by the curvature of the satellite surface to between 5 and 10 R/A corresponding to a total of 150 R if the shuttle mechanism is operating on the AE satellite. The baffle of the AE airglow photometer extrudes 8 cm above the surface, and bearing in mind the short decay length of the shuttle glow, we estimate that of the total 150 R only 30 R would be detected. The total measured intensity is 60 R and we suggest that half the measured high-altitude glow on the AE surfaces arises from the mechanism that has been attributed to OH and half from the shuttle mechanism that has been attributed to NO2. Table 2 compares the resultant relative intensities with those measured above 160 km. The agreement is close. A more quantitative study is in progress.

We believe the OH mechanism also operates on the shuttle but is weak compared to the NO_2 mechanism in the visible. It may be detectable between 1 and 2μ if the calculations of Langhoff et al. [1983] are

appropriate.

Acknowledgments. This research was supported in part by the Air Force Geophysics Laboratory under contract F19628-88-0034, by the Aeronomy Program of the National Science Foundation under Grant ATM-84-07314, and by NASA Grant NAGW-496 to the University of Michigan.

References

Abreu, V. J., W. R. Skinner, P. B. Hays, and J-H. Yee, Optical effects of spacecraft-environment interactions: Spectrometric observations by DE-B satellite, J. Spacecraft and Rockets, 22, 177-180, 1985.

Auerbach, D. J., H. E. Pfnur, C. T. Rettner, J. E. Schlaegel, J. Lee, and R. J. Madix, Kinetic energy and angular dependence of activated dissociative absorption of N₂ on W(110): Observed insensitivity to incidence angle, J. Chem. Phys., 81, 2515-2516, 1984.

- Balooch, M., M. J. Cardillo, D. R. Miller, and R. E. Stickney, Molecular beam study of the apparent activation barrier association with the absorption and desorbtion of H on Copper, <u>Surf. Sci.</u>, <u>46</u>, 358-392, 1974.
- Banks, P. M., P. R. Williamson, and W. J. Raitt, Space Shuttle glow observation, Geophys. Res. Lett., 10, 118-121, 1983.
- Engebretson, M. J., and K. Mauersberger, The impact of gas-surface interactions on mass spectrometric measurements of atomic nitrogen, J. Geophys. Res., 84, 839-844, 1979.
- Fontijn, A., C. B. Meyer, and H. I. Schiff, Absolute quantum yield measurements of the NO-O reaction and its use as a standard for chemiluminescent reactions, J. Chem. Phys., 40, 64-70, 1964.
- Green, B. D., Atomic recombination into excited molecular nitrogen-A possible mechanism for Shuttle glow, Geophys. Res. Lett., 11, 576-579, 1984.
- Hays, P. B., G. Carignan, B. C. Kennedy, G. G. Shepherd, and J. C. G. Walker, The Visible-Airglow Experiment on Atmospheric Explorer, Radio Science, 8, 369-377, 1973.
- Kenner, R. D., and A. E. G. Ogryzlo, Orange chemiluminescence from NO₂, J. Chem. Phys., 80, 1-6, 1984.
- Kofsky, I. L., Spectroscopic consequences of Papadopoulos' discharge model of spacecraft ram glows, Radio Science, 19, 578-586, 1984.
- Kuwabara, S., K. Kuwata, I. Nishiyama, and I. Hanazaki, Acoustically oscillating emission from NO₂* produced by infrared photosensitized reaction in SF₆+NO₂, Chem. Phys. Lett., 106, 540-543, 1984.
- Langhoff, S. R., R. L. Jaffe, J-H. Yee, and A. Dalgarno, The surface glow of the Atmosphere Explorer C and E satellites, Geophys. Res. Lett., 10, 896-899, 1983.
- Mende, S. B., O. K. Garriott, and P. M. Banks, Observations of optical emissions on STS-4, Geophys. Res. Lett., 10, 122-125, 1983.
- Mende, S. G., P. M. Banks, and D. A. Klingelsmith, Observation of orbiting vehicle induced luminosities on the STS-8 mission, Geophys. Res. Lett., 11, 527-530, 1984a.
- Mende, S. B., G. R. Swenson, and K. S. Clifton, Preliminary results of the Atmospheric Emissions Photometric Imaging Experiment (AEPI) on Spacelab 1, Science, 225, 191-193, 1984b.
- Mende, S. B., G. R. Swenson, K. S. Clifton, R. Gause, L. Leger, and O. K. Garriott, Space vehicle glow measurements on STS 41-D, J. Spacecraft and Rockets, submitted, 1985.
- Papadopoulos, D., On the Shuttle glow (the plasma alternative), Radio Science, 19, 571-577, 1984.
- Paulsen, D. E., W. F. Sheridan, and R. E. Huffman, Thermal and recombination emission of NO2, J. Chem. Phys., 53, 647-658, 1970.
- Schwartz, S. E., and H. S. Johnston, Kinetics of nitrogen dioxide fluoresence, J. Chem. Phys., 51, 1286-1302, 1969.
- Slanger, T. G., Conjectures on the origin of the surface glow of space vehicles, Geophys. Res. Lett., 10, 103-132, 1983.
- Swenson, G. R., S. B. Mende, and K. S. Clifton, Ram vehicle glow spectrum: Implication of NO₂ recombination continuum, Geophys. Res. Lett., 12, 97-100, 1985.
- Torr, M., and D. G. Torr, A preliminary spectroscopic assessment of the Spacelab 1/Shuttle optical environment, <u>J. Geophys. Res.</u>, <u>90</u>, 1683-1690, 1985.

Yee, J-H., and V. J. Abreu, Optical contamination on the Atmospheric Explorer-E Satellite, SPIE Proceedings, 338, 120-129, 1982.

Yee, J-H., and V. J. Abreu, Visible glow induced by spacecraftenvironment interaction, Geophys. Res. Lett., 10, 126-129, 1983.

Yee, J-H., and A. Dalgarno, Paper AIAA-03-2660-OP, Radiative lifetime analysis of the Shuttle optical glow, Environment and Operations Meeting, 191-197, 1983.

Yee, J-H., and A. Dalgarno, Radiative lifetime analysis of the Shuttle optical glow, J. Spacecraft and Rockets, submitted, 1985.

Yee, J-H., V. J. Abreu, and A. Dalgarno, Characteristics of the spacecraft optical glow, Geophys. Res. Lett., 11, 1192-1194, 1984. Yee, J-H., V. J. Abreu, and A. Dalgarno, The Atmosphere Explorer

Yee, J-H., V. J. Abreu, and A. Dalgarno, The Atmosphere Explorer optical glow near perigee altitudes, Geophys. Res. Lett., submitted, 1985.

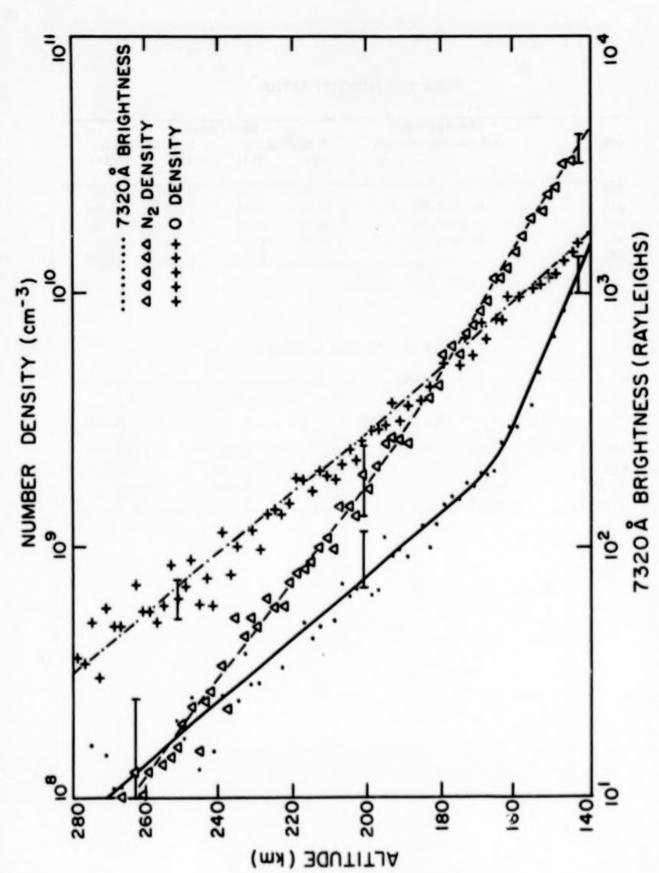


Fig. 1. The Atmosphere Explorer glow at 732 nm in Rayleighs as a function of altitude.

TABLE 1. INTENSITY RATIOS*

	Theoretical	Empirical			
(nm)	O-H recombination	O-mechanism		N2-mechanism	
		(i)	(ii)	(1)	(ii)
732	1.00	1.00	1.00	1.00	1.00
656	0.18-0.13	0.71	0.68	0.09	0.08
428	0.05-0.03	0.02	0.02	0.06	0.06
337	0.06-0.02	0.05	0.04	0.21	0.17
280		0.08	0.03	0.19	0.08

* (1) $k(\lambda)/k(732)$ (11) $\frac{k(\lambda)}{\Delta(\lambda)}$ $\frac{\lambda(732)}{\Delta(732)}$

TABLE 2. AE GLOW SPECTRUM

	OH*	NO ₂	$^{\mathrm{I}}$ _{OH} $^{+\mathrm{I}}$ _{NO2}	K _o (Yee et al.,
	(Langhoff et al., 1983)	(Swenson et al., 1985)		1985
7320 X	1.000	1.00	1.000	1.000
6563 X	0.159	1.00	0.580	0.679
4278 Å	0.030	0.05	0.040	0.021
3371 Å	0.022	-	0.012	0.036

ORBITER GLOW OBSERVATIONS AT HIGH SPECTRAL RESOLUTION

David J.W. Kendall and Richard L. Gattinger

Herzberg Institute of Astrophysics National Research Council of Canada

Edward J. Llewellyn and Ian C. McDade

Institute of Space and Atmospheric Studies University of Saskatchewan

Steven B. Mende

Lockheed Palo Alto Research Laboratory

Abstract. An experiment flown on mission STS 41-G as part of the Canadian complement of experiments was designed to obtain relatively high resolution spectra of the Orbiter glow phenomenon over limited spectral regions centered on prominent upper atmospheric emissions. Observations were carried out successfully at altitudes of 360 km and 230 km although those at the lower altitude were limited by degradation of the image intensifier. Definitive glow results were obtained at the end of a thruster firing which showed the spectrum to be a continuum at a resolution of approximately 0.4 nm centered at a wavelength of 630 nm. Results at other wavelengths in the absence of any firings strongly suggest that the Orbiter glow is a continuum throughout the spectral region 550 nm to 760 nm. A discussion is presented that considers the reaction NO + 02* as being a possible candidate for the mechanism producing the shuttle glow.

Introduction

In 1984, an opportunity arose to fly a complement of experiments onboard the shuttle to be performed by a Canadian payload specialist. One of the experiments accepted for flight was given the acronym OGLOW and consisted of an imaged intensified camera system onto which was attached a series of filters or a transmission grating spectrograph. The filters were selected to be centered on prominent atmospheric emissions of interest to the WAMDII (Wide Angle Michelson Doppler Imaging Interferometer) instrument that will be flown onboard the shuttle in 1989 [Shepherd et al., 1985]. The purpose of the OGLOW experiment was to obtain relatively high spectral resolution images of the Orbiter glow phenomenon and of the selected atmospheric emissions in order to provide knowledge of these emissions from above the atmospheric source region and to provide quantitative values of the shuttle glow intensity and spectral shape at these wavelengths.

The OGLOW experiment was flown successfully on mission 41-G in October 1984 and produced results both of the glow phenomenon and of atmospheric emissions. Further details on the instrument and the varied scientific objectives may be found in Kendall et al. [1985].

Observations

For the STS 41-G flight, narrow bandpass interference filters (0.4 nm) were employed with a central wavelength, for normal incidence, slightly longer than that of the atmospheric emissions. As the camera operated in a true imaging mode, this choice of central passbands afforded both spectral scanning [Shepherd et al., 1965] and some protection against wavelength shift due to temperature change. The specifications of the filters are listed in Table 1. For the observations of shuttle glow the Orbiter was positioned with the payload bay pointing in the nadir, with the velocity vector in the -Y direction with respect to the Orbiter body X,Y,Z coordinate axis system, and with the 100 km atmospheric layer bisecting the rear stabilizer as observed from the aft windows of the cabin. In this way it was possible to compare the shuttle glow directly with known atmospheric emissions.

For the atomic line emissions (557.7, 630.0, 731.9, and 777.4 nm) this procedure is straightforward as the limb enhancement may be readily calculated. However, for the molecular emissions (0₂ atmospheric band at 762.0 nm and the 8-3 OH Meinel band at 730.2 nm) the change of the filter capture fractions with the shift of passband, due to spatial scanning, must be considered. Studying the glow at the wavelengths of the atmospheric emissions also allows inversion of the emission profiles to determine boundary values for both temperature and species concentration [McDade and Llewellyn, 1984].

The crew activity plan for the mission afforded two opportunities to make shuttle glow measurements during two entire night passes. The first of of these was on mission day 2, when the Orbiter was at an altitude of 360 km, and the second occurred on mission day 5 at an altitude of 230 km. An 8-second exposure photograph from day 2 with the 630.8 nm filter is shown in Figure 1 and fails to reveal an obvious shuttle glow. The dimensions of the Orbiter stabilizer, on the digitized image, were carefully measured and compared with those obtained from an image taken under non-glow conditions. In practice, the equations for the surfaces of the OMS pod and the upper stabilizer were determined using a least-squares fitting routine and then used to register subsequent images. The estimated error in this procedure is ±2 cm. The extension of the ring pattern throughout the entire atmosphere attests to the extended nature of the airglow emission while the ring pattern across the tail demonstrates the albedo of the shuttle. The presence of albedo away from the bright ring is due to both scattered moonlight and other airglow emissions, notably the airglow continuum and the OH Meinel bands. Similar photographs were obtained with the other filters and failed to reveal any Orbiter glow. Unfortunately, the intensifier was damaged, with a consequent loss of sensitivity, at the end of this night pass.

By comparing the airglow limb brightness with that measured on the tail of the Orbiter, upper limits for the shuttle glow at 360 km can be determined. These values are presented in Table 2. It should be noted that while these values are expressed in terms of a continuum brightness, the present results cannot be used to conclude that the glow is in fact a continuum at this altitude.

On mission day 5 the Orbiter was again positioned so that the velocity vector was in the -Y direction and the same o serving program

was repeated. The only group of exposures, all taken with the 630.8 nm filter, that revealed a definitive glow were those taken after a thruster firing and before the induced glow had entirely disappeared. One of these exposures is shown in Figure 2. Through the cooperation of the entire shuttle crew it was possible to avoid exposures that included a thruster firing. A video tape, obtained from a payload bay CCTV camera operated during this entire night pass, indicates that there were only three vernier thruster firings that caused a noticeable shuttle glow during the observing period. The presence of this glow along the entire leading face of the stabilizer, except for the region shadowed by the OMS pod, indicates that at this resolution (0.4 nm) the thrusterinduced glow is a continuum. As for the high altitude observations, upper limits for the spacecraft glow at 230 km have been determined. These values are also presented in Table 2. Due to the loss of sensitivity of the intensifier, these upper limits are significantly larger than those obtained for the high-altitude observations. Attempts to correlate the induced glow photographs with the video tape are continuing although it has been noticed that each vernier thruster firing appears in three distinct parts, each less intense than its predecessor. The final brightening is close to the stabilizer and it is probably this final part that is present in Figure 2.

The width of the induced glow has been determined from the digitized image of Figure 2 to be approximately 15 cm; this value is in reasonable agreement with the values reported by Yee and Dalgarno [1983] and Swenson et al. [1985]. If the continuum nature of the glow observed at 630.8 nm also extends to the rest of the emission spectrum, then it would appear that for instruments intended to look at narrow line emissions, e.g., WAMDII and WINDII, there is no major problem from the vehicle glow. For observations over an extended spectral range this may

not apply.

Discussion

If the vehicle glow, both the normal ram glow and that induced from the thruster firing, is a true continuum, it is reasonable to suppose that it arises from a recombination that forms NO2 as suggested by Swenson et al. [1985]. In Figure 3 the glow spectra of Swenson et al. have been replotted together with those of Torr and Torr [1985] when the ISO instrument, flown on Spacelab 1, was pointing directly into the velocity vector. These latter values have been normalized to unity at the longest wavelength, i.e., 800 nm. The continuum from NO + 0 [Fontijn et al., 1964; Paulsen et al., 1970] and that from NO + 0_3 [Greaves and Garvin, 1959] have also been included in the figure. Here the values have been normalized to unity for the maximum intensity within the plotted spectral region. Recently Kenner and Ogryzlo [1984] have presented observations of an orange chemiluminescence from NO2 and these are also included in the figure. It is readily apparent that while none of these spectra exactly match the shuttle glow observations, those from Kenner and Ogryzlo [1984] are in closest agreement. This is particularly true when the uncertainty in the longer wavelength glow measurements is recognized. These latter investigators concluded that the orange glow was due to the reaction of NO with vibrationally excited 0,*, where the latter species was formed according to the reaction:

$$0_2(A^3\Sigma_{11}^+) + 0_2 \rightarrow 0_3^* + 0$$
 (1)

and where the $0_2(A^3\Sigma_0^+)$ state was formed through the heterogeneous recombination of oxygen atoms on a nickel mesh. In their analysis, Kenner and Ogryzlo [1984] concluded that the primary losses of vibrationally excited ozone were due to wall quenching and through reaction with NO. However, if the measurements of the loss of vibrationally excited ozone with oxygen atoms are considered [West et al., 1976, 1978], it appears that the analysis of Kenner and Ogryzlo [1984] could be in error. An alternate possibility is that the excited ozone state referred to by Kenner and Ogryzlo is a low lying electronic state as conjectured by McGrath et al. [1983]. In the following analysis, we have considered both the Kenner and Ogryzlo scheme and a direct reaction between 1 and 0_2^* as suggested by Harteck and Reeves [1964]. In their analysis Kenner and Ogryzlo derived the expression:

I (orange glow) =
$$\frac{k[O_2^*][O_2][NO]}{[M]}$$
 (2)

where the effective rate constant $k = 5 \times 10^{-13}$ cm molecule sec and each of the other terms have their usual meaning. The concentration of excited oxygen molecules close to the nickel screen for essentially zero flow conditions, would be given by:

$$[0_2^*] = \frac{\xi[0]}{k_1[0] + k_2[0_2] + A}$$
 (3)

where ξ is the efficiency of the surface recombination; $k_1[0]$ represents the loss rate of 0_2 * through 0; $k_2[0_2]$ is the loss rate through 0_2 ; and A is the radiative loss. For the model atmosphere shown in Table 3, the concentration of 0_2 * is equal to $\xi \times 10$ " at all altitudes. If the surface layer of 0_2 * does not build up during the flight, then the production rate would equal the loss rate from the surface. Thus the production rate of orange glow emitters is equal to $2 \times 10^3 \xi [\text{NO}]$ at 200 km and 3.6 x $10^5 \xi [\text{NO}]$ at 300 km. Hence the surface brightness over the entire spectrum at 200 km is 260ξ kR and 9.3ξ R at 300 km. For any reasonable value of the efficiency [Black and Slanger, 1981] this is unable to match the glow intensity reported by Mende et al. [1984] or the upper limits obtained here.

An alternative approach is to consider the direct reaction of O_2 * and NO as postulated by Harteck and Reeves [1964]. In this case we have a production rate expression given by:

I (orange glow) =
$$\frac{E[0]k_3[NO]}{k_1[0] + k_2[0_2] + A}$$
. (4)

Under these conditions at 200 km, the surface brightness is equal to 9 x 10^{-2} kg, and 1 x 10^{-2} kg, at 300 km. If kg is gas kinetic and $\xi=10^{-2}$ the effective surface brightness is 90 kR at 200 km and 100 R at 300 km. These values do not contradict the presently available measurements although it should be noted that the glow forming reaction is in the gas phase. The surface simply provides a source of 0.2^{+2} and an opportunity for the effective NO concentration to be doubled. The high speed of the emitting molecules is simply due to the mechanics of the collision. The

thruster glow would of course follow both this reaction and the normal NO + O reaction. This latter reaction would deplete [0] so that the normal shuttle glow would be enhanced; the loss of 0,* through collisions with 0 is decreased. However, after the thruster firing, the 0,*concentration on the shuttle surface would be reduced and the vehicle glow could be reduced, at least for a short time. As Ogryzlo and Slanger (private communications, 1985) have noted, different materials have different efficiences as catalysts for the surface recombination of oxygen atoms, so that it is to be expected that vehicle glow is material dependent.

An alternative hypothesis has been presented by Swenson et al. [1985] who suggested that the glow recombination reactions essentially followed the surface formation of an NO monolayer. However, the departure of the observed glow spectrum from that of NO + O allows us to question that mechanism. A mechanism in which oxygen atoms adsorbed on the surface react with impacting NO molecules and then are extracted from the surface has been suggested by Thrush et al. [1968]. Although such a mechanism could indeed shift the NO2 spectrum to longer wavelengths, Kenner and Ogryzlo [1984] have shown that such a process is unnecessary for the formation of the orange glow. It should also be noted that a potential source of enhanced NO concentration could be the reaction between incident N atoms and O2* molecules residing on the surface.

Acknowledgments. We wish to acknowledge the assistance provided by B.H. Long, G.R. Swenson, and G.J. Buttner is the present work. This experiment has been supported by the Canada Centre for Space Science of the National Research Council of Canada; the lockheed Palo Alto Research Laboratory; and the Universities Space Research Association.

References

- Black, G., and T.G. Slanger, Production of O2(a' Ag) by oxygen atom recombination on a pyrex surface, J. Chem. Phys., 74, 6517-6519, 1981.
- Fontijn, A., C.B. Meyer, and H.I. Schiff, Absolute quantum yield measurements of the NO-O reaction and its use as a standard for the chemiluminescent reactions, J. Chem Phys., 40, 64-70, 1964.
- Greaves, J.C., and D. Garvin, Chemically induced molecular excitation: Excitation spectrum of the nitric oxide-ozone system, J. Chem. Phys., 30, 348-349, 1959.
- Harteck, P., and R.R. Reeves, Formation and reaction of the excited O2(A32,) solecule, Disc. Faraday Soc., 37, 82-86, 1964.
- Kendall, D.J.W., R.L. Gattinger, R. Wlochowicz, M. Garneau, G.J. Buttner, S. Mende, G.R. Swenson, E.J. Llewellyn, W.A. Gault, G.G. Shepherd, B.H. Solheim, and L.L. Cogger, OGLOW - An experiment to measure Orbiter and Earth optical emissions, Canad. Aeronaut. Space J., in press, 1985.
- Kenner, R.D., and E.A. Ogryzlo, Orange chemiluminescence from NO, J. Chem. Phys., 80, 1-6, 1984.
- McDade, I.C., and E.J. Llewellyn, Atomic oxygen concentrations in the
- auroral ionosphere, Geophys. Res. Lett., 11, 247-250, 1984. McGrath, W.D., J.M. Maguire, A. Thompson, and J. Trocha-Grimshaw, The production of electronically excited ozone by flash irradiation, Chem. Phys. Lett., 102, 59-63, 1983.

Mende, S.B., P.M. Banks, and D.A. Klingelsmith, III, Observations of orbiting vehicle induced luminosities on the STS-8 mission, Geophys. Res. Lett., 11, 527-530, 1984.

Paulsen, D.E., W.F. Sheridan, and R.E. Huffman, Thermal and recombination emission of NO2, J. Chem. Phys., 53, 647-658, 1970.

Shepherd, G.G., C.W. Lake, J.R. Miller, and L.L. Cogger, A spatial spectral scanning technique for the Fabry-Perot spectrometer, Appl. Opt., 4, 267-272, 1965.

Shepherd, G.G., W.A. Gault, D.W.Miller, Z. Pasturczyk, S.F. Johnston, J.W. Haslett, D.J.W. Kendall, and J.R. Wimperis, WAMDII: Wide Angle Michelson Doppler Langing Interferometer for Spacelab, Appl. Opt., in press, 1985.

Swenson, G.R., S.B. Hende, and K.S. Clifton, Ram vehicle glow spectrum: Implication of NO₂ recombination continuum, <u>Geophys. Res. Lett.</u>, 12, 97-100, 1985.

Thrush, B.A., C.J. Halstead, and A. McKenzie, Chemiluminescence in gases: Reactions yielding electronically excited sulfue dioxide, J. Phys. Chem., 72, 3711-3714, 1968.

Torr, M.R., and D.G. Torr, A preliminary spectroscopic assessment of the Spacelab 1/shuttle optical environment, J. Geophys. Res., 90, 1683-1690, 1985.

West, G.A., R.E. Weston, and G.W. Flynn, Deactivation of vibrationally excited ozone by O(3P) atoms, Chem. Phys. Lett., 42, 489-493, 1976.

West, G.A., R.E. Weston, and G.W. Flynn, The influence of reactant vibrational excitation on the O(P) + O₃[†] bimolecular reaction rate, Chem. Phys. Lett., 51, 429-433, 1978.

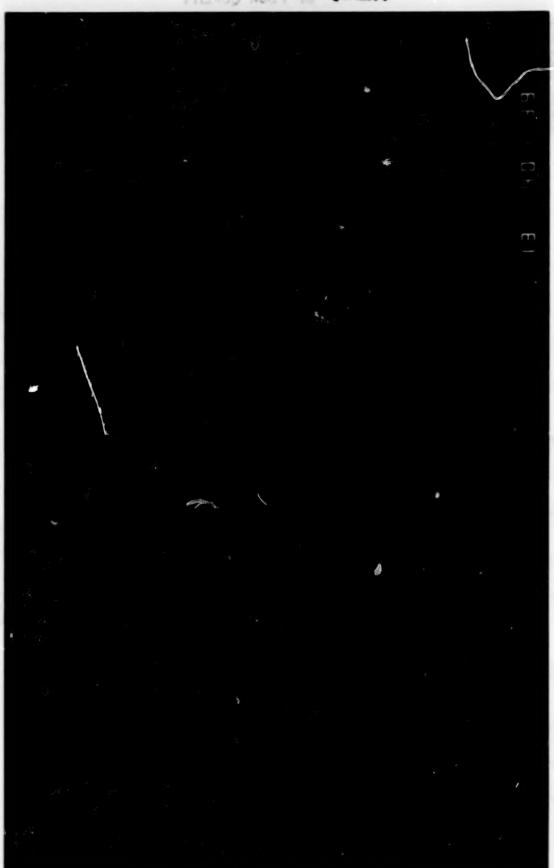
Yee, J.H., and A. Dalgarno, Radiative lifetime analysis of the shuttle optical glow, <u>AIAA-83-CP838</u>, AIAA Shuttle Environment and Operations Meeting, 191-196, 1983.

ORIGINAL PAGE IS OF POOR QUALITY



Fig. 1. Ram glow photograph of the rear stabilizer taken with the 630.8 nm filter at 360 km altitude; exposure time 8 sec.

ORIGINAL PAGE IS OF POOR QUALITY



Ram glow photograph of the rear stabilizer taken with the 630.8 nm filter at 230 km altitude following a thruster firing. Pig. 2.

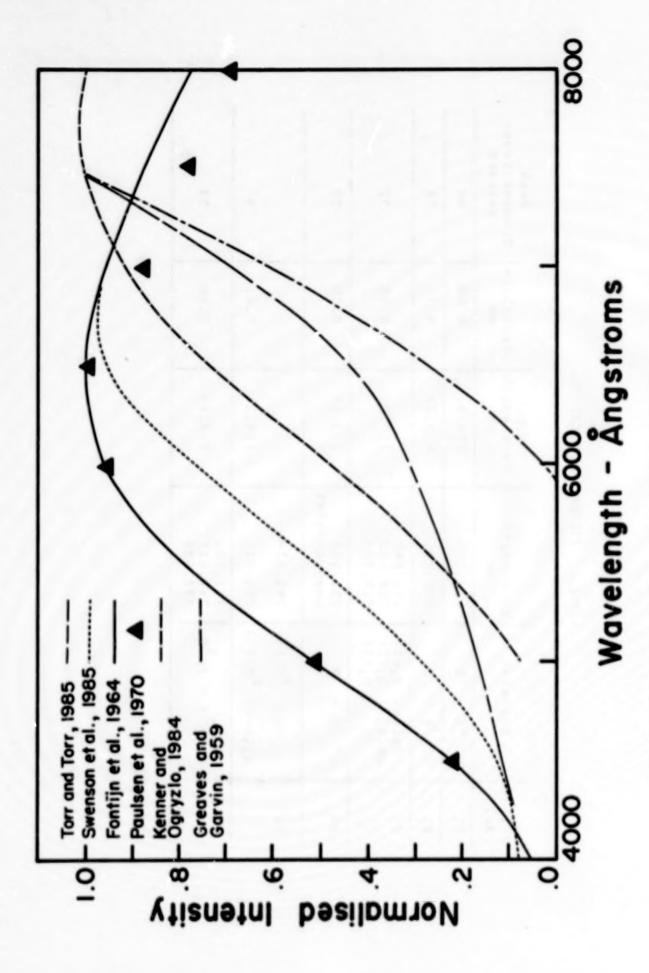


Fig. 3. Comparison of Orbiter glow and NO2 continuum spectra.

TABLE 1. FILTER SPECIFICATIONS

Filter No.	Enission	Wavelength	Center Wavelength	Bandwidth	Peak Transmittance percent
-	St - dt 0	557.735	558.30	07.0	44
12	0 3p - 4D	630.031	630.78	0.31	58
2	Meinel Q ₁ (1) OH(8,3) Q ₁ (2) Q ₁ (3)	727.840 728.638 729.780	730.08	0.38	52
9.4	0+ 2p - 2p	731.984 mean-doublet	733.18	0.40	52
4	Atm PQ(11)	763.959			
	02(0-0) PP(11)	764.071	764.24	0.41	47
2	0 38 S - 3p Sp	777.194	778.42	07.0	15

TABLE 2. UPPER BOUNDS FOR SHUTTLE GLOW INTENSITY ON MISSION 41-G

Wavelength nm	360 km	ow Intensity (R/A) 230 km*	222 km (STS-8)
557.7	<40	<100	150
630.0	<50	<200	300
730.2	<75	<200	400
762.0	<90	<300	550

^{*} These values have been modified from those presented at the workshop by reason of more recent analysis.

	TABLE 3.	MODEL ATMOSPHERE	FOR GLOW	ANALYSIS
Altitude km	[0]	[NO]	[0 ₂]	[M]
KM	Cm	Cin	Cin	Car
200	3 x 10 ⁹	5 x 10 ⁵	4 x 10 ⁸	6 x 10 ⁹
300	4 x 10 ⁸	103	6 x 10 ⁶	5 x 10 ⁸

NEUTRAL MASS SPECTROMETER MEASUREMENTS IN THE SHUTTLE BAY ENVIRONMENT

E. Miller Space Science Laboratory NASA Marshall Space Flight Center, Huntsville, AL

> G. Carignan Space Physics Research Laboratory University of Michigan, Ann Arbor

Abstract. A neutral mass spectrometer, flown as part of the Induced Environment Contamination Monitor (IECM), is briefly described. Results from STS-2, -3, -4, and Spacelab 1 are qualitatively summarized. The gases observed were, for the most part, those with molecular weights below 45 amm with sources attributable to instrument background, shuttle-induced environment, and the ambient atmosphere. The most abundant gases were H₂O, N₂, and He. Heavier gases consisted primarily of fluorocarbons.

Introduction

A neutral mass spectrometer was flown as part of the Induced Contamination Monitor (IECM) on shuttle flights STS-2, -3, -4, and Spacelab 1 [Miller, 1983a,b, 1984] (Figure 1). It will also fly on Spacelab 2. The mass spectrometer covered the mass range from 2-150 amu with a nominal resolution of 1 amu over the range. The instrument field-of-view was collimated by a three-stage skimmer to 0.1 sr (Figure 2). Gas entering at angles greater than 10° to the view axis are skimmed into a matrix of zirconium oxide getters where active atoms and molecules are pumped providing the collimation. Nonreactive gases such as helium and argon are not pumped by these getters and thus are not collimated.

In normal operation, a 600-s cycle format was employed during which each mass number from 2 to 150 amu was sampled for 2 s and during the subsequent 300 s, mass 18 (H₂O) was sampled continuously with a 2-s integration period. Other formats, selectable by the astronauts, reduced the integration period to 0.2 s and/or truncated the mass range to 2-50 amu. With both options selected the mass range from 2-50 was sampled each 10 s. The instrument was sealed in an ultra-clean vacuum prior to launch and opened to the environment after the shuttle was in orbit.

The IECM was mounted in the payload bay such that the view axis of the mass spectrometer was along the -Z axis. On STS-2, -3, and -4, with the bay doors open, there was very little shuttle surface in the entire 2π front hemisphere, so that virtually all arriving contaminant gases were scattered from atmospheric gases. Interpretation of the arriving flux in terms of its source strength or column density thus involves consideration of the scattering cross section of the 8 km/s collisions between contaminants and the atmosphere. On STS-4, the IECM was grappled by the Remote Manipulator Arm and a survey was made with

the instrument axis looking back in toward the bay and wing surfaces. On Spacelab 1 the IECM was located well below the sill line so that much of the aft bulkhead and instrument surfaces were within the uncollimated field-of-view.

The IECM and the mass spectrometer functioned well on all four flights. There were some anomalies and minor problems, but for the most part, operation was nominal. The quantitative interpretation of the mass spectrometer measurements was expected to be difficult and it has been. The major limitation of the spectrometer measurements has been the relatively large background of previously pumped gases over the zirconium oxide getters. Despite the difficulties and the limitations of the system, some success has been achieved in characterizing the gaseous environment in the vicinity of the shuttle.

Results

A qualitative summary of the measurements will be presented here describing the interpretation of the gaseous contributors to each of the mass numbers from 2-44 and a few others at greater mass number.

Mass 2--Molecular hydrogen that is almost entirely background of the zirconium oxide getters. No significance can be attached to the mass 2 measurement.

Mass 3-Statistically insignificant (SI).

Mass 4-Helium. This is the best measurement made by the instrument. There is virtually zero background contribution at mass 4. Helium is not collimated or otherwise affected by the getters and so the instrument field-of-view is 2π sr. Atmospheric helium is observed and its quantification is in good agreement with model values on all flights. Helium is also a major contaminant of the shuttle (10^{-9} torr on Spacelab 1) and is observed even in the wake [Naumann et al., 1985].

Mass 5--SI.

Mass 6--SI.

Mass 7--SI.

Mass 8--SI.

Mass 9--SI.

Mass 10--SI.

Mass 11 -- Small but statistically significant; possibly borane.

Mass 12--All carbon bearing molecules contribute to this peak.

Mass 13-Mostly a product of dissociative ionization of CH4. This peak together with 14, 15, and 16 is used to separate methane from other contributors to these mass numbers.

Mass 14-A complex sum of doubly and dissociatively ionized N_2 , doubly ionized CO, and dissociatively ionized CH_b. Its abundance is heavily modulated by angle of attack because of the N_2 contribution and is also modulated by methane producing events.

Mass 15--Almost exclusively from methane; a very small fraction from the 15 isotope in nitrogen compounds. It is the mass of choice for quantifying the methane source density because it is uncontaminated by atomic oxygen and is almost equally sensitive of methane as the mass 16 peak.

Mass 16-Methane and atomic oxygen. Ambient atomic oxygen does not survive the many surface collisions before ionization. It combines to form ${\rm CO}$, ${\rm CO}_2$, and ${\rm O}_2$. The contribution to the mass 16 peak is thus indirect through dissociative ionization of oxygen bearing molecules. Methane is a substantial background gas over the zirconium oxide getters. It also appears to be catalytically produced in the instrument from some effluent associated with thruster firings. It is postulated that it is formed on the getter surfaces by conversion of unoxidized or partially oxidized thruster fuel, monomethyl hydrazine.

Mass 17--Dissociatively ionized H20, i.e., OH+. The amplitude of the mass 17 peak is about 40 percent of the mass 18 peak due to water.

Mass 18--Water. The density of $\rm H_2O$; in the ion source is the sum of the instrument background and contaminant $\rm H_2O$ from various shuttle sources. In most observation geometries, the contaminant $\rm H_2O$ observed is the consequence of scattering by the ambient atmosphere into the instrument orifice, giving source densities of about $\rm 10^7/cm^3$ and column densities of $\rm 10^{12}/cm^2$.

Mass 19--A statistically significant but unknown contaminant. It is possibly an ionization product of a fluorine compound, but the associated spectral peaks have not been identified.

Mass 20-Mostly doubly ionized argon with a small contribution from the oxygen 18 isotope in H₂O. A small impurity in the neon 22 used for calibration is observed during calibrations.

Mass 21--Statistically insignificant except during calibration using isotopically labeled neon. Neon 22 was used for the calibration; contributions at masses 20 and 21 resulted from impurities and, in the case of mass 21, a slight cross-talk from the large mass 22 peak.

Mass 22-Doubly ionized CO_2 , except during calibration when the isotopically labeled neon 22 caused count rates in excess of 2 X $10^6/2$ s at mass 22.

Mass 23--SI.

Masses 24, 25, 26, and 27--Small, but measurable, products of an instrument contaminant of unidentified origin.

Mass 28-Molecular nitrogen (ambient and contaminant) and carbon monoxide which is a relatively large instrument background over the zirconium oxide getters and other metal surfaces. At small angles of attack the mass 28 peak is dominated by streaming ambient molecular nitrogen, and the quantitiative interpretation of the peak yields reasonable values for ambient density. During the contamination survey taken on STS-4 with the IECM looking into the payload bay the fluxes of molecular nitrogen appear to be about half that of water. This would lead to a column density for N2 contaminant of 1.0 X 10¹²/cm². The survey also showed that the major N2 contamination source was in the vicinity of the aft bulkhead (Figure 3).

Mass 29-Mostly No with one atom of nitrogen 15.

Mass 30--Probably NO with large peaks observed during thruster firings.

Mass 31 -- Not analyzed.

Mass 32--Molecular oxygen mostly of atomspheric origin through the recombination of atomic oxygen. The level of molecular oxygen contamination is very low, probably below the instrument background.

Mass 33--SI.

Mass 34--Not analyzed; partly 016-018.

Mass 35 -- SI.

Mass 36-An unknown minor contaminant, possibly HCl, plus a small component of argon 36.

Masses 37, 38, 39, 41, and 42-Small but statistically significant peaks characteristic of propene.

Mass 40-Argon. Analysis of the mass 40 peak at low angles of attack yields reasonable values for ambient argon densities. There is an argon contaminant on at least some of the flights. The STS-3 door closing event showed a steep rise in mass 40.

Mass 44--CO2. Mostly instrument background with some small contribution from the shuttle that is too low with respect to background to quantify.

Masses 50, 81, and 100--Fractionation spectrum of C₂F₄ (tetra-fluoroethene) observed on Spacelab 1 flight.

Masses 85, 87, 101, 103, 125, and 137--Fractionation spectrum of freon 114, C₂Cl₂F₄ from a known 6.2 cm³/day leak in the Spacelab cooling loop on Spacelab 1.

Masses 67 and 69--The principal peaks of electron impact-inoized Freon 21, CHCl₂F, are presumably from a leak in the shuttle cooling loop. Strong signatures of Freon 21 were observed on STS-4 during the contamination survey and during the payload bay door cycling events.

References

- Miller, E. R. (editor), STS-2, -3, -4 Induced Environment Contamination Monitor (IECM) Summary Report, NASA TM-82524, 1983a.
- Miller, E. R., Update of Induced Environment Contamination Monitor Results, presented at AIAA Shuttle Environments and Operations Meeting, Washington, D.C., 1983b.
- Miller, E. R. (editor), Induced Environment Comtamination Monitor -Preliminary results from the Spacelab 1 flight, NASA TM-86461, 1984.
- Naumann, R. J., G. R. Carignan, and E. R. Miller, Space Shuttle molecular scattering and wake vacuum measurements, <u>Journal of Vacuum</u> Science and Technology, in press, 1985.

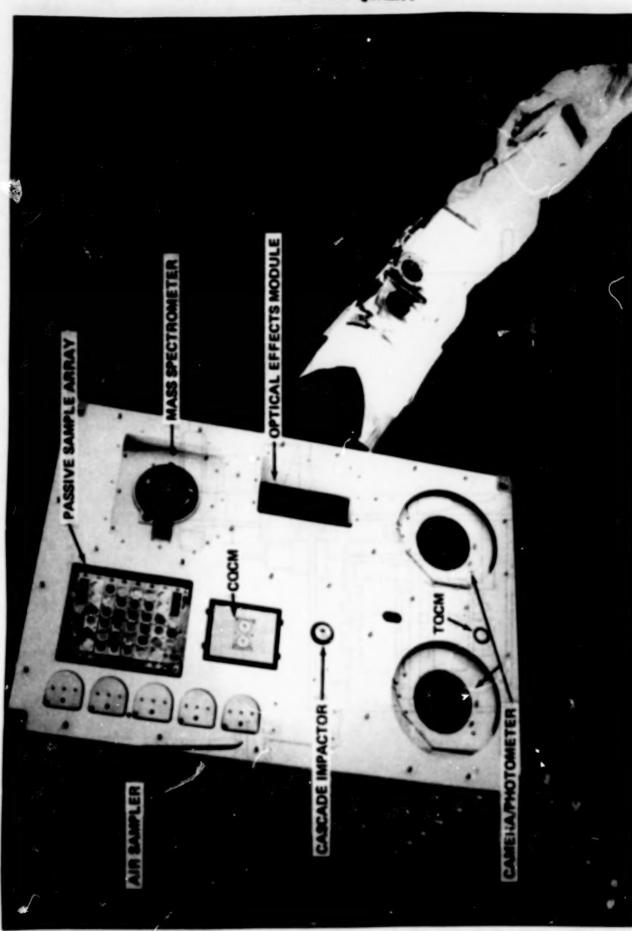


Fig. 1. IECM during remote contamination survey.

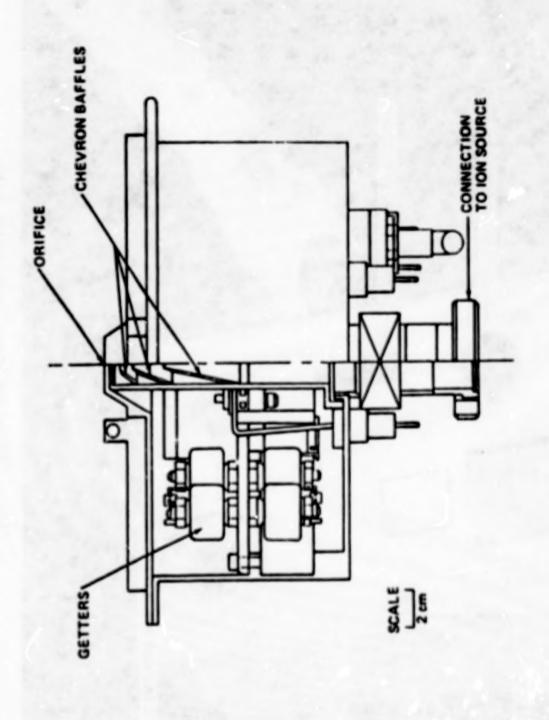


Fig. 2. Mass spectrometer collimator.

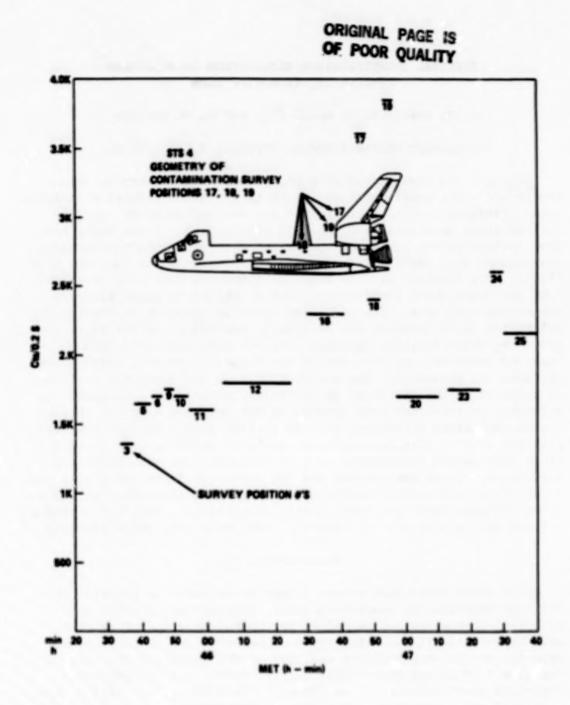


Fig. 3. Mass 28 during the remote contamination survey on STS-4.

The Model

The relative velocity, in excess of 7 km/s, between forward facing orbiting surfaces and ambient particles provides a collisional interaction energy of 5 eV for oxygen atoms. This energy is considerably in excess of the 1.9 eV difference between the 1D and 3P states which leads to red emission lines at 6300 Å and 6364 Å (Figure 1). If losses during the collision were sufficiently low, then the 4.2 eV difference between the 3P normal state and the 1S state might be provided which leads to emissions in the green at 5577 Å and ultraviolet at 2972 Å. States requiring excitation energies greater than 5 eV are neglected for simplicity.

Also shown (Figure 1) is an approximation of the spreading that might be expected as discrete energy levels of a free atom are converted into energy bands of a solid. No attempt has been made to calculate densities of states for the poorly characterized case of an atom striking typical orbital surfaces, but the general trend can be noted by observing what occurs as progressively larger numbers of atoms are involved. Results for band calculations starting with six hydrogen atoms in a line show splitting of levels into six lines forming bands dependent upon lattice constant [Kittel, 1965]. Kittel also gives results for noble metals as a function of internuclear separation.

If specular reflection is assumed for an oxygen atom striking a surface with a speed of 8 km/s, it is easily determined that the atom would spend approximately 5×10^{-14} s within an atomic diameter on the surface. This is sufficient time for the atom to communicate at the speed of light with a large number of lattice atoms (within a hemisphere of radius 10^{-4} cm), which satisfies at least one requirement for producing many states within the bands. If it is necessary for the atom to become part of the lattice, it can be seen by comparison to self-diffusion coefficients that 5 eV minus 2 eV would leave sufficient energy to exceed most barriers to incorporation of the atom into a lattice (activation energies for self-diffusion are typically less than the 60 kcal/(g-atom) available from a kinetic energy of 3 eV [Askill, 1971]).

A broadband spectrum can be produced, assuming that the energy band structure is reasonably represented (Figure 1). Also, the peak intensity should be in the general vicinity of the discrete lines, though shifted, and have an asymmetrical distribution. A spectrum from STS 41-D [Mende et al., 1985] exhibits characteristics of this nature, with the peak shifted toward a longer wavelength and with a bandwidth in excess of 1.5 eV.

Model Testing

To test the model it seems appropriate that spectra of some type dependent upon solid state band structure should be compared to glow spectra. Soft x-ray emission spectra provide information on some band structures [Kittel, 1965] which arise when inner K and L levels are ionized by electron impact and outer electrons make transitions to the

inner vacancies. Since inner levels are relatively sharp because of shielding by the outer electrons, the bandwidths observed in the emission spectra are mostly due to the occupied width of the band from which the outer electrons made their transitions. The K emission band of lithium was found to have a full width of approximately 3 eV [Skinner, 1940], which should represent a good measure of the filled portion of the conduction band. Bandwidths of other materials are generally of the order 1 eV to 10 eV. Optical absorption coefficients versus wavelengths should also provide information about transitions between bands [Kittel, 1965]. Major absorption peaks for Cu and Au are 2000 Å to 3000 Å wide and peaked in the visible. Thus, the bandwidth for the glow is of the correct order compared to other spectra dependent upon solid state bandwidths (toward lower limit).

To provide a higher probability for glow from the surface the lifetime of the excited oxygen state should be less than the time spent traveling one atomic diameter during reflection ($<10^{-14}$ s, as mentioned earlier) or less than a period of lattice vibration ($\sim10^{-13}$ s), if the atom is adsorbed. The exclusion principle $\Delta E * \Delta t \sim h$ provides a means of comparing linewidths to mean lifetimes [White, 1934]. Taking 0.7 eV for the half width of the spectral peak from STS 41-D data [Mende et al., 1985], and assuming the same uncertainty applies when $\Delta E = 0.7$ eV and Δt is the mean lifetime of the excited state, we obtain

$$\Delta t \sim \frac{h}{0.7 \text{ eV}} \approx 6 \times 10^{-15} \text{ s}$$
 (1)

In the derivation of pressure broadening of atomic spectra the collision damping contribution, which broadens the lines, has a correction added due to alteration of the energy levels due to the close approach of the second atom [White, 1934]. The initial and final states of the excited atom are not modified equally by collision since an excited, or outer, state is affected more than an inner tightly bound state. The effect is a shift toward lower frequencies for atoms emitting while spaced less than 10 Å. Asymmetry and redshifting of the spectral lines occur. This does not conflict in general with the appearance of the STS 41-D spectrum and the fact that a solid would produce greatly modified states.

Ground-based studies of airglow [Young, 1966] found a number of gases acted as quenching agents, reducing radiative de-excitations by collision losses. Carbon dioxide was particularly noted for this effect. If carbon dioxide or other contaminants have a high coverage on the surface, one might speculate quenching of the excitation or de-excitation of the incident atoms; this would provide for differences in glow intensities for different materials. Those materials producing a minimum of gaseous products, but exposing a cleaner, lattice-type structure might be expected to glow with more intensity (the opposite of what might be expected for chemical reactions providing the glow). The data from STS 41-D may show such a trend [Mende et al., 1985]. This could be further tested by using a high glow intensity surface coated with a thin plastic film. When the film is burned away, the glow should intensify. Using a half coated disk rotated behind an aperture and also phase-sensitive

detection would provide a low-noise measurement. Dosing of gases onto surfaces could also be used if limited so effects in the gaseous state above the surface did not dominate. If successful, such techniques (with acceptable gases or materials) might be useful for controlling shuttle glow. The distribution of oxygen atoms reflected from an orbiting surface (measurements by J.C. Gregory and P.N. Peters, to be published) may indicate a higher accommodation than would be predicted by hard sphere collision models. Mechanisms such as excitation/radiation which would deplete a large fraction of the particle's incident energy could help explain excessive accommodation coefficients where measured values exceed theoretical predictions. It should also be possible to measure incident energy thresholds for enhanced adsorption and glow if variable energy neutral oxygen atom sources are developed. If accommodation is found to be an adjustable parameter, numerous applications of this parameter to studies for understanding and controlling drag and torques in low-Earth orbits are possible.

As a solid state model, no mechanism is provided to explain glow emanating above surfaces.

Conclusions

A hypothetical solid state model appears to explain a number of features for glow emanating from a surface in low-Earth orbit. A specific case of oxygen atoms impacting the surface with 5 eV energy may provide the atom excitation, energy level broadening, and shortened lifetimes necessary to produce an appropriate spectrum. The model does not provide a mechanism for glow emanating above surfaces.

References

Askill, J., Tracer diffusion in metals, in <u>Handbook of Chemistry and Physics</u>, edited by R. C. Weast, 52nd ed., pp. F-48-F-51, The Chemical Rubber Company, Cleveland, Ohio, 1971.

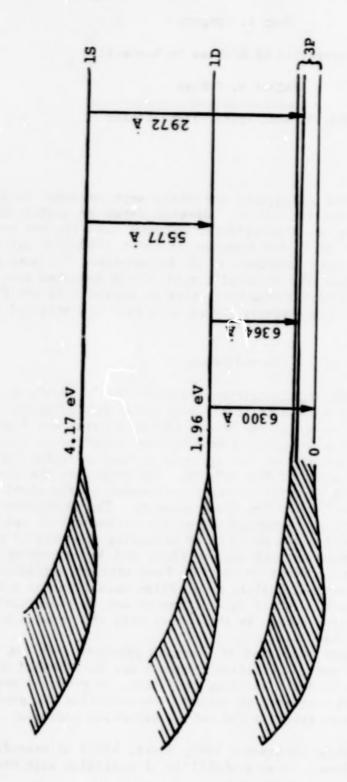
Kittell, C., Introduction to Solid State Physics, 2nd ed., pp. 275-268, 318, 310, and 319, Wiley & Sons, New York, 1965.

Mende, S. B., et al., Shuttle glow measurements on STS 41-D, Final Report to Space Telescope Program Office, MSFC, Alabama, 1985.

Skinner, H.W.B., Trans. Roy. Soc., A239, 95, 1940.

White, H. E., Introduction to Atomic Spectra, pp. 423-432, McGraw-Hill, New York, 1934.

Young, R. A., The airglow, Scientific American, 214, 102-110, 1966.



A hypothetical representation of oxygen atom energy levels being spread on impacting surface. Fig. 1.

THE PRODUCTION OF GLOW PRECURSORS BY OXIDATIVE EROSION OF SPACECRAFT SURFACES

John C. Gregory

The University of Alabama in Huntsville

Palmer N. Peters

NASA, Marsall Space Flight Center

Abstract. Erosion rates of organic materials were measured during a recent flight of the shuttle (STS-8). Several forms of carbon and a variety of thermosetting and thermoplastic polymers were exposed to the ram beam of atomic oxygen. Arrhenius energies of about 1000-2000 cal mole were measured from the rate dependencies on temperature. If some simple assumptions are made about the chemical nature of the desorbed species, the data can be used to estimate production rates at surfaces in orbit under different conditions of temperature, oxygen atom flux and material surface conditions.

Introduction

Erosion of carbon and organic polymer surfaces by "active" or atomic oxygen has been known for decades [e.g., Blackwood and McTaggart, 1959; Hansen et al., 1965]. Gregory and Peters [1975] pointed out that the atmosphere in orbit at a few hundred km altitude would be at least as reactive and proposed the use of the returnable Long Duration Exposure Facility (LDEF) for a study of the effects. Although, at the time of writing, this spacecraft is still in orbit, a version of the atomic oxygen instrument was flown in 1983 on the STS-8 mission. The objectives of the experiment were to begin an investigation of the mechanisms of interaction of 5 eV oxygen atoms with solid surfaces by measuring the rate of reaction as a function of temperature and oxygen flux, and by examining the scattered distribution of atoms re-emitted from certain surfaces. In addition, a number of optical quality metal films were prepared and exposed to investigate the growth of their oxide films or any morphological changes induced by the oxygen atom beam. In this paper only the results on carbon and solid polymers is discussed.

In the context of glow, emission of reaction products from the surface may be relevant in two ways. Oxidation products may be desorbed in excited states which subsequently decay emitting radiation, or products may suffer reactive collision with another 5 eV oxygen atom producing new products in excited states. Evidence favoring the latter mechanism includes:

- (a) New calculations [Rantanen, 1985; Brock, 1985] of mean-free-path of emitted species indicate large probability of collision with the ambient stream.
 - (b) Energetic collisions of organic molecules with oxygen atoms are

expected to have a significant probability for reaction producing excited products.

(c) Emission lines from C, species were observed [Torr and Torr,

1985] on Spacelab 1.

(d) An extended (tens of meters) glow around the orbiter in the unresolved infrared was observed [Witteborn, 1984] from the ground during a recent shuttle flight.

Experimental Approach

The experimental approach used was necessarily very simple as no electromechanical devices such as lids, shutters, etc. were available, and no intermediate measurements could be made; i.e., only a single integral effect could be measured for each sample. Samples were nominally 1-inch discs, with the hot-plate discs only being k-inch diameter. For the case of the erodible materials discussed here, a bar-pattern of small rectangles of niobium was deposited on the surface using a photo-resist technique (Figure 1). The niobium was sputtered on as a uniform film ~2000 € thick. Although it oxidized heavily, it still served to protect the underlying carbonaceous material. The scanning electron microscope picture in Figure 2 shows both the eroded portion of a vitreous carbon disc and the part covered and protected by the niobium film. The height of the step on this sample was about 50,000 Å (5 µm). The bar-pattern allowed multiple measurements of the step-height to be made using a Dektak stylus profilometer. Amplitudes were checked using the SEM micrographs. Half of each sample was covered at all times before and during the flight, and served as a control.

Erodible surfaces studied included single crystal graphite (basal and prismatic planes), vitreous (or glassy) carbon from various manufacturers, polymethyl methacrylate (lucite), bisallyl diglycol carbonate (CR-39, a

high quality optical plastic), and diamond.

The exposure obtained during the STS-8 mission was ideal from the point of view of the materials experiment in that about 95% of the atom fluence was accumulated while the vehicle attitude was held so that the ambient atom beam was within 1° of the normal to the material surfaces. The rest of the mission was spent at much higher altitudes or with the payload bay doors closed. Pertinent exposure data are shown in Table 1.

Table 1. STS-8 ATOMIC OXYGEN EXPOSURE DATA

Payload bay forward facing: t = 41.2 hrs.

Altitude: 120 nautical mi. (225 km)

Velocity: 7.8 km s⁻¹

Mean oxygen atom density (calculated): 2.65 x 10⁹ cm⁻³

Surface impact frequency: 2.07 x 10¹⁵ cm⁻² s⁻¹

Integral fluence: 3.5 x 10²⁰ atoms cm⁻²

Erosion observed by this experiment ranged from a thousand angstroms for diamond (which appears to be particularly resistant to oxidation under these conditions), to about 200,000 Å for the polycarbonate resin, CR-39, which was the most heavily eroded sample reported on any space flight exposure.

The temperature dependence of the oxidative effects was measured by conducting the erosion measurements at three temperatures spanning about 120°C. The Arrhenius activation energy, AE, was estimated, assuming:

where r is the rate of the reaction and A is a constant assumed independent of temperature T. These studies were performed for six materials, vitreous carbon, two graphites, CR-39, silver, and osmium. All activation energies were small and positive.

Fesults

The conclusions from the measurements on various forms of carbon exposed in the STS-8 mission appear applicable to organic solids in general. They may be summarized as follows:

- 1. Measured erosion was linear with total fluence.
- 2. No induction time observed before onset of erosion.
- 3. Erosion rate linear with oxygen flux (i.e., reaction probability independent of flux) measured over a small range 1.5 to 2.5 x 10^{15} atoms cm⁻² s⁻¹.

These results show that erosion and production of gas molecules at the surface can proceed indefinitely at such surfaces as long as oxidizable material remains exposed, in contrast with outgassing behavior which generally shows exponential decay of evolution rate with time. It should be emphasized, however, that our experiment used very pure materials and real or engineering materials may be contaminated either on the surface or by inclusions in the bulk. Such contamination, if less oxidizable than the matrix itself, may then serve to protect the rest of the matrix material from erosion. As erosion proceeds the density of these screening particles or films on the surface grows and the erosion rate may drop from its prior value.

4. Arrhenius activation energies forthe reactions were measured as follows:

Vitreous Carbon 1200 (cal mole⁻¹) Graphite (basal plane) 1400 CR-39 1050

- 5. Reaction probabilities depend on temperature as shown in (4) above. Reaction probabilities for carbons exposed at ~300°K ranged from 0.1 to 0.15 where reaction probability equals the number of carbon atoms lost divided by the number of incident oxygen atoms.
- 6. Reaction probabilities for more complex organic materials have been expressed in cm³ x 10⁻²⁴ of material lost per incident 0 atom. For present purposes we use two examples at approximately 300° K:

 CR-39 (C₁₂H₁₈O₇)_n (this work): ~6 x 10⁻²⁴ cm³ atom⁻¹

Kapton [Leger et al., 1984]: 3 x 10-24 cm3 atom-1

Rates of Production of Volatile Species

Our assumption is that the erosion of carbonaceous materials in orbit was caused by the interaction of 5 eV oxygen atoms with a surface of the material, forming volatile products which evaporated into space. We have performed no experiments to measure the nature or composition of the volatile species, and must, therefore, make intelligent guesses. In the case of the pure carbons the range of choice is limited. From the published literature (at higher temperature) the main product is expected to be CO rather than CO. The mechanism for this production is not discussed here. In the cases of polymeric films, paints and other solid organic surfaces, the chemistry is likely to be much more complex and quite undefined by experiment. A survey of the experimental data for reactions with commonly used polymers has been given [Leger et al., 1984]. the data from 5 and 6 above we may then calculate the emission rates of product molecules from the eroding surfaces in the idealized case. The emitted flux of CO from carbon is given simply by the product of the reaction probability, P, times the flux of oxygen. Calculation of the molecular loss rate from polymers, on the otherhand, requires some assumption of mean molecular weight of the desorbed species.

For the polymers we assumed a mean molecular weight of 28 amu of solidderived component (i.e., not including the atomospheric component). Since the product mixture may well be complex, and different components will differ radically in their capacity for reactive collision excitation to a glow condition, this level of understanding is clearly inadequate.

For the STS-8 mission, with an oxygen atom flux of 2 x 1015 cm 2 s 1,

we have:

Substrate	Emitted Species	Rate of Emission (molecules s 1 cm 2)
Carbon	CO	3 x 1014
Kapton	(28+) amu	1.9 x 1014
CR-39	•	3.0 x 1014

Before these rates are used in any modeling of the gas cloud surrounding the shuttle it should be emphasized that they apply only to unprotected and rather pure organic surfaces. The extent to which impurities reduce the rate of mass loss requires further definition, and it is already quite clear that simple procedures of overcoating with oxidation-resistant materials can reduce mass loss by orders of magnitude. Model calculations of the dynamics of scattering of surface-desorbed species with ambient atmospheric species have suggested that the probability of collision with a streaming oxygen atom is quite high. Under these conditions a large fraction of all organic molecules leaving this shuttle surface may emit one or more photons, contributing to an extended ball of glowing gas around the vehicle, with the upper limit (for 1 mol E 1 photon) for the integral number of photons emitted per second equaling the total number of glow precursors leaving the entire surface per second.

References

Blackwood, J. D., and F. K. McTaggart, Austral. J. Chem., 12, 114, 1959. Brook, F. S., these proceedings, 1985.

Gregory, J. C., and P. N. Peters, The Interaction of Atomic Oxygen with Solid Surfaces at Orbital Altitudes, experiment proposal to NASA, Langley Research Center, June 1975; see also, The Long Duration Exposure Facility (LDEF) Mission One Experiments, NASA SP-473, p. 14, NASA Headquarters, 1984.

Hansen, R. H., J. V. Pascale, T. Benedictis, and P. M. Renzepis, J. Polymer Sci:PtA, 3, 2205, 1965.

Leger, L. J., J. T. Visentine, and J. F. Kuminecz, AIAA Paper No. 84-9548, January, 1984.

Rantsnen, R., these proceedings, 1985.

Torr, M., and D. G. Torr, A preliminary spectroscopic assessment of the Spacelab 1/shuttle optical environment, J. Geophys. Res., 90, 1683, 1985.

Witteborn, F., unpublished results presented at the First Workshop on Spacecraft Glow, NASA/MSFC, 1984

Acknowledgements

We are grateful to the University of Alabama Research Institute for a grant to build the instrument hardware. Part of the analysis at the University of Alabama in Huntsville was supported by Contract NASS-36189.

ORIGINAL PAGE IS DE POOR QUALITY

Fig. 1. One-inch-diameter vitreous carbon disc exposed to the atomic oxygen stream normal to its surface in a 225-km orbit. Rectangles are thin films of niobium. The lighter annulus round the edge of the sample is protected by its holder and remains highly specular, while the inner circle shows the light-absorbing nature of the eroded surface.

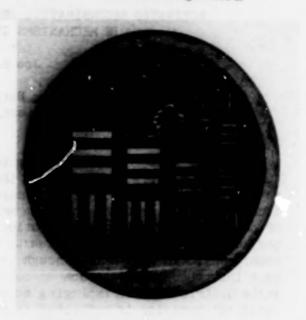


Fig. 2. Scanning electron micrograph of a sample similar to Figure 1 which has been cut through one of the niobium rectangles. Viewing direction is in the plane of the sample. The height of the step (a few µm) indicates the amount of carbon eroded.



N86-13258

ACTIVATED RECOMBINATIVE DESORPTION: A POTENTIAL COMPONENT IN MECHANISMS OF SPACECRAFT GLOW

Jon B. Cross

Los Alamos, New Mexico

Abstract. The concept of activated recombination of atomic species on surfaces is capable of explaining the production of vibrationally and translationally excited desorbed molecular species. Equilibrium statistical mechanics predicts that the molecular quantum state distributions of describing molecules is a function of only the surface temperature when the adsorption probability is unity and independent of initial collision conditions. In most cases though the adsorption probability is dependent upon initial conditions such as collision energy or internal quantum state distribution of impinging molecules. From detailed balance, such dynamical behavior is reflected in the internal quantum state distribution of the desorbing molecule. A number of surface-atom recombination systems demonstrate this "nonthermal" behavior: H2-Cu,N2-Fe,CO2-Pt, etc. It is proposed that this concept, activated recombinative desorption, may offer a common thread in proposed mechanisms of spacecraft glow. Groundbased experiments are proposed which will complement flight investigations probing the mechanism of the glow phenomenon. Using molecular beam techniques and equipment available at Los Alamos, which includes a high translational energy 0-atom beam source, mass spectrometric detection of described species, chemiluminescent/laser-induced fluorescence detection of electronic and rovibrationally excited reaction products, and Auger detection of surface-adsorbed reaction products, we propose a fundamental study of the gas-surface chemistry underlying the glow process. This would lead to the development of materials that could alter the spectral intensity and wave length distribution of the glow.

Introduction

Interaction of the low-Earth orbit (LEO) environment with ram-oriented spacecraft surfaces may involve both gas-surface and gas-phase components whose relative importance is poorly understood. From conservation of flux arguments the ram pressure can be 30 to 100 times the ambient LEO pressure depending upon the extent of gas-phase equilibration with the surface temperature. At low-altitude pressures as high as 10-5 torr may be present near ram surfaces, which could produce glow from the low rates of rotational and vibrational excitation produced by collisions with ram-directed 0-atoms (5 eV) or No (11 eV) as well as ion or electrons. An alternative mechanism to gas-phase excitation lies in desorption of vibrationally excited recombination or surface reaction products through activated recombination. Molecules not normally found in LEO can be formed by recombination of oxygen and nitrogen atoms on spacecraft surfaces as well as reactions of 0-atoms with the surface substrate atoms forming species such as OH, CO, CO2, CN, NO, etc.; all of which may contribute to chemiluminescent glow through activated desorption.

Activated Recombinative Desorption

Figure 1 is a schematic potential energy representation of molecular and atomic particle interactions with a solid surface which illustrates the concept of activated recombinative desorption. Collisions of gasphase molecules with a surface can result in physisorption of the molecule into a precursor van der Waals potential well or chemisorption into a dissociative atomic state by crossing from the molecular to the atomic state curve. In many cases a barrier must be surmounted to cross to the atomic state resulting in an activation energy for adsorption in molecule-surface collisions while adsorption of atomic species is rarely limited by barriers. The reverse process, molecular desorption, is accompanied by the release of molecules having a high translational energy; i.e., atomic recombination occurs with the molecule being born at an elevated potential and leaves the surface with this energy. A number of examples [Comsa and David, 1982; Kubiak et al., 1984; Robota et al., 1985] involving hydrogen can be found in the literature which show that Ho desorbs with translational temperatures as high as 2000 K and with vibrational populations 50 times greater than expected from an equilibrium ensemble at the surface temperature of 300 K. Molecular nitrogen [Thorman and Bernasek, 1978] exhibits high vibrational excitation in the ground electronic state when desorbing from iron. Vibrational excitation of CO₂ produced by oxidation of CO on platinum [Brown and Bernasek, 1985] has been observed with the extent of excitation decreasing with increasing surface coverage of oxygen. In these cases the desorbing molecule loses memory of the initial conditions prevailing before desorption and is only influenced by its position at birth.

Even though there can be extensive etching of surfaces in LEO, oxygen or nitrogen atom reactions with spacecraft surfaces to produce excited products seem to be ruled out by the fact that most surfaces exposed to the ram direction glow with intensity variations of 2 to 3, i.e., that the glow is independent of surface composition. This suggests that surfaces simply act as a third body to catalyze recombination of existing atomic species found in LEO, most probably oxygen and nitrogen atoms. Since the altitude dependence of the glow intensity follows that of atomic and not molecular species, N₂ seems to be ruled out as a reaction partner with 0-atoms, but it has been proposed [Swenson et al., 1985] that nitrogen atoms may be the reactant controlling the glow intensity. This suggests that the following reaction sequence may be one of the major components in the glow mechanism

$$O(s) + N(s) + surface + NO(s) + surface$$
 (1)

$$O(s) + NO(s) + surface + NO_{2}(g) + surface$$
 (2)

where the surface acts as a third body to stabilize the newly formed molecules before desorption. Many investigations have been performed on the reaction

$$0_3 + NO + 0_2 + NO_2$$
 (3)

which have shown that NO2 can be formed with substantial vibrational [Kahler et al., 1984] energy, and our work [van den Ende et al., 1982]

shown in Figure 2 shows both internal and translational excitation of the NO $_2$ product. Though it may be stretching the point a bit to consider (3) as a reaction of 0-atoms on an oxide surface (0 $_2$) with NO, nevertheless the results indicate that NO $_2$ formed from this reaction possesses the characteristics needed to fit the glow data, i.e., long life time (tens of microseconds) and strong spectral emission in the infrared (1-3 μ). Indeed it has been demonstrated [Brown and Bernasek, 1985] that vibrationally excited CO $_2$ is produced through oxidation of CO on platinum surfaces and chemiluminescence is observed in the gas phase. Satellite mass spectrometer measurements [Engebretson and Mauersberger, 1979] have shown formation of NO and NO $_2$ on surfaces in the ion source region, but no direct measurements of nitrogen oxide desorption from spacecraft surfaces have yet been made to confirm this hypothesis. High signal-to-noise mass spectrometric investigations of the spacecraft environment will be needed to identify the presence of NO $_2$.

Gas-Phase Excitation

Even though activated recombinative desorption seems an attractive idea to explain spacecraft glow, there is no conclusive evidence from LEO experiments to support it and there may in fact be several mechanisms in operation which come into play as the concentration of species changes. NO₂ could indeed be formed at high surface coverages of oxygen and desorb in its ground state with subsequent excitation by gas-phase collisions with ion, electron, or neutral species. A combination of molecular beam scattering experiments and theory will be needed to determine cross sections for high energy O-atom excitation processes in order to realistically assess the contribution of gas-phase collisions to the glow phenomenon.

LEO Experiments

Extensive experimental data are needed from LEO in order to narrow down the possible mechanisms of spacecraft glow. Both high-resolution spectroscopic information and simultaneous mass spectrometer detection of surface-desorbed species will be necessary to distinguish between various proposed models. To study etching and glow mechanisms a mass spectrometer with high sensitivity and differential pumping and the ability to use modulation techniques will be needed in order to determine concentrations of reactants as well as surface reaction products. Existing mass spectrometers could be retrofitted with ion counting detectors, choppers for performing modulated molecular beam detection, and molecular shields for differential pumping. A strong emphasis should be placed on using state-of-the-art techniques in future LEO experiments.

Los Alamos LEO Simulation Facilities

A 5-eV O-atom source is being developed [Cross and Cremers, 1985] at Los Alamos that will be capable of delivering fluxes of 10¹⁵⁻¹⁷ O-atoms/cm²-s to a sample surface for materials testing, ground-based calibration of flight hardware, and fundamental investigations of etching and

glow mechanisms. The source is based upon the use of CO2-laser-sustained discharge techniques and using a 70-W laser has demonstrated translational temperatures of 9000 K in xenon. Calculations predict that similar discharges in helium will produce velocities in excess of 10 km/s but will require laser powers of 1 kW or greater. We have recently demonstrated operation of this concept at 400 W of laser power in argon and 30% oxygen for 2 hours using a boron nitride nozzle. We are presently integrating this laser (maximum power of 700 W) with the Los Alamos Molecular Beam Dynamics Apparatus 1 (LAMBDA 1) to obtain 0-atom beam velocity distributions.

LAMBDA 1, [Cross, 1984] shown in Figure 3, is being configured to test and calibrate a mass spectrometer (provided by AFGL) which is to be flown on STS to detect surface-desorbed etching reaction products as well as reactants in the ambient atmosphere. Our objective will be to use the high-energy laser sustained 0-atom source to 1) determine detection sensitivity for 5-eV O-atoms and etching reaction products, 2) demonstrate the advantage of modulated phase-sensitive detection techniques in LEO experiments, 3) determine the contribution to LEO observations from gas-surface reactions occurring in the ion source, and 4) calibrate the AFGL mass spectrometer against the LAMBDA 1 mass spectrometer detector in order to relate ground-based investigations to LEO observations. This effort will provide the unique ability to directly compare future studies of etching mechanisms with LEO experiments and to provide an O-atom testing facility for use in materials development programs. LAMBDA 1 has demonstrated [Pack et al., 1982] high sensitivity and resolution in measurements of gas-phase collision dynamics and could also be used to measure elastic, inelastic, and reactive high-energy 0-atom collision cross sections that would be used in future glow modeling.

Though LAMBDA 1 can be configured to also detect chemiluminescence, LAMBDA 2, shown in Figure 4, is better suited for these types of experiments and provides the instrumentation to detect reaction products from beam-surface scattering by 1) mass spectrometry, 2) chemiluminescence, or 3) laser-induced fluorescence in a UHV environment as well as providing surface characterization using Auger or XPS/UPS spectroscopy. Beam sources developed for the LAMBDAs are interchangeable between the two instruments, thus allowing comparison of results. We propose using this machine to investigate surface-catalyzed, gas-phase chemiluminescence produced by the interaction of high-energy oxygen and nitrogen beams with spacecraft materials. Representative surfaces would be exposed to an N/O atom beam, and measurements of 1) translational energy using time of flight techniques and 2) internal energy using laser-induced fluorescence would be performed to determine the extent of excitation. Through the combined use of LAMBDA 1 and 2 a complete picture of etching and glow mechanisms can be obtained, which would lay the basis for design of materials and processes for use in low-Earth orbit.

Conclusion

To achieve a sustained presence in low-Earth orbit new and novel materials will need to be developed that can resist the effects of long-term 0-atom exposure. Heat rejection systems will require high temperature surfaces that will not erode or alter their IR emissivity over long periods of time (20 years). High strength-to-weight ratio epoxy-fiber composite structural materials will need protective coatings for long-term,

maintenance-free operation while silver interconnects on solar cell panels will require coatings or be replaced with more inert material. Methods for controlling or eliminating ram surface glow need to be devised to provide optimum conditions for infrared astronomy and Earth viewing. Before new materials can be devised, a basic understanding of etching and glow mechanisms will be required after which optimum design parameters for materials can be decided upon. Activated recombinative desorption of reaction products from surfaces may be a common thread in mechanisms of spacecraft glow, but a great deal of basic research into gas-phase and gas-surface dynamics will be needed to fully explain this phenomenon.

Los Alamos is uniquely equipped with instrumentation and staff to collaborate with NASA in fundamental investigations of LEO material problems. A traditional strength of the Laboratory is materials chemistry and physics from which facilities have been developed for ion microprobe investigations of subsurface bulk diffusion processes [Thompson et al., 1983], surface chemistry and physics [Campbell and Paffett, 1984], and theory [Doll, 1985] of gas-surface processes. The combination of LAMBDA 1 used for mass spectrometric angular and translational energy particle detection, LAMBDA 2 used for internal state and fixed laboratory angle translational energy detection, and the high-energy 0-atom source represents an additional unique resource that can be focused to provide solutions to the challenges of extended operation in low-Earth orbit.

References

Brown, L. S., and S. L. Bernasek, J. Chem. Phys., 82, 2110, 1985. Campbell, C. T., and M. T. Paffett, Surf. Sci., 139, 396, 1984; 143, 517, 1984.

Comsa, G., and R. David, Surf. Sci., 117, 77, 1982.

Cross, J. B., Thirteenth Space Simulation Conference, October 8-11, 1984, Orlando, Florida, NASA Conference Publication 2340.

Cross, J. B., and D. A. Cremers, AIAA 23rd Aerospace Sciences Meeting, January 14-17, 1985, Reno, Nevada, AIAA Paper #85-0473.

Doll, J. D., Monte Carlo Fourier Path Integral Methods in Chemical Dynamics, J. Chem. Phys., in press, 1985.

Engebretson, M. J., and K. Mauersberger, J. Geophys. Res., 84, 839, 1979. Kahler, C. C., E. Ansell, C. M. Upshur, and W. H. Green, Jr., J. Chem.

Phys., 80, 3644, 1984 (and references therein).

Kubiak, G. D., G. O. Sitz, and R. N. Zare, J. Chem. Phys., 81, 6397, 1984.
Pack, R. T., J. J. Valentini, and J. B. Cross, J. Chem. Phys., 77, 5486, 1982.

Robota, H. J., W. Vielmaber, M. C. Lin, J. Segner, and G. Ertl, Surf. Sci., in press, 1985.

Swenson, G. R., S. B. Mende, and K. S. Clifton, Geophys. Res. Lett., 12, 97, 1985.

Thompson, K. A., W. P. Ellis, T. N. Taylor, S. M. Valone, and C. J. Maggiore, Nucl. Instr. and Methods Phys. Res., 218, 475, 1983. Thorman, R. P., and S. L. Bernasek, J. Chem. Phys., 74, 6498, 1978.

van den Ende, D., S. Stolte, J. B. Cross, G. H. Kwei, and J. J. Valentini, J. Chem. Phys., 77, 2206, 1982.

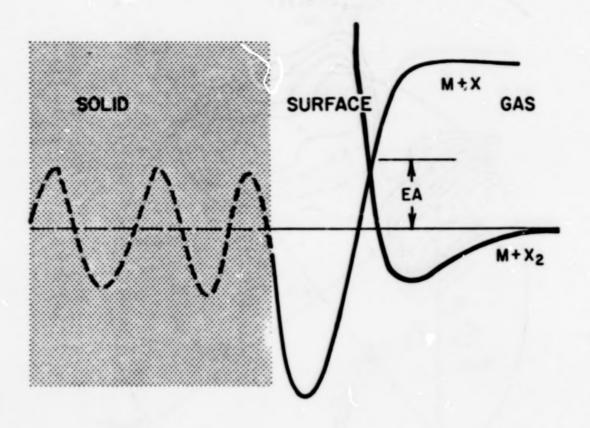


Fig. 1. Potential energy diagram representing activated desorption.

Molecules colliding with a surface can be trapped in a
molecular precursor well or with sufficient collision energy
to surmount the barrier EA and cross to the dissociative
atomic state curve and be chemically trapped. In most cases,
desorption occurs with the expulsion of molecules X2 rather
than X, and the molecule exits the surface with energy EA.
In some cases (see Comsa and David [1982]), the two-dimensional
surface has holes in it and molecules can exit over the barrier
and are not affected by surface temperature, while other molecules come from states without barriers and are accommodated to
the surface conditions.

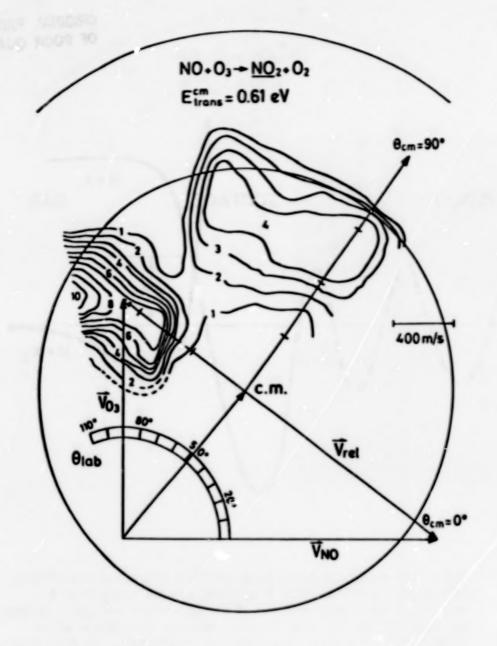


Fig. 2. Center-of-mass contour map of the NO₂ flux distribution obtained from laboratory angular and time-of-flight distribution measurements by performing a 1-Newton diagram transformation of the gas-phase data. There is a narrow backward NO₂ peak and a broad sideways peak which are clearly separated. The outer circle indicates the velocity of NO₂ when all available energy is put into translation while the inner one gives the maximum velocity at which chemiluminescence is possible. The majority of product has high internal excitation. NO₂ formed by recombination of NO + O on oxide surfaces may exhibit similar dynamics.

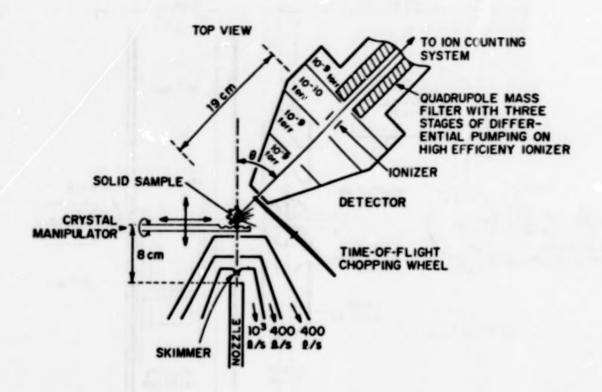


Fig. 3. Los Alamos Molecular Beam Dynamics Apparatus 1 (LAMBDA 1) showing the central portion of the instrument including the molecular beam source, sample manipulator-molecular beam intersection zone, and a portion of the movable detector. The detector is an electron bombardment ionizer-quadrupole mass spectrometer suspended from the rotatable lid of the main vacuum chamber for the measurement of angular distributions. Also shown is a time-of-flight chopping wheel, which allows for 50% transmission efficiency and time-of-flight measurement by cross correlating the data with the sequence. Pumping on the scattering chamber is accomplished with a liquid nitrogen cryoliner, turbomolecular pump, and a closed-cycle gaseous helium cryopump. Pressures of 10-8 to 10-9 torr are obtained in the scattering chamber.

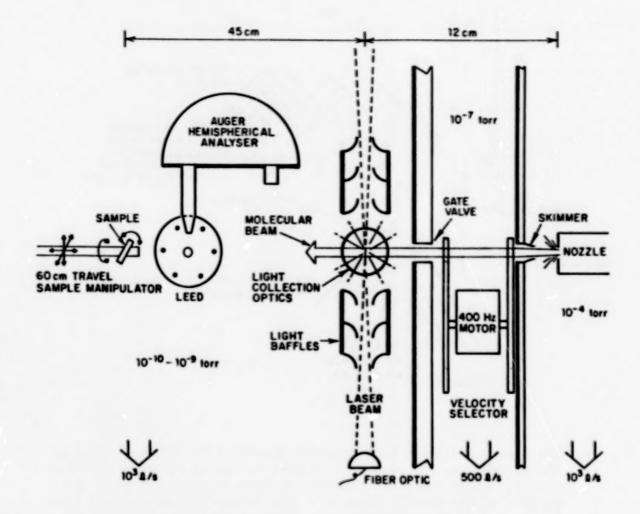


Fig. 4. LAMBDA 2. This figure shows a detailed view of the central portion of the apparatus that consists of a nozzle chamber, a differential pumping chamber containing flags, choppers, and a slotted disk velocity selector; and a UHV (10-10 torr) chamber containing a cyroshroud, sample manipulator, surface analysis equipment consisting of LEED and Auger units, provision for collecting fluorescence light and laser-induced fluorescence signals. A quadrupole mass spectrometer (not shown) with two stages of differential pumping and a cross correlation time-of-flight chopper is opposite the LEED unit and is limited to a fixed laboratory angle.

LABORATORY MEASUREMENTS

OPTICAL RADIATION FROM THE INTERACTION OF ENERGETIC ATOMS, IONS, ELECTRONS, AND PHOTONS WITH SURFACES

N. H. Tolk, R. G. Albridge, R. F. Haglund, Jr., and M. H. Mendenhall

Department of Physics & Astronomy, Vanderbilt University

J. C. Tully

AT & T Bell Laboratories

Abstract. Heavy particle, electron, and UV photon bombardment of solid surfaces has been recently observed to result in the emission of infrared, visible, and ultraviolet radiation. This effect occurs over a wide range of incident projectile energies. Line radiation arising from transitions between discrete atomic or molecular levels may be attributed to the decay of excited particles which have been sputtered or electronically/chemically desorbed from the surface. Broadband continuum radiation, which is also observed, is believed to arise either from fluorescence of the near surface bulk or from the radiative decay of desorbed excited clusters. The spectral characteristics of the optical radiation as well as the efficiencies for producing it may vary substantially with the identity, form and cleanliness of the surface, and on the identity and energy of the bombarding particle. Spacecraft, in the ambient near-Earth environment, are subject to such bombardment. The dynamics of energetic particle and photon beam interactions with surfaces which lead to surface erosion and glow phenomena will be treated. Ir addition, projected experimental and theoretical studies of oxygen and nitrogen beam-surface interactions on materials characteristic of spacecraft surfaces will be discussed.

Introduction

Exterior surfaces of spacecraft in near-Earth orbit are bombarded by a formidable assortment of neutral and ionized atoms and molecules, in addition to electrons and ultraviolet photons. Heavy particle bombardment arises largely from the motion of the vehicle through the ambient environment. However, enhanced solar activity and artificial environments associated with disturbed nuclear atmospheres and directed energy beams may increase the energy and intensity of the bombarding particles.

Over a wide range of bombarding energies, particle and photon interactions with surfaces have been shown to result in the efficient desorption of surface atoms and molecules. Many of these are desorbed in excited states which subsequently emit characteristic infrared, visible, and ultraviolet radiation. We will review recent work on this topic and discuss future studies of ion-, electron-, and photon-induced erosion and glow phenomena.

Photon Emission from Ion and Neutral Particle Impact on Surfaces

In the experimental observations to be treated below, three distinct kinds of collision-induced optical radiation have been identified.

The first of these is line radiation due to sputtering with simultaneous excitation. The interaction of the impinging ion or neutral beam with the surface results in the sputtering of neutral atoms, neutral molecules, and ions from the surface. A significant portion of the sputtered particles leaves the surface in excited electronic states which then decays and gives rise to optical line radiation characteristic of surface constituents [Tolk et al., 1977].

The second kind of radiation observed has a similar nature but arises from backscattered excited beam particles which have escaped the surface after having experienced collisions in the bulk material [Leung et al., 1978]. To the extent that the momentum-changing collisions do not effect the final excited state configuration of the emerging particles, this class of phenomena is identical to the beam foil radiation phenomenon. Studies of backscatter radiation provide more complete information on final states than conventional charge state measurements and give important insights into the nature of the interaction of the emerging particle with the surface.

The final and perhaps least understood type of radiation is the broad continuum of radiation that is observed from many of the solid materials studied. In the case of metals, for a given beam projectile at a given energy, the shape of the continuum is observed not to change for a variety of metal surfaces [White et al., 1976]. For insulators, the shape of the continuum as a function of wavelength is entirely characteristic of the material and independent of the beam particle species. An important conclusion from these studies is that the collision participants, both the solid itself as well as the escaping atomic and molecular fragments, in general are in excited states following the collision interaction. The collision participants may then produce the observed photons by radiative decay or may undergo radiationless de-excitation processes such as Auger de-excitation.

Motallic Targets

The spectra of radiation observed when Ar* ions at 4000 eV impact on Ni and Cu targets are shown in Figure 1. Most of the prominent lines in these spectral scans have been identified as arising from low-lying energy levels of neutral Ni and Cu, sputtered off the surface in excited states by the incident ion beam. In addition to spectral lines from the surface target materials, radiation is also often observed which is characteristic of surface contaminants [Tolk et al., 1973]. The molecular radiation centered at 4300 A and 3900 A has been identified as arising from the A2A + X2II and B²Σ - X²II electronic transitions of the CH molecule. This radiation is believed to originate from collisional excitation of adsorbed hydrocarbon surface contamination. The prominent line which is often observed at approximately 5900 A is the NaD line doublet which is assumed to arise from sodium contaminants deposited on the surface. The surface can be cleaned to such an extent that the contaminant radiation is negligible by prolonged exposure (approximately 20

minutes) to a 3-keV argon ion beam or by heating the target. Our measurements show that for metallic targets, beams of neutrals and ions (of the same species) produce photons due to sputtering with equal efficiency. Low-velocity ions with sufficiently large ionization potential impacting on a metal surface are neutralized by non-radiative processes several angstroms in front of the surface, well before the sputtering interaction occurs. It is reasonable then to assume that the radiation which results from the sputtering interaction should be the same for beams of ions or neutrals at the same velocity. This assumption has been verified experimentally using a bolometer to independently measure the neutral "current." These results consequently suggest a means of directly measuring neutral beam flux in the low-energy region. It follows from the above discussion that the ratio of the intensity of the optical line radiation produced when a metallic target is bombarded with neutrals to that produced when the same target is bombarded with ions is equal to the ratio of the neutral to ion fluxes thus leading to a direct measurement of the neutral "current." In principle, this technique could also be extended to non-metallic surfaces using

Insulator Targets

a more complicated calibration scheme.

The spectral distribution of radiation arising from excited sputtered particles due to the impact of nitrogen molecules (N2) at a beam energy of 3.5 keV on aluminum oxide (Al20,), lithium fluoride (LiF), and quartz (SiO2) is shown in Figure 2. Optical scans taken using neutral beams of neon, argon, and other heavy particles give similar results. Neutral beams rather than ion beams are used for the bombardment of insulators in order to avoid ion beam energy decrease and defocusing due to charge buildup on the insulator surface. Ion beams may also be used, however, if the insulator surface is bathed in electrons emitted from a nearby heated filament. In Figure 2, the more intense lines are identified as arising from the decay of excited states of neutral aluminum, lithium, silicon, and hydrogen. Because the line widths are found in these experiments to be equal to the instrumental resolution (about 1 angstrom), we may assume that the radiation originates from individual atoms and molecules which have been sputtered off the surface in excited states which subsequently decay by photon emission. The Balmer lines of neutral hydrogen are believed to arise from the sputtering of surface contaminants.

For all cases studied-metals, semiconductors and insulators-optical radiation has been observed due to sputtering with simultaneous excitation. However, in the insulator case, the excitation efficiency is observed to be much larger than for metals. For the case of metals, typical prominent lines are estimated to have excitation efficiencies of the order of 10⁻⁵ (photons per incident ion) while in the insulator case, the excitation efficiencies are measured to be two or three orders of magnitude higher [Tolk et al., 1977].

Optical Radiation from Electronically Described Particles

For the case of heavy-particle induced sputtering as discussed above, understanding the influence of surface parameters on the final state of sputtered particles is complicated by the fact that the ejection of atoms and molecules results from both electronic and momentum changing processes. Electron- and UV photon-stimulated desorption of atoms and molecules, on the other hand, involves only electronic interactions.

Even though it is known that the most abundant products of electronically induced desorption are neutral atoms and molecules, most studies have involved desorbed ions. This is due primarily to the eare of detection of ions. In only a few cases have neutrals desorbed by electron and photon impact been directly studied.

It is useful to describe the mechanisms of electron and photoninduced descrption as a three-stage process: (1) the initial deposition
of electron energy by, for example, the creation of a hole, two
holes, an exciton, or a defect; (2) a fast electronic rearrangement
leaving a surface atom or group of atoms in a localized repulsive
or energetic state; and (3) further particle-surface electronic
interaction as the atom, or molecule, or cluster leaves the surface.
Although not treated here, recent observations of strong elliptic
polarization of optical radiation following grazing incidence of
9-keV protons on crystal surfaces contribute unique information
on stage (3) electronic processes [Tully et al., 1981]. Studies
of these phenomena promise to provide new insight into the electronic
aspects of atomic collisions in solids [Tolk et al., 1981b]. In
this paper we discuss recent measurements of electronically described
neutrals obtained by observing optical radiation which arises from
neutrals described in excited states.

Electron Stimulated Desorption (ESD) of Excited Particles

Although it is now generally accepted that the most abundant products of desorption from surfaces induced by electronic transitions, stimulated by energetic electrons or UV/soft x-ray photons, are neutral atoms and molecules, only a very few results have been published about neutral desorption. These experiments confirm the leading role of neutrals in the desorption process.

Our approach to the detection of described neutrals is based on analysis of the optical radiation emitted by decays after descrition [Tolk et al., 1981a]. The experimental equipment included an ultrahigh vacuum chamber, a primary excitation source, and an optical detection/analysis system with a monochromator and computer-controlled data processing. Initially, the excitation source was an electron beam. Figure 3 shows spectra of atomic and molecular radiation emitted by described atoms and molecules from NaCl, NaF, and LiF surfaces, principally from excited alkalis, hydrogen, OH, and an unidentified molecular species.

In marked contrast to ion bombardment and gas discharges, the only sodium and lithium radiation detected in these experiments are first resonance lines. This indicates that for alkali halides there exists a strong nonstatistical state selection mechanism of an as-yet undetermined nature. Energy-dependent measurements show

onsets correlated to core hole formation relating to the initial energy deposition process. Electron-stimulated erosion of alkali halides is usually attributed to the creation of defects which results in the ejection of halogen atoms and leaves excess alkali atoms to desorb thermally from the surface. This does not appear to be adequate to explain the emission of excited neutrals. It is likely that this latter process involves the creation of a long-lived localized surface excitation, perhaps an exciton, which results in ejection of a surface atom and in addition supplies the excited electron.

Photon Stimulated Desorption (PSD) of Excited Particles

Description of excited particles was recently observed when UV photons from the University of Wisconsin synchrotron storage ring, with energies of 40-200 eV, were incident on alkali-halide surfaces [Tolk et al., 1982]. As shown in Figure 4 photon energy dependent measurements were taken of optical radiation arising from the decay of desorbed excited Li atoms. These data are compared with PSD measurements of positive ions from the same LiF sample. Both measurements showed pronounced energy-dependent structure similar (though not identical) to soft x-ray absorption coefficient measurements also presented in Figure 4. It should be noted that the yield of excited neutrals was measured to be at least 3 orders of magnitude greater than the corresponding yield of desorbed ions. Similar to the ESD case, only the first resonance level is observed. In light of these observations, a plausible three-step desorption scheme for excited neutrals may be hypothesized [Tolk et al., 1983, 1984]: (1) The incoming photon creates a core or valence excitation near the surface which provides electronic energy to the system. (2) One or a series of secondary electronic processes occur, resulting in a localized valence excitonic state, which leaves the surface alkali atom in a highly energetic or repulsive state. (3) As the alkali atom departs. the lowest excited state is preferentially populated because it is both at lower energy and more localized than the higher excited states.

Laboratory Studies of Spacecraft Glow

At Vanderbilt University, we have initiated studies of the dynamics of particle— and photon-beam interactions which lead to surface erosion and glow phenomena, emphasizing materials and surface conditions relevant to spacecraft in the near-Earth environment. This research uses facilities available at Vanderbilt and at the University of Wisconsin sychrotron storage ring for studying the interactions of directed beams of ions, neutrals, electrons, and UV photons with well-characterized surfaces under carefully controlled vacuum conditions.

Work is progressing toward the development of a high-flux beam of energetic neutral oxygen and nitrogen atoms using an existing ion source at Vanderbilt to compare ion bombardment with corresponding neutral bombardment on relevant surfaces. Desorption experiments are also in progress on metallic surfaces with controlled doses of relevant adsorbates (e.g., N₂ and O₂), to ascertain changes in surface electronic and bonding properties induced by contaminants. Finally, experiments on possible synergistic effects—as in simultaneous ion-electron and ion-photon bombardment—are now feasible and will

Conclusions

As discussed above, when particles impact on surfaces, many complex interrelated processes occur as the incident energy is transformed into electronic and sometimes thermal excitations. Previous studies of electronically-induced desorption have shown much of the incident energy may be channeled into bond-breaking and desorption processes leading to ejection of surface atoms and molecules from metal oxides and insulators. Thus, electronic, chemical, and thermal processes stimulated by energetic beams can play a major role in surface modification and damage, through erosion, changes in tribological properties, and migration of electronically-induced defects. The primary effort is to understand the fundamental mechanisms underlying these processes. These studies will generate an increasingly detailed microscopic view of the dominant modes through which incident energy is absorbed, localized, and redirected to desorption. This, in turn, leads to a comprehensive macroscopic picture of material ejection, erosion, and ablation from surfaces and of the associated optical emissions.

References

- Leung, S. Y., N. H. Tolk, W. Heiland, J. C. Tully, J. S. Kraus, and P. Hill, Optical radiation from low-energy hydrogen atomic and molecular ion-surface collisions, Phys. Rev., A18, 447, 1978.
- Tolk, N. H., D. L. Simms, E. B. Foley, and C. W. White, Photon emission from low-energy ion and neutral bombardment of solids, Radiation Effects, 18, 221-229, 1973.
- Tolk, N. H., I.S.T. Tsong, and C. W. White, In-situ spectrochemical analysis of solid surfaces by ion beam sputtering, Analytical Chemistry, 49, 16A, 1977.
- Tolk, N. H., L. C. Feldman, J. S. Kraus, M. M. Traum, and J. C. Tully, Optical radiation from electron stimulated desorption of excited particles, Phys. Rev. Lett., 46, 134, 1981a.
- Tolk, N. H., L. C. Feldman, J. S. Kraus, J. C. Tully, M. Hass, Y. Niv, and G. M. Temmer, The role of surface interactions in beam foil excited state formation, Phys. Rev. Lett., 47, 487, 1981b.
- Tolk, N. H., M. M. Traum, J. S. Kraus, T. R. Pian, W. E. Collins, N. G. Stoffel, and G. Margaritondo, Optical radiation from photon-stimulated desorption of excited atoms, Phys. Rev. Lett., 49, 812, 1982.
- Tolk, N. H., W. E. Collins, R. J. Morris, T. R. Pian, J. S. Kraus, M. M. Traum, N. G. Stoffel, and G. Margaritondo, The electronic desorption of excited alkali atoms from alkali halide surfaces, chapter in Desorption Induced by Electronic Transition, edited by N. H. Tolk, M. M. Traum, J. C. Tully, and T. E. Madey, Springer-Verlag, Heidelberg, 1983.
- Tolk, N. H., P. Bucksbaum, N. Gershenfeld, J. S. Kraus, R. J. Morris, D. E. Murnick, J. C. Tully, R. R. Daniels, G. Margaritondo, and N. G. Stoffel, Desorption induced by electronic transitions, Nucl. Instr. and Meth. in Physics Research, B2, 457, 1984.

- Tully, J. C., N. H. Tolk, J. S. Kraus, C. Ran, and R. Morris, Polarization on surfaces, chapter in <u>Springer Tracts in Chemical Physics</u>, edited by W. Heiland and E. Taglauer, p. 196, Springer-Verlag, Heidelberg, 1981.
- White, C. W., N. H. Tolk, J. S. Kraus, and W. F. van der Weg, Continuum optical radiation produced by low-energy heavy particle bombardment of metal targets, Nucl. Instr. and Meth., 132, 419, 1976.



Spectra of radiation produced by the impact of Ar (at 4 keV) on copper (top) and nickel (bottom). Lines arising from excited states of sputtered copper, nickel, and various contaminants are observed in this wavelength interval. Fig. 1.

ORIGINAL PAGE IS OF POOR QUALITY

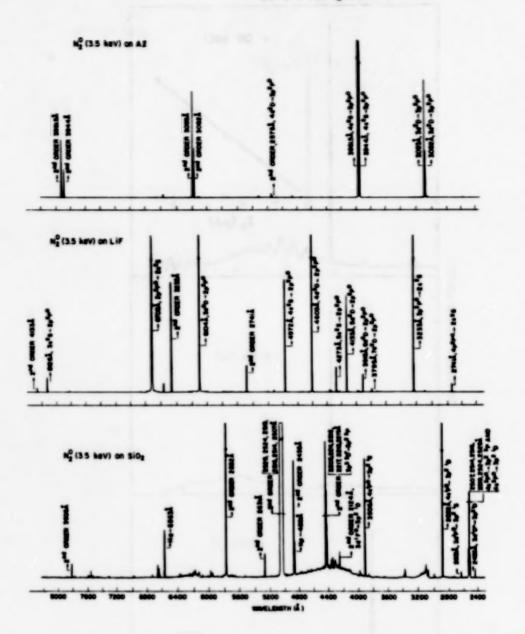


Fig. 2. Spectrum of radiation produced by the impact of N₂^O (3.5 kiloelectron volts) on Al₂O₃, LiF, and SiO₂. Lines arising from excited states of neutral aluminum, lithium, and silicon are observed in this wavelength interval. The wavelength and electronic transition are indicated beside each line. Two Balmer lines of neutral hydrogen, H_Q and H_B, are observed on the SiO₂ scan.

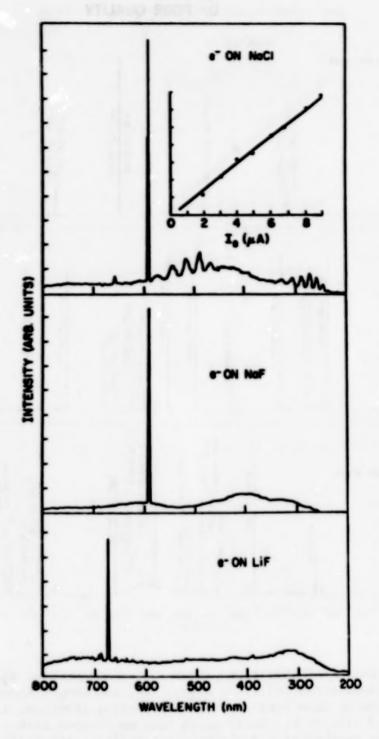


Fig. 3. Spectra of radiation produced by 1-keV e impact of NaCl, NaF, and LiF, obtained at approximately 90° to the surface normal. The inset shows the linear behavior of the intensity of the NaD line as a function of incident e current. A straight line has been drawn through the data points.

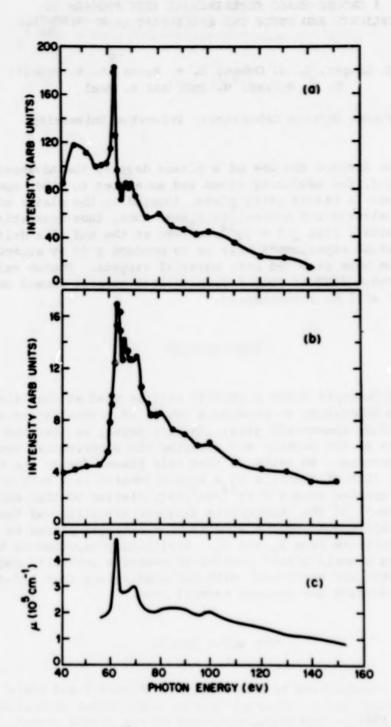


Fig. 4. (a) Li (670.7 nm) optical emission dependence on soft x-ray energy using a (100) single-crystal LiF sample at room temperature.

(b) Positive-ion yields as a function of incident photon energy using the same sample at about 250 °C. (c) Photon absorption coefficient measurements.

A GROUND-BASED EXPERIMENTAL TEST PROGRAM TO DUPLICATE AND STUDY THE SPACECRAPT GLOW PHENOMENON

W. D. Langer, S. A. Cohen, D. M. Manos, D. H. McNeill R. W. Motley, M. Ono, and S. Paul

Plasma Physics Laboratory, Princeton University

Abstract. We discuss the use of a plasma device, the Advanced Concepts Torus-I, for producing atoms and molecules to study spacecraft glow mechanisms. A biased metal plate, located in the plasma edge, will be used to accelerate and neutralize plasma ions, thus generating a neutral beam with a flux $\gtrsim 5 \times 10^{14}/\text{cm}^2/\text{sec}$ at the end of a drift tube. Our initial experiments will be to produce a 10 eV molecular and atomic nitrogen beam directed onto material targets. Photon emission in the spectral range 2000 to 9000 Å from excited species formed on the target surface will be investigated.

Introduction

The Advanced Concepts Torus-I (ACT-I) will be used at the Princeton Plasma Physics Laboratory to produce a source of neutral atoms and molecules to study spacecraft glow. In this paper, we list the characteristics of the machine and describe the experimental arrangement and research program. We estimate that this plasma device can be used to produce the flux of neutrals on a sample located in a test chamber outside ACT-I greater than $5 \times 10^{14}/\text{cm}^2/\text{sec}$, similar to that encountered in the environment of the Atmosphere Explorer satellite and the space shuttle. We made spectroscopic studies of a nitrogen plasma in ACT-I and detected emission from N₂ and N₂. Preliminary experiments have been conducted using a small biased limiter to generate neutrals, and the measured currents are consistent with our predictions that ACT-I has the properties to produce the desired neutral flux.

The ACT-I Device

ACT-I is a steady-state toroidal machine (Figure 1 and Table 1) built primarily to study radio frequency heating and current generation in plasmas [Wong et al., 1981]. The characteristics of the plasma formed in ACT-I are such that it can be converted into a copious source of neutrals with energies of 3 to 100 eV. The plasma characteristics for both steady-state and pulsed operation are given in Table 1. The machine consists of 26 sets of toroidal field coils which produce up to a 5.5 kg steady-state magnetic field. The vacuum chamber has 26 toroidal segments with large ports (10 cm

x 40 cm). A 600 kW motor-generator set provides steady-state power to the coils which are cooled by pressurized de-ionized water. ACT-I has been operated with a variety of gases, including H, He, Ne, Ar, N_2 , and air.

A Neutral Source

Ions formed in ACT-I are confined for about 1 msec and most of them are lost by drifting radially outward across field lines onto the outer wall. A fraction of these ions (~0.3) can be intercepted on a metallic plate, a so-called limiter, where they are neutralized and reflected. calculation of reflectivity of neutrals formed in this manner using the TRIM code [Biersack and Haggmark, 1980] predicts that a high percentage of the incoming particles is reflected with nearly their full energy if the mass of the atoms making up the target (limiter) is much greater than that of the incoming particles. Furthermore, the code predicts that by positioning and orienting the limiter appropriately a high percentage of the neutrals will be directed out of the machine where they can enter a drift tube (Figure 2). A target will be mounted in a test chamber at the end of this tube and the glow resulting from the neutral-surface interaction will be observed in this chamber. The limiter may be biased to accelerate the ions and produce neutrals with an adjustable range of energies.

Estimate of Neutral Flux

What makes this device an effective plasma source for the glow problem is that it can sustain a dense plasma with a warm bulk ion temperature $(T_i > 1 \text{ eV})$, with sufficient volume, to produce a large steady-state source of plasma with $T_e = 1$ to 15 eV. The plasma source can readily be converted into a large flux of energetic neutrals as described above. The ion source from the entire plasma, S_i , can be estimated as

$$s_i = \frac{nv_p}{\tau_c} = 1 \times 10^{20}/\text{sec}$$
, (1)

[see Table 1 for the symbols and values used in Eq. (1)]. The neutral source, S_n , depends on the fraction of ions that intersect the biased limiter as they drift outward. Ions from the center of the plasma travel roughly half way around the torus in the time they drift radially outward. By inserting the biased limiter a few centimeters into the plasma about a third of the partiples can be intercepted. In practice, the port opening to the drift tube restricts the fraction that can be used to about a quarter of the ion source. The energy will depend on the bias voltage applied to the limiter. The flux onto the sample depends on the fraction of neutrals reflected into a solid angle at the end of the drift tube, Ω_s . The reflected particles are forward-peaked giving $\Omega_s = \pi d^2$ where d is the distance from the limiter to the sample. Though the TRIM code predicts about eighty percent reflection, we assume only fifty

percent to make a conservative estimate of the neutral flux. Therefore, $S_n \approx S_i/8$, and the flux on a target located 1 meter away is

$$\Gamma_{\rm n} = \frac{\rm s_{\rm n}}{\rm sd^2} \sim 5 \times 10^{14}/{\rm cm^2/sec}$$
 (2)

Diagnostics and Spectroscopy

We will install diagnostics to look at the plasma source, the energetic neutrals in the drift tube, and the molecular emission in the test chamber. The plasma temperature and density are measured with a triple Langmuir probe and microwave interferometer; the spectroscopic signature of the plasma is also monitored. This information is needed to optimize the plasma for production of neutrals and identification of any contribution of the plasma light to the background in the test chamber.

Screening of Background Light and Velocity Selection

In the test chamber, it is crucial to screen out the background plasma light. An effective technique for screening is to use a rapidly rotating slotted chopper disk on the port end of the drift tube (Figure [Vots and Cohen, 1982]. The flight time for 5 to 10 eV neutrals down a 1-meter tube is about 100 microseconds, and the rotor speed must be about 10,000 rpm for the configuration used here. The chopper can be used as a velocity selector if two slotted disks are mounted with a phase shift between the slots in the blades. Such devices have been built at PPPL and used for experiments with hydrogen neutrals produced by charge exchange within the Princeton Large Torus. The following techniques will also be employed to reduce the background light: (1) the position of the biased limiter over the port will obscure the lineof-sight to the bulk of the plasma (Figure 2), and (2) baffles in the drift tube to block light reflections. The sample will be mounted perpendicular to the drift tube and the line-of-sight will graze the target and pass into a light dump so that only photons from the glow should be detected. Prior to the installation of a rapidly rotating chopper a slow chopper containing open and glass slots can be used to subtract any remaining background light.

Spectroscopy

We estimate a photon source in the visible of $5 \times 10^{10}/\text{sec}$ produced on a sample with an area of 10^2 cm², assuming an efficiency of photon production in the visible of 10^{-6} due to the interaction of the neutrals with the surface. Because most of the glow will appear within 10 cm of the target surface, the photon production rate coefficient within the emitting volume (10^3 cm³) is $\phi = 5 \times 10^7/\text{cm}^3/\text{sec}$. We shall use

calibrated interference and/or color filters with photomultipliers for initial, sensitive broadband detection of glow effects. The sample will be viewed at different angles from 2000 to 9000 Å using two or more calibrated Czerny-Turner spectrometers. The spectra from a 1 cm wide slice of the volume will then be measured with 25 Å resolution using a f/4.8, 0.32 m monochromator with a 1200/mm grating. With this configuration the counting rate in the visible should be 4 × 10² pulses/band/sec assuming a detector quantum efficiency of 0.1 and a light source spread uniformly over a hundred bands from 3500 to 6000 Å. A larger counting rate is expected in the infrared regime, 6000-9000 Å, because the increased photon production due to the neutral-surface interaction will more than offset the decrease in detector sensitivity. Once any glow has been detected, we will observe the spectra with higher resolution and extend the observations into the infrared to 2 microns.

Characterization of the neutral beam is important and an in-line quadrupole mass spectrometer will be employed at the end of the drift tube to determine the relative concentration of atoms and molecules. Initially, the beam intensity will be estimated by the rise in gas pressure at the end of the drift tube. Later we will install a direct low-energy beam monitor, such as a pyroelectric detector.

Experimental Results

Our spacecraft glow experiment began in mid-April and, presently, we are studying the operation and characteristics of a nitrogen plasma. The spectrum of an ACT-I nitrogen plasma over 5000-9000 Å with 8 Å resolution is shown in Figure 3. Structure of bands from the first positive system of N2 can been seen clearly between 5500 and 8000 A. The spectrum shown here rolls off above 9000 A because the GaAs photomultiplier loses sensitivity and below 5000 A because a long pass filter with a 5000 A cutoff was used to eliminate higher order signals in the spectrum. The figure includes a relative sensitivity curve, which must be multiplied by the spectrum intensity to give the relative intensity of the plasma light as a function of wavelength. Higher resolution spectra at 3500-4200 Å (Pigure 4) show the first negative spectrum of No and the second positive spectrum of No. We also see in this figure features which may tentatively be identified as belonging to CN and trace amounts of other carbon containing species. The temperature and density of the bulk plasma in these discharges were ~ 3 \times 10¹² cm⁻³ and T_a ~ 5 eV, and the N₂ filling pressure was ~ 1.6 \times 10⁻⁴ Torr. The plasma was operated in a pulsed mode with 10 ms pulses and a duty cycle of one-half driven by a 5 A electron beam produced by a filament biased to > 200 V. Viewing the plasma by eye shows that the beam is responsible for a large fraction of the optical excitation observed in our data.

A test version of the biased limiter, 2 cm \times 4 cm, was mounted near one of the ports during this startup phase. The current was measured on the limiter to determine the rate at which ions were neutralized. We measured about 1.2 amps of current on the limiter at 20 eV (this voltage should produce 10 eV neutrals), corresponding to a collection rate of 7.5 \times 10¹⁸ ions s⁻¹, or 7.5 percent of the plasma ion source, S₁

[Equation (1)]. We estimate that the maximum plasma volume that this limiter could intercept corresponds to a collection efficiency of 15 percent, and, in practice, should be less. We conclude that the biased limiter is functioning as intended and that when we install a larger limiter a quarter of the ions will be collected in front of the opening to the drift tube.

The drift tube and sample chamber are under construction and will be installed in a few months along with spectroscopic diagnostics. Initially, measurements will be made to characterize the neutral source's composition, flux, density, and velocity, and for the presence of excited states. Various sample materials of the kind tested on spacecraft for glow will be mounted in the test chamber and exposed to the neutral flux. We will search for glow produced by the interaction of nitrogen on the surface and measure its intensity and spectral composition. The effect of impact energy on the glow will be studied by changing the biasing voltage on the limiter.

Acknowledgments. This work was supported by the National Aeronautics and Space Administration Grant No. NAG8-521 and the U.S. Department of Energy Contract No. DE-AC-2-76-CHO-3073.

References

Biersack, J. P., and Haggmark, L.G., A Monte Carlo computer program for the transport of energetic ions in amorphous targets, Nucl. Instrum. Methods, 174, 257, 1980.

Voss, D. E., and Cohen, S. A., Low-Energy Neutral Atom Spectrometer, Rev. Sci. Instrum., 53, 1696, 1982.

Wong, K. L., Ono, M., and Wurden, G. A., ACT-I: A steady-state torus for basic plasma physics research, Princeton Plasma Physics Laboratory Report, No. TM-354, 1981.

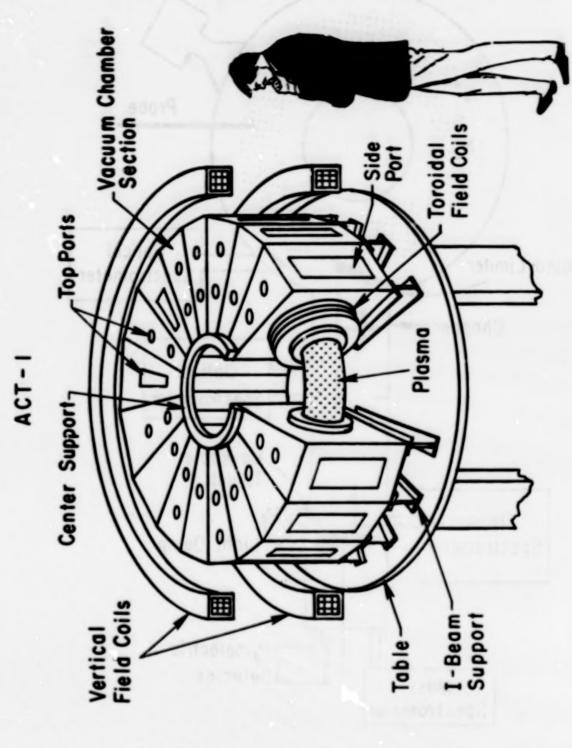


Fig. 1. Schematic of the ACT-I device.

432

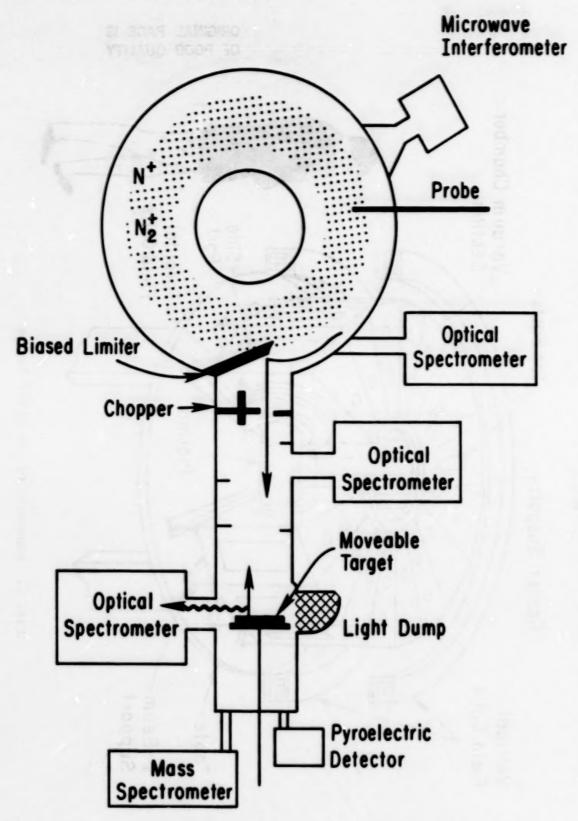
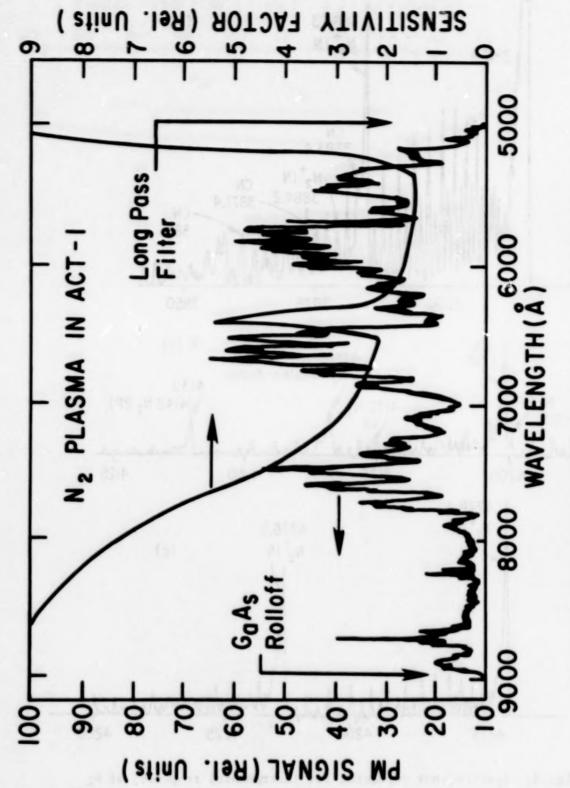


Fig. 2. Schematic of the experiment showing the drift tube, test chamber (not to scale), and diagnostics. The probe and interferometer measure the plasma density and temperature. Baffles (indicated by short lines on the sides) block reflected light.



The spectrum of a nitrogen discharge in ACT-I taken using a double monochromator with a FWHM bandpass of 8 A. The multiplicative sensitivity factor can be used to scale the observed spectral intensity. Fig. 3.

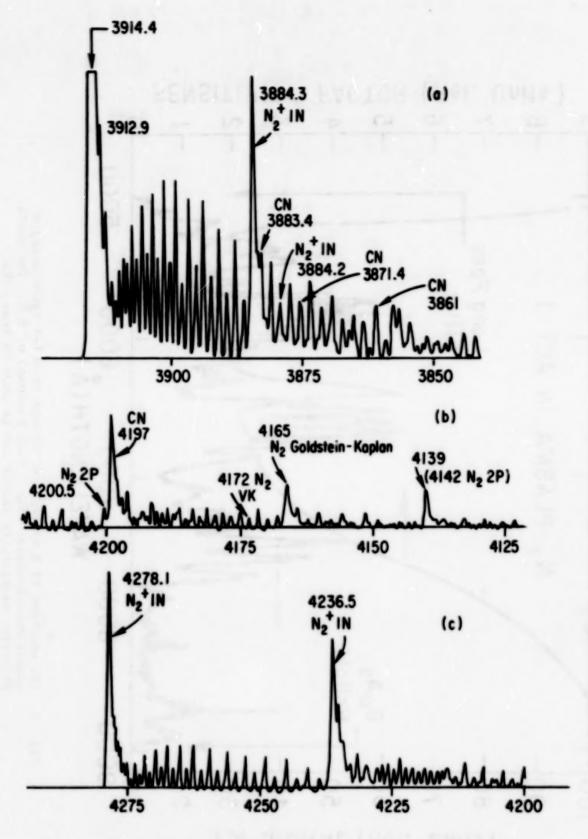


Fig. 4. Spectra, not corrected for instrumental response, of N₂ plasmas in ACT-I using a 0.66 m monochromator with a FWHM bandpass of 0.5 Å. The N² first negative (indicated by 1N) system dominates the spectrum. The shoulders on the 1N(1,1) band may come from CN emission.

TABLE 1. PHYSICAL AND PLASMA CHARACTERISTICS OF ACT-I

			Comments
r	Minor radius:	10 cm	
R	Major radius:	59 cm 1.2 x 10 ⁵ cm ³	
v	Volume:	1.2 x 10° cm	
r_	Plasma radius:	7 cm	
V.	Plasma volume:	6 × 10 cm3	
v _p	Electron density:	6 × 10 ⁴ cm ³ 10 ¹² cm ⁻³ 10 ¹³ cm ⁻³	continuous operation pulsed (20 µsec) with 20% duty cycle
T _e	Electron temperature:	<15 eV	up to 50 eV in the high energy tail
T _i	Ion temperature:	1-5 eV	without rf heating (in H ₂)
T _C	Confinement time:	1 msec	

APPLICATION OF AN ATOMIC OXYGEN BEAM FACILITY TO THE INVESTIGATION OF SHUTTLE GLOW CHEMISTRY

Graham S. Arnold and Daniel R. Peplinski

Chemistry and Physics Laboratory The Aerospace Corporation El Segundo, California

Abstract. A facility for the investigation of the interactions of energetic atomic oxygen with solids is described. The facility is comprised of a four-chambered, differentially pumped molecular beam apparatus which can be equipped with one of a variety of sources of atomic oxygen. The primary source is a DC arc-heated supersonic nozzle source which produces a flux of atomic oxygen in excess of 10¹⁵ cm⁻² sec⁻¹ at the target, at a velocity of 3.5 km sec⁻¹. Results of applications of this facility to the study of the reactions of atomic oxygen with carbon and polyimide films are briefly reviewed and compared to data obtained on various flights of the space shuttle. A brief discussion of possible application of this facility to investigation of chemical reactions which might contribute to atmosphere-induced vehicle glow is presented.

Introduction

A spacecraft in the altitude range of 200-700 km experiences bombardment by an atmosphere whose primary constituent is neutral atomic oxygen [Hedin et al., 1977]. Although the ambient gas temperature is only on the order of 1000 K, the 8 km sec⁻¹ velocity of the spacecraft causes the oxygen atoms to strike satellite surfaces at a relative kinetic energy of 500 kJ mole⁻¹ (5 eV). At shuttle altitudes, the atomic oxygen density is on the order of 10⁹ cm⁻³, which corresponds to a flux of about 10¹⁵cm⁻² sec⁻¹. These conditions present a regime of gas-surface chemistry which has been the subject of very little experimental investigation because of the difficulties inherent in reproducing them in the laboratory. A variety of effects observed on NASA and USAF spacecraft have been ascribed to the action of the ambient atmosphere. These include material erosion [Leger et al., 1983, 1984], optics degradation [Arnold et al., 1982], and luminescence [Banks et al., 1983; Yee and Abreu, 1983].

This paper describes a facility assembled specifically for the investigation of the interactions of energetic atomic oxygen with solid surfaces. The major elements of this facility, which are described below, are the four-chambered, differentially pumped molecular beam apparatus, the provisions for mounting and interrogating solid samples, and the DC arc-heated supersonic atomic beam source. Results of experimental work using this facility which demonstrate its utility in

performing its appointed task are briefly presented along with a brief assessment of the potential for application of this facility to investigation of chemistry which may contribute to vehicle glow.

Facility Description

Vacuum System

Figure 1 shows a schematic representation of the molecular beam apparatus. The vacuum system is comprised of four differentially pumped stainless steel chambers. The first three chambers are 0.46 m³ boxes equipped with Viton or Buna-N "O-ring" seals. Each is pumped by an oil diffusion pump. The pumps on the second and third chambers are equipped with gate valves and liquid nitrogen cooled baffles.

The fourth chamber is a cylindrical clean chamber utilizing crushed metal seals. It is recessed into chamber 3 to reduce the total length of the facility (as measured from the source). This chamber is equipped with a high vacuum gate valve (Huntington model GVAP-600) and a 570 l-sec turbomolecular pump (Balzers model TPU 510). The turbomolecular pump is used in preference to more conventional UHV pumping technology because of the large helium load which this chamber must bear.

Sample and Analysis Systems

The facility is equipped with a quadrupole mass spectrometer (Extranuclear Laboratories, Inc.) comprised of a crossed-beam electron-impact ionizer, a quadrupole mass filter with 17 mm diameter rods, and a Johnston MM-I particle multiplier. The mass spectrometer has been used so far only for beam source characterization.

When solid samples are to be bombarded, they may be mounted either in chamber 2, when it is desirable to maximize the available beam flux on target, or in chamber 4 when sample cleanliness is the paramount concern. A liquid nitrogen cooled shroud surrounds samples in chamber 2 to inhibit contamination. The beam is typically collimated to subtend a circular spot of approximately 7 mm in diameter when samples are mounted in this shroud, however, spots as large as 17 mm are possible. A three-axis-plus-rotation precision manipulator is provided for mounting solid samples. Active temperature control on the range of 300-450 K is typical.

The only in situ diagnostics currently available in this facility are optical. Transmission measurements of samples mounted in either location are possible. Figure 2 shows a schematic representation of the optical path for transmission measurements in chamber 4. Ultraviolet transmission has been used to measure the rate of oxidation of carbon by high velocity atomic oxygen [Arnold and Peplinski, 1984a] and infrared transmission has been used to measure the effect of atomic oxygen on clean and contaminated infrared optics [Arnold et al., 1982].

Atomic Oxygen Sources

The primary beam source used in this facility is a DC arc-heated supersonic nozzle source which relies on a modified, commercially available plasma torch. The beam source has been described in detail elswhere [Silver et al., 1982; Arnold and Peplinski, 1984b]. Typical beam source operating conditions and performance specifications are summarized in Table 1.

Two other beam sources for producing atomic oxygen are available for use in this facility: a microwave discharge source [Arnold et al., 1982] and a resistively-heated thermal dissociation source [Henderson et al., 1969] for which iridium or rhenium source tubes with a variety of orifice diameters are available. Both sources are capable of producing substantial fluxes of atomic oxygen, but with velocities on the order of 1 km sec 1. These lower velocity sources are needed to gain a more complete understanding of the kinetics of the reactions of atomic oxygen with solids.

All three of the sources produce light as well as atomic beams. This light presents a potential interference to experiments aimed at measuring luminescence. In the case of the microwave discharge source, this problem can be circumvented by introducing a bend in the source between the discharge region and the nozzle. For the other two sources this is not possible.

Since the beam from either the DC arc source or the thermal dissociation source is comprised of neutral atoms and molecules, separation of the beam from the light can only be readily effected by a mechanical chopper. A two-segment slotted-disk velocity selector of 40% nominal transparency has been designed for this facility [Fluendy and Lawley, 1973]. The role of this device is not to prepare a beam of narrow velocity distribution, but merely to block species, such a photons, traveling at velocities in excess of the selected velocity. Since the selector has only two disks, it naturally has an infinite number of low-velocity side bands. This device has not heretofore been used for experiments performed in this facility.

Facility Applications

Reaction of Atomic Oxygen with Solids

This facility has been used to investigate the rate of reaction of atomic oxygen with two types of carbon [Arnold and Peplinski, 1984a, 1985a] and with Kapton film, a polyimide material manufactured by E.I. du Pont de Nemours & Co., Inc. [Arnold and Peplinski, 1985b] The results of these investigations are summarized very briefly below.

Carbon. Pigure 3 shows an Arrhenius plot (in carbon surface temperature) of the probability of reaction of atomic oxygen with carbon including data from ground-based measurements and flight experiments and other observations from various flights of the space shuttle. The reaction probability plotted is defined as the probability that an oxygen atom impact will remove a carbon atom from the surface,

regardless of its final state of aggregation. (For a detailed discussion of these data the reader should consult [Arnold and Peplinski, 1984a] and works cited therein.)

The open circles and open triangle represent the results of measurements performed in this facility. The dashed line labeled "Park" is a fit to several laboratory measurements of the rate of reaction of atomic oxygen with various forms of carbon, under more or less thermal conditions [Park, 1976]. The other data include limits on the reaction probability inferred [Arnold and Peplinski, 1984a] from removal of carbon surfaces on the STS-3 Plasma Diagnostics Package (G.B. Murphy. University of Iowa, Department of Physics and Astronomy, Iowa City, IA, private communication, 1982) and on the STS-4 Marshall Space Flight Center's Induced Environment Contamination Monitor Passive Sample Array [Peters et al., 1983], a probability calculated from the observed thickness loss of vitreous carbon included on the STS-5 Evaluation of Oxygen Interaction with Materials (EOIM) passive sample array [Arnold and Peplinski, 1985a], and the reaction probability calculated from the observed rate of mass loss from and amorphous carbon-coated temperaturecontrolled quartz crystal microbalance on the Goddard Space Flight Center's Contamination Monitor Package flown as a "Get-Away Special" on STS-8 (J.J. Triolo, NASA/Goddard Space Flight Center, Greenbelt, MD, private communication, 1984).

These data lead one to the conclusion that the rate of reaction of atomic oxygen with carbon, at collision energies of up to 100 kJ mole⁻¹ (1 eV), does not depend strongly on the translational energy of impact. Indeed when one compares laboratory and flight data for similar samples of carbon, the evidence that rates occurring on-orbit are significantly different from the thermal rate of reaction of 0 atoms with carbon is not strong. However, the results of Gregory and Peters (not shown on Figure 4), who infer probabilities in excess of 0.1 from STS-8 EOIM results, militate against drawing an unambiguous conclusion in this matter (J. C. Gregory, Chemistry Department, the University of Alabama at Huntsville, private communication, 1985).

Kapton. Table 2 shows a comparison between the average probabilities for the reaction of atomic oxygen with Kapton measured in this facility [Arnold and Peplinski, 1985b] and inferred from the STS-5 and STS-8 EOIM experiments [Leger et al., 1983, 1984]. In this case, the reaction probability is conventionally defined as the thickness of material removed divided by the fluence of atomic oxygen incident on the sample.

The agreement between the laboratory and flight data is quite good in comparison to the uncertainties in the various data. This relatively good agreement suggests that there is not a great dependence on 0 atom impact energy of the average efficiency of the reaction of atomic oxygen with Kapton over a range of impact energy from 1 to 5 eV.

Luminescent Reactions

Several possible contributing mechanisms have been proposed to explain the vehicle glow phenomenon. These include surface catalyzed recombination of atmospheric radicals [Torr et al., 1977; Reeves, 1982],

production of excited products from oxygen reactions with materials [Slanger, 1983], recombination collisionally dissociated of nitrogen [Green, 1984], and vehicle plasma interactions [Papadopoulos, 1984].

Considering the complexity of the problem and the scarcity of unambiguous data, one cannot yet make any definitive assessment of the relative importance of these various processes in creating the observed glows. However, one can proceed reasonably to investigate these processes experimentally, with both flight and laboratory experiments. It is a valid and important point that there appears to be no way to simulate the "shuttle glow" in the laboratory. The shuttle environment is too complex and uncertain. However, simulation is not necessarily the proper function of laboratory investigations of spacecraft environmental phenomena. Rather, their role is to elucidate mechanistic details which are difficult to address in flight experiments on account of operational constraints, background interferences, scarcity of opportunities, or expense.

Visible luminescence from surface catalyzed excitation. In the earliest published reference to atmosphere-induced vehicle glow [Torr et al., 1977], it was hypothesized that recombination of adsorbed atmospheric 0 and NO to produce excited NO₂ in the gas phase was responsible for the observed visible emission. This explanation has subsequently been proposed repeatedly. [Reeves, 1982; Mende and Swensen, 1985].

The production of excited products by surface catalyzed radical recombination is a well-documented phenomenon [Mannella and Harteck, 1961]. However, both Mende and Swenson and Torr et al. have suggested that for the 0 + NO recombination luminescence to account for the majority of the observed glows, the spectrum of the NO₂ product must be shifted compared to the spectrum obtained from 3-body gas-phase recombination [Golde et al., 1973]. There is not sufficient information from experiments in which the spectrum of the product NO₂ is not perturbed by subsequent gas-phase collisions to answer whether this mechanism is important in the creation of the observed shuttle glow.

Clearly one wishes to investigate the luminescence from surfacecatalyzed NO₂ production under "single collision" conditions so that one measures the spectrum of the nascent products. This suggests that molecular beam techniques be used. A schematic representation of such an experiment is shown in Figure 4.

One may estimate the signal from such an experiment as follows. The number density of NO₂ product near a surface on which O and NO are recombining may be formally expressed as

$$[NO_2^*] \approx k_1 F_0 [NO_{ads}]/v_1 + k_2 F_{NO} [O_{ads}]/v_2 + k_3 [O_{ads}] [NO_{ads}]/v_3$$
 (1)

where three different processes are considered to be operational:

1. Reaction of an incident O atom with an adsorbed NO molecule;

- 2. Reaction of and incident NO molecule with an adsorbed O atom;
- 3. Reaction of an adsorbed 0 atom with an adsorbed NO molecule.

In equation (1) the rate coefficients k_1 and k_2 have units of area (reaction cross-section) and k_3 has units of area/time (like a diffusion coefficient). The quantities v_1 are the average velocities with which the product is ejected as a result of each of the three formation processes.

In practice, to make a rough estimate of the photon emission rate from such an experiment, one approximates equation (1) by assuming that the NO₂ production rate will be limited by one or the other of the reagent fluxes. Therefore one obtains

$$[NO_2^*] = pF_1/\langle v \rangle \tag{2}$$

where F_1 is the limiting flux, p is some effective probability, and $\langle v \rangle$ is an average velocity of the product.

If one approximates the volume emission rate as $[NO_2^*]$ divided by the average radiative lifetime, τ_{rad} , and assumes collection with f/l optics from an 0.5 cm volume, then the rate at which photons fall on the detector per unit wavelength, S, is given by

$$s = \frac{17_1}{10 \langle v \rangle_{T_{rad}} \Delta \lambda}$$
 (3)

If one presumes that it is the 0 atom flux that limits the reaction rate, then one needs to envoke a value of about 10^{-7} for p to rationalize the orbital observations. In this facility 0 atom fluxes on the range of 10^{14} – 10^{15} cm⁻² sec⁻¹ are easily realized. The product $\langle v \rangle_{T}$ can be expected to range from 3-20 cm. The bandwidth, $\Delta \lambda$, is expected to be approximately 3000 Å. Thus total photon arrival rates range from 10–1000 photon/Å/sec. Using cooled, a red-sensitive photomultiplier tube, with photon counting detection, measurement of a moderately well resolved spectrum at these signal levels should be possible.

Infrared Luminescence

The observation of moderately intense luminescence in the visible near spacecraft surfaces naturally raises the question of whether there is also a significant infrared component associated with the glow. At least one of the proposed mechanisms for glow production suggests such to be the case [Slanger, 1983]. Observation of the shuttle from the ground suggests that there may be more near infrared emission from the shuttle than can be explained by thermal emission or scattering from other sources (F. Witteborn, NASA/Ames Research Center, private communication, 1985).

The long lifetimes associated with infrared emission render the laboratory investigation of infrared luminescence under "single collision conditions" difficult. Excited molecules tend to leave the

detector field-of-view or to strike chamber walls in times much less than their radiative lifetimes. Newever, the technology for direct, laser-induced fluorescence (LIF) measurement of internal state distributions of reaction products, from which one may readily calculate net emission spectra, is well established [Kinsey, 1977]. Recently this technology has begun to find application in gas-surface scattering research [Cardillo, 1985].

Because of the wide use of carbon, carbon-filled, and carbon-containing materials on spacecraft surfaces, the internal state distribution of the CO product of the $0 + C_{\rm S}$ reaction is of interest. Since LIF is a number density detector, one again needs to estimate the number density or "effective pressure" of products to ascertain whether a measurement is feasible. This number density is given by

$$[CO] \cong pF_0/v_{CO} \tag{4}$$

where p is the reaction probability, F_0 is the flux of atomic oxygen, and v_{CO} is the product velocity. For a reaction probability of 0.01, a flux of 4 x 10^{14} cm 2 sec $^{-1}$, and a thermal product velocity, one estimates the CO number density to be approximately 8 x 10^7 cm $^{-3}$, which is roughly equivalent to a pressure at room temperature of 3 x 10^{-9} Torr.

Detection of CO internal state distributions by LIF can be accomplished by excitation of the A-X transition at approximately 148 nm. Hepburn has reviewed the technology for coherent VUV generation for this application [Hepburn, 1984]. He estimates the detection limit for CO (at 300 K) to be 10⁻¹⁰ Torr. Thus, by the application of established technology, a useful experiment to assess the potential for non-thermal infrared luminescence from vehicles in LEO is feasible.

Summa ry

A facility which has proven to be useful in the investigation of oxygen atom interaction with materials has been described. Order-of-magnitude estimates of signal strengths suggest that this facility will be useful in the investigation of surface-catalyzed excitation reactions and of energy disposal in gas-solid reactions which produce volatile products. Both of these processes have been suggested as contributors to the "shuttle glow."

Acknowledgments. This work was supported by the Aerospace Sponsored Research program.

References

Arnold, G.S., and Peplinski, D.R., Reactions of high velocity atomic oxygen with carbon, AIAA 22nd Aerospace Sciences Meeting, Reno, NV, AIAA Paper #84-0549, 1984a.

- Arnold, G.S., and Pelinski, D.R., A facility for Investigating interactions of energetic atomic oxygen with solids, 13th Space Simulation Conference, NASA Conference Publication 2340, pp. 150-168, 1984b.
- Arnold, G.S., Peplinski, D.R., and Herm, R.R., Atmospheric effects in low Earth orbit and the DMSP ESA offset anomaly, SD-TR-82-81, The Aerospace Corporation, El Segundo, CA, 1982.
- Arnold, G.S., and Peplinski, D.R., Reaction of atomic oxygen with vitreous carbon laboratory and STS-5 data comparisons, AIAA Journal, in press, 1985a.
- Arnold, G.S., and Peplinski, D.R., Reaction of atomic oxygen with polyimide films, AIAA Journal, accepted for publication, 1985b.
- Banks, P. M. Williamson, P. R., and Raitt, W. J., Space shuttle glow observations, Geophys. Res. Lett., 10(2), 118-121, 1983.
- Cardillo, M. J., Concepts in gas-surface dynamics, Langmuir, 1(1), 10-23, 1985.
- Fluendy, M.A.D., and Lawley, K.P., Chemical Applications of Molecular Beam Scattering, Chapman and Hall, London, pp. 97-104, 1973.
- Golde, M.F., Roche, A.E., and Kaufman, F., Absolute rate constant for the 0 + NO chemiluminescence in the near infrared, SRCC Report #187, University of Pittsburgh, Pittsburgh, PA, 1973 (and references cited therein).
- Green, B.D., Atomic recombination into excited molecular states-A possible mechanism for Shuttle glow, Geophys. Res. Lett., 11, 576-579, 1984.
- Hedin, A.E., Reber, C.A., Newton, G.P., Spencer, N.W., Brinton, H.C., Mayr, H.G., and Potter, W.E., A global thermospheric model based on mass spectrometer and incoherent scatter data MSIS 2, composition, J. Geophys. Res., 82, 2148-2156, 1977.
- Henderson, W.R., Fite, W.L., and Brackmann, R.T., Dissociative attachment of electrons to hot oxygen, Phys. Rev., 183, 157-166, 1969.
- Hepburn, J.W., Coherent vacuum ultraviolet in chemical physics, CP-244 (Beams 83-7), University of Waterloo Chemical Physics Research Report, Waterloo, Ontario, Canada, 1984.
- Kinsey, J.L., Laser induced fluorescence, Annual Rev. Phys. Chem., 28, 349, 1977.

- Leger, L.J., Spiker, I.K., Kuminecz, J.F., Ballentine, T.J., and Visentine, J.T., STS flight 5 LEO effects experiment, background description and thin film results, AIAA Shuttle Environment and Operations Meeting, Washington, D.C., AIAA Paper #83-2631-CP, 1983.
- Leger, L.J., Visentine, J.T., and Kuminecz, J.F., Low Earth orbit atomic oxygen effects on surfaces, AIAA 22nd Aerospace Sciences Meeting, Reno, NV, AIAA Paper #84-0548, 1984.
- Mannella, G., and Harteck, P., Surface-catalyzed excitations in the oxygen systems, J. Chem. Phys., 34 (6), 2177-2180, 1961 (and references cited therein).
- Mende, S.B., and Swensen, G.R., Measurements of vehicle glow characteristics during STS 41-D, AIAA Paper #85-0475, AIAA 23rd Aerospace Sciences Meeting, Reno, NV, 1985.
- Papadopoulos, K., Shuttle glow (the plasma alternative), Radio Sci., 19, 576-579, 1984.
- Park, C., Effect of atomic oxygen on graphite ablation, AIAA Journal, 14, 1640-1642, 1976.
- Peters, P.N. Linton, R.C., and Miller, E. R., Results of apparent atomic oxygen reactions on Ag, C, and Os exposed during the Shuttle STS-4 orbits, Geophys. Res. Lett., 10, 569-571, 1983.
- Reeves, R.R., Surface catalyzed excitation-Laboratory observations of solid catalyst induced molecular light emission in atomic oxygen and/or atomic nitrogen environment, NASA Induced Shuttle Luminosity Meeting, McLean, VA, 1982.
- Silver, J.A., Freedman, A., Kolb, C.E., Rahbee, A., and Dolan, C.P., Supersonic nozzle beam source of atomic oxygen produced by electric discharge heating, Rev. sci. Instrum., 53(11), 1714-1718, 1982.
- Slanger, T.G., Conjectures on the origin of the surface glow and space vehicles, Geophys. Res. Lett., 10, 130-132, 1983.
- Torr, M.R., Hays, P.B., Kennedy, B.C., and Walker, J.C.G., Intercalibration of airglow observatories with the Atmosphere Explorer Satellite, <u>Planet. Space Sci.</u>, 25, 173-184, 1977.
- Yee, J.H., and Abreu, V.J., Visible glow induced by spacecraftenvironment interaction, Geophys. Res. Lett., 10, 118-121, 1983.

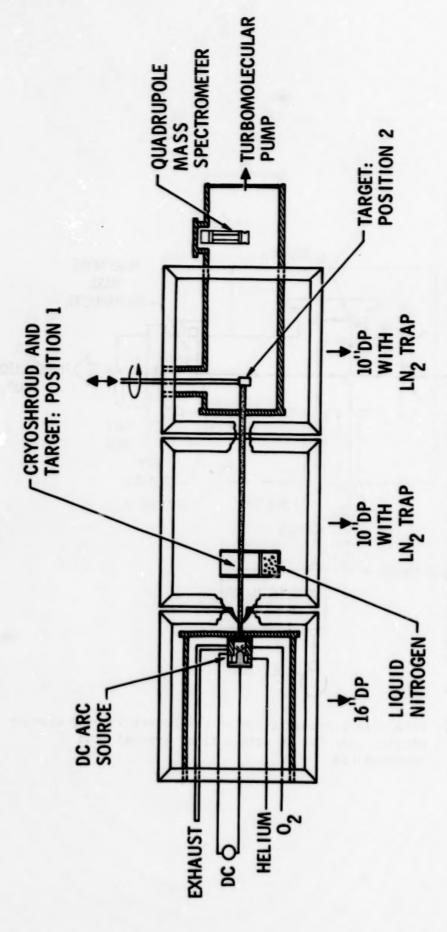


Fig. 1. Schematic representation of the atomic oxygen beam facility.

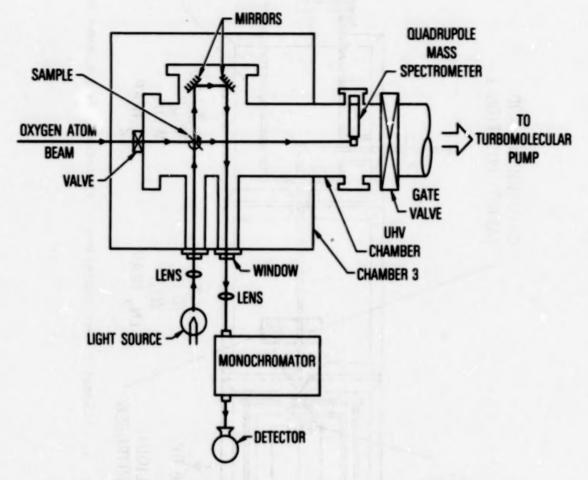


Fig. 2. Schematic representation of the fourth (clean) chamber showing path for in situ optical transmission measurements.

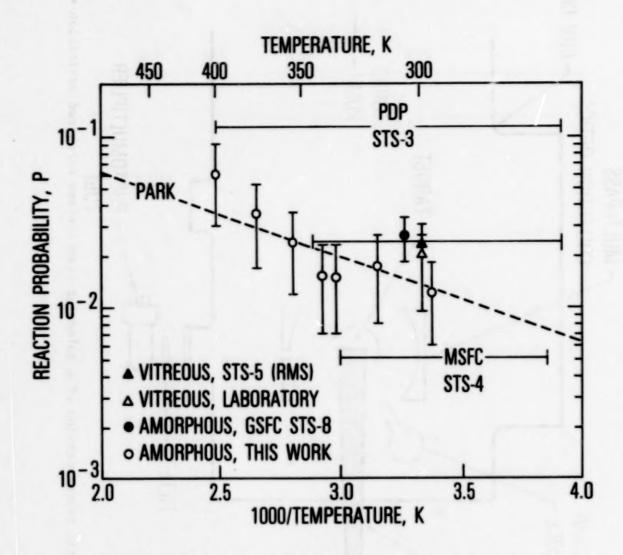


Fig. 3 Arrhenius plot (in carbon surface temperature) of the probability of the reaction of atomic oxygen with carbon. Various laboratory and flight data are shown. (See text.)

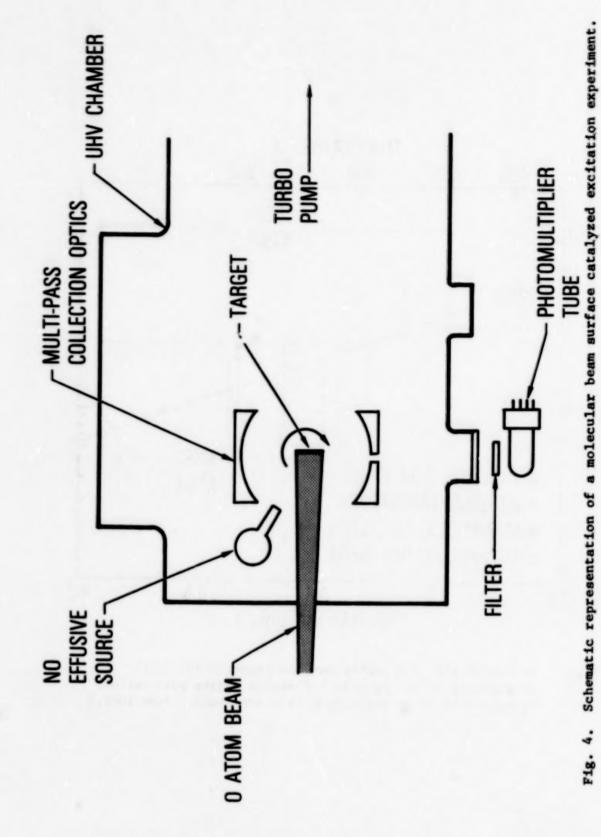


TABLE 1. TYPICAL BEAM SOURCE CHARACTERISTICS

Feed Gas	He:0 ₂ /98:2
Flow Rate	265 SCFH (2 1-atm sec 1)
Power Dissipated	16 kW
O Flux on Targeta	$5.0 \times 10^{15} \text{ cm}^{-2} \text{sec}^{-1}$
02 Flux on Targeta	7.5x10 ¹⁵ cm ⁻² sec ⁻¹
Beam Velocity (oxygen atoms)	3.5 km sec ⁻¹

Target mounted in chamber 2; see Figure 1.

TABLE 2. COMPARISON OF LABORATORY AND FLIGHT MEASUREMENTS OF THE AVERAGE PROBABILITIES FOR THE REACTION OF ATOMIC OXYGEN WITH KAPTON

Kapton Temperature (k elvin)	La boratory ^a	Reaction Probability 10 ⁻²⁴ cm ³ /O atom	
		STS-5b	STS-8 ^c
300	2.1+1.1 1.7+0.9	2.3+0.9	
338	1.4+0.9	2.0+0.8	3.0+1.2
393	1.5+0.9	2.1+0.9	2.9+1.2

Arnold and Peplinski [1985b].

See Table 3 of Leger et al. [1983]; Nominal uncertainty is +40%.

See Table 5 of Leger et al. [1984]; Nominal uncertainty is +40%.

FUTURE EXPERIMENTS

PRECEDING PAGE BLANK NOT FILMED

AN ASSESSMENT OF THE IMPACT OF SPACECRAFT GLOW ON THE HUBBLE SPACE TELESCOPE

John T. Clarke Space Telescope Project NASA Marshall Space Flight Center

Summary of Existing Observations and Theory

Visible spacecraft glow was first observed on the Atmospheric Explorer spacecraft by Torr [1983] and studied in some detail with the Visible Airglow Experiment (VAE) on the AE-E spacecraft by Yee and Abreu [1983]. The AE-E was a spin-stabilized spacecraft without thrusters at an altitude of 140-280 km. The VAE contained six visible-wavelength photometers that measured a glow spectrum which: a. rose steeply in the red, b. decreased with a cos dependence from pointing into the ram direction of the spacecraft orbital motion, and c. decreased in intensity with increasing altitude with the same dependence as the measured atomic oxygen number atmospheric density [O] and not with the measured molecular nitrogen density [Na]. Yee and Abreu [1983] proposed that the glow is produced by chemical reactions on the spacecraft surface as it sweeps through the atmospheric O, with roughly 5-8 eV per O atom available for excitation from the orbital motion of the spacecraft. This glow may in principal be produced by any of a number of species, including molecular band emission from OH, NO, and NO, (see Figure 1). The physical picture for the estimation of the surface brightness of the glow emanating above a surface is therefore:

column photon production = [0] x (orbital speed) x (efficiency)

where: [0] at 590 km =
$$4 \times 10^{5}$$
 cm⁻³ (solar min average)
[0] at 590 km = 3×10^{7} cm⁻³ (solar max average)

and the efficiency for optical photon production (4000-8000Å) is 10⁻⁵ to 10⁻⁶ (measured on STS-3 and AE-E).

It has been proposed by Slanger [1983] and by Langhoff et al. [1983] that the observed glow on AE-E is from the excitation of the OH Meinel band system, which may be capable of producing all of the observed glow above 160 km altitude. This identification is supported by the detection of two spectral lines of the OH system with the Fabry-Perot spectrometer on the Dynamics Explorer [Abreu et al., 1983]. The existence of OH band emission would imply that there exists a much brighter near-IR glow than observed to date in the visible (see Figure 2), and thus poses a risk for the development of second-generation IR SI's for Space Telescope.

Observations on the shuttle indicate that there are several different "glows" operating, and the functional dependencies governing the brightness of these different glows are not well understood. The situation is complicated by the existence of thruster firings on the shuttle, as well as the generally larger size of the spacecraft and resulting greater residual atmosphere and induced plasma and spacecraft charging. The early pictures of the shuttle tail and aft bulkhead taken on STS-3,-4,-5, and -9 revealed a glow which varied in brightness with the surface material, varied with

the timing with respect to the thruster firings, showed a cos 1/2 dependence in brightness with pointing away from the orbital ram direction, and exhibited a spectrum similar to that observed on AE-E. Ground-based imaging of STS-9 at wavelengths of 1.6 and 2 microns detected the shuttle (as a whole) only at 2 microns, as would be expected from OH band emission, but the intensity of the emission was uncertain due to tracking difficulties [Witteborn et al., 1985]. A hand-held movie camera operated by Owen Garriott revealed a dramatic brightening of the shuttle tail and aft bulkheads following the firings of the vernier thrusters. This emission appeared a few seconds after the thrusters fired and decayed a few seconds later. However, the surface glow has been observed on the shuttle even when the thrusters were not firing (STS-3). Two far-UV cameras flown on Spacelab 1 (FAUST and WFC) both showed considerable fogging of their film, which may have been due to any of a combination of atmospheric twilight emissions, tropical arc OI 1304 and 1356 & emissions, or an additional far-UV glow on the Shuttle.

Moderate resolution (3-6 Å) spectroscopy was performed on the STS-9 mission with the Imaging Spectrometric Observatory (ISO) from 1150-8000 A [Torr and Torr, 1985]. Specific observations for glow were performed in a dedicated pointing into the ram direction and tangent to the Earth at an altitude of 250 km, although the instrument did not view any direct surfaces. The ISO spectrometers were capable of detecting line and/or band emission but not continuum glow due to uncertain detector background caused by rapid temperature changes. The detected UV and visible spectra are shown in Pigures 3 and 4. The emissions shown in these spectra are a combination of atmospheric and potential glow emissions: more detailed analysis of these data will be required to identify which of the observed features may be due to glow. The visible band emission observed from 4000-8000 Å has a spectral slope consistent with that observed on AE-E, but the brightness of the visible glow reported at 250 km is similar to that observed by AE-E at 140-145 km. These band spectra suggest a contribution from the N, first positive system, and at different times the brightness of the emission at all wavelengths was observed to vary by at least an order of magnitude.

Theoretical studies of the glow have been performed to study the physical processes responsible for the glow. Yee and Dalgarno [1983] have determined the lifetime(s) of the glowing species (0.3 ms) from the spatial decay of the emission above the shuttle surface [Banks et al., 1983]. They conclude that OH band emission is unlikely to explain all of the observed shuttle glow, but may still radiate strongly in the IR. Swenson et al. [1985] propose NO, recombination continuum as the dominant source of radiation based on energetic arguments and the apparent lack of band structure in the glow at 30 Å resolution from 4000-8000 Å. There are no near-IR observations available to test either of these hypotheses. Torr and Torr [1985] identify N, first positive band emission from their STS-9 spectra. There is additionally a plasma theory for the glow, in which a surface plasma layer heated by non-linear plasma-wave interactions provides the glow excitation. The required plasma density is known to exist near the shuttle, but only under sunlit conditions, and the AE-E glow data showed no dependence on daytime/nighttime electron density variations [Yee et al., 1985]. The plasma theory also predicts blue/UV enhanced glow emission, which has never been observed.

Scaling Observed Glows to Space Telescope

Accurately scaling the observed glows to Space Telescope requires much better information about the physical processes producing the glow and the functional dependencies of the glow brightness than is currently available. Many different species have been proposed as glow emitters (OH, NO₂, NO, No₂), making the spectral character of the glow uncertain. The glow brightness is believed to depend on atmospheric density, which varies quite strongly with solar activity at a given altitude (see Figure 5). Other functional dependencies to be determined are:

- -the quantitative effect of thruster firings (not an issue for ST other than to interpret shuttle glow observations)
- -changes in the glow spectrum during thruster firings
- -dependence of glow on spacecraft size
- -dependence of glow on spacecraft materials and cleanliness
- -dependence of glow on angle to the orbital ram direction
- stence of extended glow above spacecraft surfaces

It must be concluded that the extrapolation to ST will be very uncertain until these factors are better understood. For example, the difference in scaling the observed glow brightnesses from AE-E and the ISO to ST altitudes by [O] is shown in Figure 6.

The actual contamination by glow in the focal plane of the Space Telescope depends not only on the surface brightness of the glow above a particular surface but also on the extent of the glow above each surface and how well the emission is baffled and thus prevented from reaching the focal plane. As long as the glow is confined to 10-20 cm above any given surface, the ST is a very well-baffled telescope and relatively little of that flux will penetrate to the focal plane. If any glow extends into the OTA field-of-view of the sky, however, the presumably isotropically emitting glow will be competing directly with the sky background to contaminate ST data. Perkin-Elmer has performed an analysis of the contribution to the total focal plane flux made by surface-localized glow using the following assumptions:

- [0] = 3 x 107 cm-3 (average solar max conditions)
- photon production efficiency 1-3 x 10-5
- glow extends 20 cm above the surface

These efficiencies were roughly measured for the ST materials (Chemglaze Z306 and anodized aluminum) on previous shuttle flights, but no information is available on the glow of Al+MgF₂. The predicted focal plane fluxes are plotted in Figure 7 as a function of angle to the ram direction. The case within 15° of upwind is uncertain since we do not know how the primary mirror will glow under direct exposure to the ambient atmospheric ram, but this will hopefully never be put to the test in flight. At all other angles the focal plane glow flux is predicted to be safely below the average sky background level of roughly 23 mag/arc sec.

The tolerable levels of extended glow emission (where "tolerable" is defined as less than or equal to the sky background) are plotted in Figure 8 as a function of wavelength in the aeronomer's units of Rayleighs/Å. Comparison with Figure 6 shows that even direct viewing glow emission should not be a problem due to the decreased [O] at 590 km. If the glow is somewhat extended and brightens in the near-IR (neither of which would be a particular surprise), however, the glow may be the limiting factor on ST sensitivity in the near-IR spectral range. An additional illustration of

the relation between glow brightness and ST detection limits is shown in Figure 9 as a plot of the sky brightness equivalent to the flux in one planetary camera (PC) pixel that would be received from the representative blue spectrum of a hot star or QSO of m = 30, which is in turn equal to the sky background per PC pixel at 5500 Å.

Work Needed to Address Immediate Concerns for Space Telescope

The information required for Space Telescope can be divided into the near-IR, visible, and UV spectral ranges. Although a better understanding of the glow phenomenon is unlikely to influence any ST hardware at this stage of the program, the existence and characteristics of any unacceptably bright glow emissions will affect both ST operations and the planning for second-generation SI's. The ST project recommendations are therefore aimed at addressing the following problems before ST launch:

1. The existence and brightness of any near-IR glow.

The indication from the existing visible spectra is that the maximum glow brightness will be observed in the near-IR spectral range. The region from 8000 Å to 5 microns is of great interest in planning for second-generation SI's and has never been observed for glow! Spectroscopy at these wavelengths is also crucial to identifying the emitting species and excitation conditions, including knowing the lifetimes of the excited states which in turn determines the extent of the glow above a surface. It should also be noted that the different theories for molecular glow predict vastly different brightnesses in the near-IR.

2. Validate the brightness and altitude dependence of the visible glow.

Although the rough spectrum of the glow from 4000-8000 Å is known, the brightness of the glow above any given surface is uncertain by 1-2 orders of magnitude due to our lack of knowledge of the excitation processes. Other factors to be studied are listed in the conclusion of this section.

3. Does there exist a UV glow?

The visible spectra suggest that the brightness of the continuum glow is decreasing into the UV, and upper limits to any UV glow derived from earlier spaceborne airglow spectrometers indicate that there is no bright UV continuum glow. None of the earlier instruments looked at surfaces exposed to the ram, however, and it is conceivable that known atmospheric UV line and band emissions may be enhanced by the passage of spacecraft through the atmosphere. Candidate atmospheric emissions are OI 1304 Å and 1356 Å (which are known to be particularly bright in the tropical arcs at +15 magnetic latitude), NO gamma and delta bands (1900-2400Å), N₂ Lyman-Birge-Hopfield bands (roughly 1000-2000Å), and various lines of NI and N₂.

For all spectral regions the functional dependencies need to be determined between glow brightness and:

-atmospheric density and species

-angle of pointing to the ram vector (including possible wake glow)

-surface material and composition

- -spacecraft charging and outgassing
- -distance above the surface (lifetimes of excited states)

-relation to thruster firings

References

Abreu, V. J., W. R. Skinner, P. B. Hays, and J. H. Yee, in Proceedings of the AIAA Shuttle Environment and Operations Meeting, p. 178, Paper #83-2657, AIAA, New York, 1983.

Banks, P. M., P. R. Williamson, and W. J. Raitt, Geophys. Res. Lett., 10, L118, 1983.

Dube, R. R. W. C. Wickes, and D. T. Wilkinson, Astrophys. J. Lett., 215, L51, 1977.

Langhoff, S. R., R. L. Jaffee, J. H. Yee, and A. Dalgarno, Geophys. Res.

Lett., 10, L896, 1983.

Mende, S. B., O. K. Garriott, and P. M. Banks, Geophys. Res. Lett., 10, L122, 1983.

Slanger, T. G., Geophys. Res. Lett., 10, L114, 1983.

Swenson, G. R., S. B. Mende, and K. S. Clifton, Geophys. Res. Lett., 12, L97, 1985.

Torr, M. R., Geophys. Res. Lett., 10, L114, 1983.

Torr, M. R., and D. G. Torr, J. Geophys. Res., 90, 1683, 1985.
Witteborn, F. C., K. O'Brien, and L. Caroff, J. Geophys. Res., submitted, 1985.

Yee, J. H., and V. J. Abreu, Geophys. Res. Lett., 10, L126, 1983.

Yee, J. H., and A. Dalgarno, in Proceedings of the AIAA Shuttle Environment and Operations Meeting, Paper #83-2660, AIAA, New York, 1983. Yee, J. H., V. J. Abreu, and A. Dalgarno, J. Geophys. Res., in press,

1985.

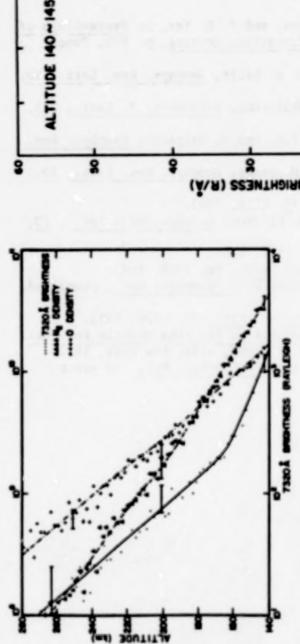


Fig. 1. The altigude variation of the glow emission at 7320 Å, along with the measured number densities of atomic oxygen and molecular nitrogen.

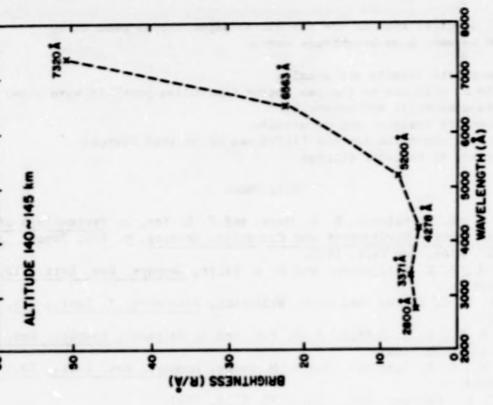


Fig. 3. The spectral variation of the glow emission at 140-145 km.

Fig. 1. Figures from Yee and Abreu [1983] showing AE glow properties.

ORIGINAL PAGE IS OF POOR QUALITY

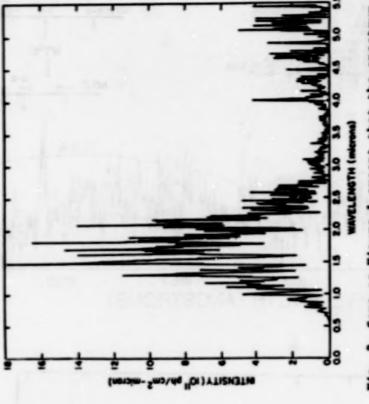
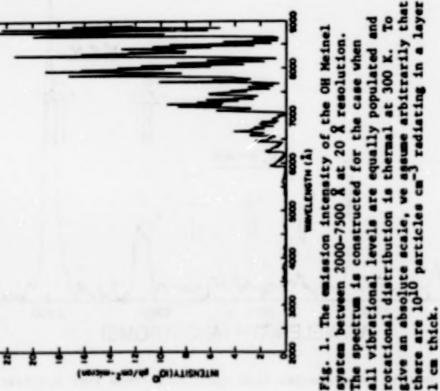
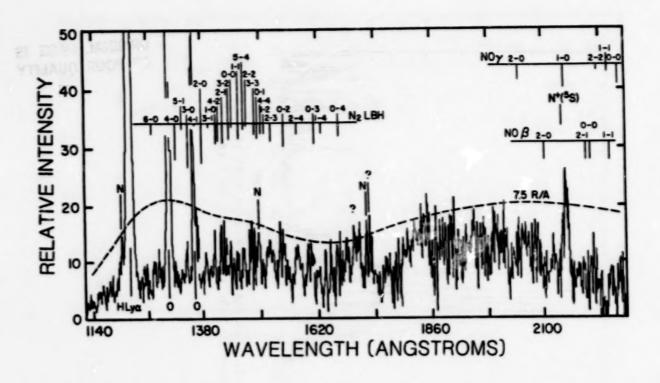


Fig. 2. Same as Figure 1 except that the spectrum is extended to 5.5µ and is at 100 Å resolution.





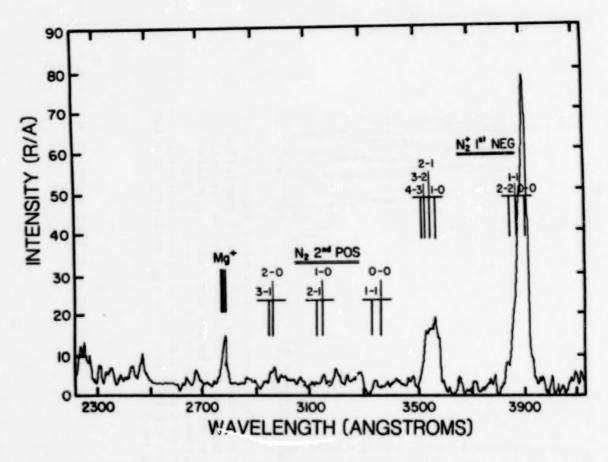
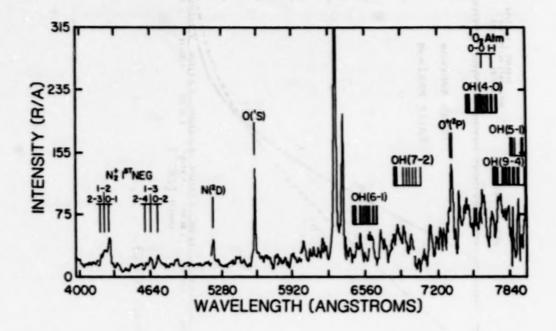


Fig. 3. Shuttle glow spectra from Spacelab 1 (from Torr and Torr [1985]).



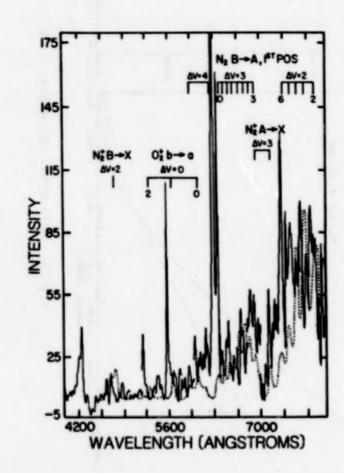
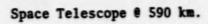
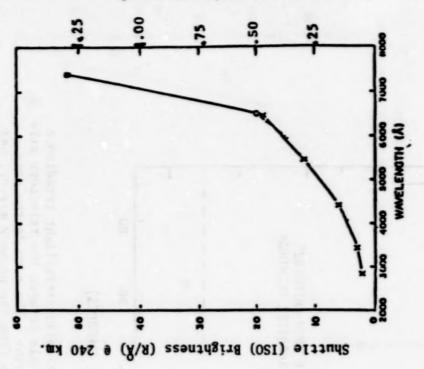
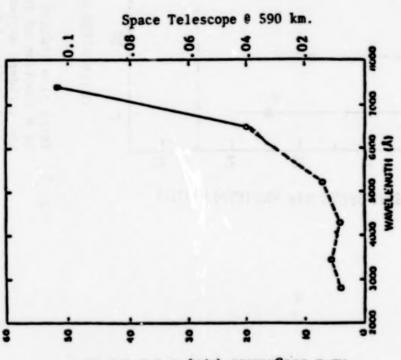


Fig. 4. Shuttle glow spectra from Spacelab 1 (from Torr and Torr [1985]).

Fig. 5. MSIS model atmospheres from A. Hedin (GSFC).







AE-E Brightness (R/A) @ 140-145 km.

Scaling observed glow brightnesses to ST altitudes (for solar max. [0] altitude profile). Fig. 6.

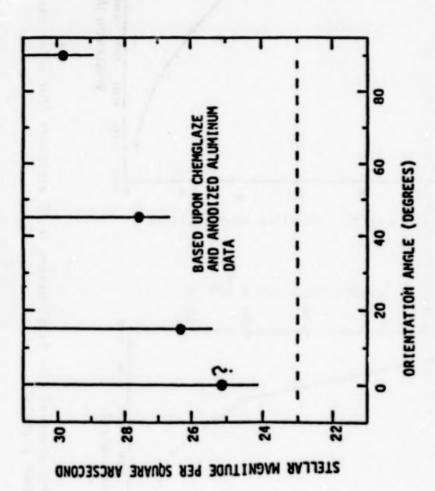


Fig. 7. Total glow induced focal plane straylight irradiance as a function of the angle between the telescope axis and incident oxygen vector. The zero degree case, being dominated by glow from the primary mirror, has the greatest uncertainty since glow from the MgF2 coating has not yet been characterized.

1st Example: Plot the expected sky background due to zodiacal light in units of Rayleighs/R

Assume average zodiacal light brightness of 60 S₁₀ units [Dube et al., 1977] at 5500 Å: 60 S₁₀ = 0.26 Rayleighs/Å = 23.3 m_V/arc sec².

Scale to other wavelengths by solar spectrum (observed to be accurate from 1800 A to 3 microns)

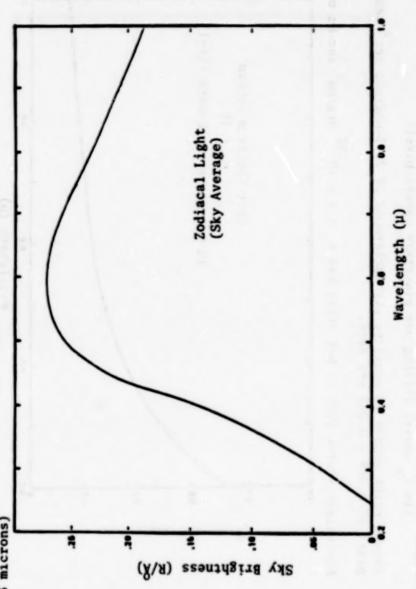


Fig. 8. Comparison of glow brightness with ST detection limits.

2nd Example: What sky brightness is equivalent to a point source with a flat spectrum (in F, units) filling one planetary camera pixel?

Assume point source is equal to sky background of 23.3 mag/arc sec scaled to 1 PC pixel of 0.048 x 0.048 arc sec2.

Equivalent source (QSO or hot star) has $F_v = 4 \times 10^{-32} \text{ erg/cm}^2$ -sec-Hz or $m_v = 30$.

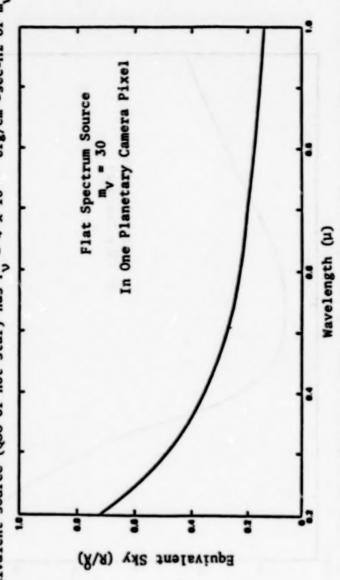


Fig. 9. Comparison of glow brightness with ST detection limits.

INFRARED MEASUREMENTS OF SPACECRAFT GLOW PLANNED FOR SPACELAB 2

Giovanni G. Fazio and David G. Koch

Smithsonian Astrophysical Observatory

Abstract. A liquid helium cooled infrared telescope (IRT) will be flown in July 1985 on Spacelab 2. The instrument was designed to measure both diffuse and discrete infrared astronomical source, including the zodiacal light, galactic, and extragalactic components, as well as to evaluate the induced Orbiter environment. The focal plane contains ten photoconductive detectors covering six broad bands from 2 to 120 microns. Each detector has a 0.6 by 1.0 deg. field-of-view optimized for detection of extended sources of IR radiation. Except for the 2-micron detector, the system noise is limited by the sky background noise.

This paper describes the measurements planned for the IRT using the 1-meter base of the Plasma Diagnostics Package (PDP), an already existing SL 2 experiment, as the glow generating surface. The measurements will be repeated changing the position of the PDP, the attitude of the Orbiter, and the ram direction in an effort to remove both the thermal component of the PDP emission and the cosmic background radiation.

Introduction

The primary intent of these observations is to obtain measurements of the glow phenomenon in the infrared produced by the base of the Plasma Diagnostics Package (PDP). The IRT is capable of obtaining data in six broad passbands: 2.0-3.0, 4.5-9.5, 6.1-7.1, 8.5-14.5, 18-30, and 70-120 microns. The two longest wavelength passbands, 18-30 and 70-120, include three detectors each. See Koch, et al. [1982] for a complete description of the instrument. Young, et al. [1981] contains a detailed description of the IR detector performance. Additional data that will be of use in interpreting the results will come from the in situ measurements by the PDP of the particles and fields associated with the ram gases. Specifically, data from the mass spectrometer will be used. Further data that will be of use are measurements available in the visible from the image-intensified camera [Mende et al., 1985]. The equatorial altitude for this mission will be 383 km and the inclination 49.5 deg.

Method of Observation

In an attempt to determine a dependence on material two observational methods will be used. One will be to see if there is any glow from the inside of the gold-coated mylar sunshade of the IRT. The other will be to look for the glow from the base of the PDP, which is covered with beta cloth and aluminum screen as the PDP is positioned near the beam of the IRT. The Orbiter Remote Manipulator System (RMS) will be used to position the PDP so that the flat base of the PDP will be in the Orbiter Y-Z plane. In both of the methods of observation described below the telescope will be fixed (stowed) and viewing along the Orbiter -Z axis (see Figure 1).

Observing Constraints

During the glow measurements, the field-of-view of the telescope must encompass regions of low infrared brightness. Such regions include the ecliptic pole or the galactic pole and must avoid regions near or crossing the galactic plane. (The preferred orbit would have the plane of the orbit pass near the ecliptic pole.) While the data are being taken the field-of-view, hence the Orbiter, must be held inertially on the sky. In addition, the data must be taken on the nighttime side of the orbit in order to observe with the lowest possible background and to permit optical photography of the glow. The velocity vector should be kept approximately normal to the base of the PDP. Data cannot be taken while near or passing through the South Atlantic Anomaly (SAA). Water dumps, operation of the flash evaporators, experiment purges, and other sources of effluent must be inhibited prior to and during data taking.

Since the thermal radiation from the PDP is substantial it will be important to have the thermal conditioning prior to and during the observing runs as nearly identical as possible.

Observing Sequence

Due to the uncertainties in both the absolute position of the PDP when manipulated by the RMS and the alignment of the telescope with respect to the Orbiter, it will be necessary to make the glow measurements by gradually cycling the PDP into and out of the field-ofview of the telescope. This will also provide a means of establishing the baseline intensity without the PDP. The intensity will be correlated with the RMS positional information. This cycling with the RMS will be repeated for each of four separate inertial positions on the sky during the 36 minutes of Earth shadow during two consecutive orbits. On the first orbit the PDP base will be pointed into the wake and on the second orbit the PDP base will be pointed into the ram, all other conditions remaining the same. During the first three inertial positions, the PDP will be moved in closer and closer to the telescope beam at about 15 cm above the sunshade aperture. During the fourth inertial position the PDP will be raised 5.7 meters above the aperture where the 1-meter PDP diameter will still fill the 15-cm telescope beam, but the thermal effects from the PDP will fill a much smaller portion of the telescope side

lobes. This alternate position is shown in Figure 2. Before each RMS cycle, the cold shutter at the focal plane will be actuated to provide an absolute flux level. On the second orbit when the PDP base is into the ram, the mass spectrometer on the PDP will be pointed into the ram to provide in situ measurements of the plasma.

Data Deconvolution

To be able to distinguish the thermal radiation of the PDP from the glow, as well as to measure the intensity scale height of the glow, the method of observation has to provide many differential experiments. These include moving the source (PDP) in and out of the telescope beam, repeating the cycles at different distances from the beam, and repeating at a different height above the aperture. Before and after each cycle the cold shutter is used to provide an absolute flux level. All of this is done first with the PDP base in the wake where there should not be any glow and only the infrared of the environment and sky is measured. Then the entire process is repeated on the next nighttime pass with the base into the ram where any difference in signal should be due to the glow. Any slight variations of the sky background due to variations in the inertial position can be corrected, since the prime objective of the IRT is to measure the large-scale structure of the sky. In addition to the many signal modulation and differentiation effects, the glow should be distinguishable spectrally from the zodiacal and the PDP thermal radiation, both of which are approximately 300 K blackbodies.

Finally, any glow off of the inner surface of the gold-coated mylar sunshade should be detectable and separable from other signals since during each cycle of the RMS, the telescope is held inertially on the sky, but during the 4 to 9 minutes of inertial hold, the orbital motion will result in the velocity vector varying from slightly into the sunshade aperture to slightly out of the sunshade. During normal IR mapping the telescope aperture will always be pitched slightly away from the velocity vector so that the inside of the sunshade is never exposed to the ram.

Expected Results

An estimate of the expected infrared flux can be made based on the following assumptions:

- The glow is due to atomic oxygen impacting the surface at 7.7 km/sec.
- The atomic oxygen flux at 400 km altitude is 1.5 x 10¹⁴/cm²/sec.
- The spectral shape of the emitted radiation will resemble that of highly excited OH.
- The decay distance from the PDP base produced by oxygen impact is 1 meter or more.

In the paper by Banks et al. [1983] the volume density of the visible photon emission was estimated to be 2 x 107 photons/cm3/sec at the 280 km altitude for STS-3. This was observed in about a

0.1 micron band so that the spectral flux is 2 x 10° photons/cm3/ sec/micron at about 0.65 microns. If the emitting species is OH we can use Langhoff's [1983] calculated spectrum to get volume densities of 1016/cm3/sec/micron at 1.3 to 2.2 microns at 280 km and 10°/cm²/sec/micron at 4.5 to 6.5 microns beyond which it drops rapidly with increasing wavelength. The IRT will look through a 100-cm-thick volume of gas that is radiating into 4x sr. Therefore, the telescope should see a flux of 8 x 1018 photons/cm2/ sec/sr/micron at 1.3 and 2.2 microns and I200 = 16 x 109 photons/cm3/sec/sr from 4.5 to 6.5 microns. From ground-based measurements of STS-9 (240 km altitude) by Witteborn et al. [1985] a flux of 5 x 1011 photons/cm2/sec/sr/micron at 1.6 microns was observed and the observed flux at 2.3 microns was attributed entirely to the diffuse reflection of the Earth thermal emissions. This would imply a factor of about six times more emission at 1.6 microns than expected from using Lan off's method.

The zodiacal emission in the 4.5-8.5 micron band is about 7 x 10° photons/cm²/sec/sr which is comparable to I₂₀₀. Since SL 2 will be at 400 km altitude, the oxygen incidence will be ten times lower, resulting in an equivalent decrease in the volume densities of photon emission. Consequently the irradiance at 400 km from "Oglow" would be I_{400 km} = 1.6 x 10° photons/cm²/sec/sr. This is only 20% of the zodiacal emission expected in the ecliptic, 90 deg. from the Sun. This irradiance would be about 60% of the zodiacal emission (away from ecliptic plane) over most of the hemisphere away from the Sun. Distinguishing the 0-glow from the zodiacal emission should be easy, since the 0-glow is not expected to contribute to the observed flux at wavelengths beyond 15 microns. Thus the 0-glow should change the ratio of the radiation in the 4.5-9.5 micron band to that in the 18-30 micron band.

Conclusions

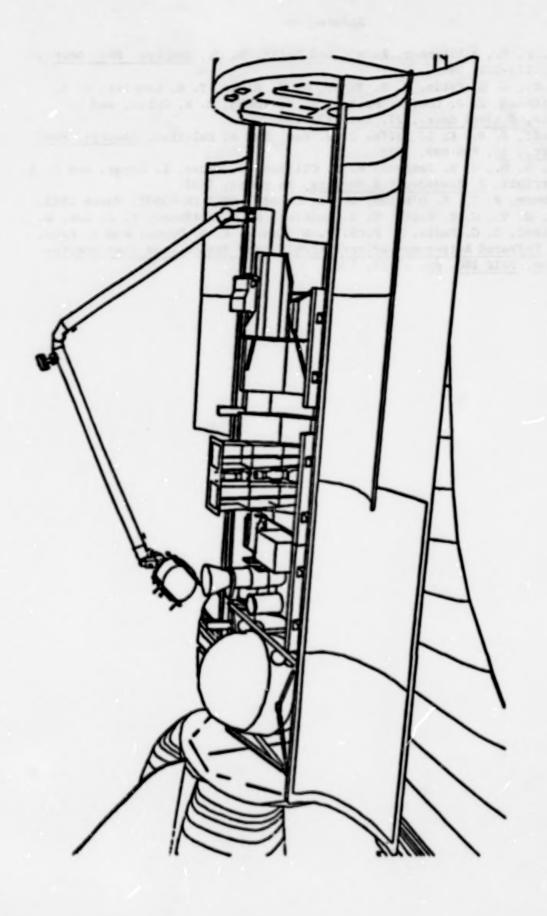
Although the plan to make the glow measurements have evolved only recently (after the final mission plan for SL 2 was formed), the opportunity to perform these IR measurements with existing hardware in so near a term has led us to dedicate two of the 18 revs. planned for IR celestial observations to making these measurements. It appears that in using the observing plan outlined above, the glow should be detectable in the near IR for the given geometry. Otherwise, the observations will put severe upper limits on the flux, limiting it to well below the zodiacal flux for the geometry described.

Acknowledgments. Funding for the IRT is provided by NASA Grant NAS8-32845. The calculations for the expected flux were performed by F. Witteborn, NASA/Ames Research Center.

References

- Banks, P. M., Williamson, P. R., and Raitt, W. J., Geophys. Res. Lett., 10, 118-121, 1983.
- Koch, D., G. G. Pazio, W. A. Traub, G. H. Rieke, T. N. Gautier, W. F. Hoffmann, F. J. Low, W. Poteet, E. T. Young, E. W. Urban, and L. Katz, Optical Engr., 21, 141-147, 1982.
- Langhoff, S. R., R. L. Jaffe, J. H. Yee, and A. Dalgarno, Geophys. Res. Lett., 10, 896-899, 1983.
- Lett., 10, 896-899, 1983.

 Mende, S. B., G. R. Swenson, K. S. Clifton, R. Gause, L. Leger, and O. K. Garriott, J. Spacecraft & Rocke's, in press, 1985.
- Witteborn, P. C., K. O'Brien, and L. Caroff, NASA TM-85972, March 1985.
- Young, E. T., G. H. Rieke, T. N. Gautier, W. F. Hoffmann, F. J. Low, W. Poteet, G. G. Fazio, D. Koch, W. A. Traub, E. W. Urban, and L. Katz, in Infrared Astronomy--Scientific/Military Thrusts and Instrumentation, SPIE 280, pp. 12-19, 1981.



View of the Spacelab 2 payload showing the Plasma Diagnostics Package being positioned above the Infrared Telescope by the Remote Manipulator System. The velocity vector is from wing-tip to wing-tip. Fig. 1.

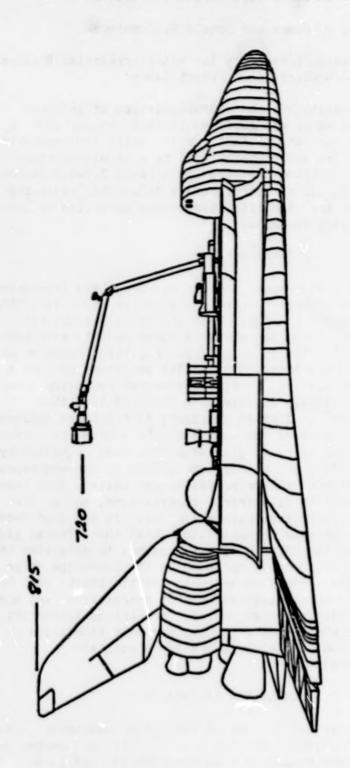


Fig. 2. View of the PDP position during the fourth inertial hold/RMS cycle.

PLANNED INVESTIGATION OF INFRARED EMISSIONS ASSOCIATED WITH THE INDUCED SPACECRAFT GLOW: A SHUTTLE INFRARED GLOW EXPERIMENT (SIRGE)

Michael J. Mumma and Donald E. Jennings

Planetary Systems Branch, Laboratory for Extraterrestrial Physics, NASA/Goddard Space Flight Center

Abstract. We will investigate the characteristics of infrared molecular emissions induced by energetic collisions between ambient atmospheric species and surfaces in Earth orbit, using low-resolution infrared spectroscopy. The spectrometer will be a liquid-nitrogen-cooled filter wheel photometer covering the wavelength range 0.9-5.5 microns with a resolving power ($\chi/\Delta\chi$) of approximately 100. This resolving power will be sufficient for identification of the molecular or atomic fluorescent species causing the glow.

Introduction

The instrument to be used for the Shuttle Infrared Glow Experiment (SIRGE) will be a liquid nitrogen cooled spectrometer flown in a GAS canister in the Hitchhiker-G program. With it, we will study the infrared (0.9-5.5 micron) component of the induced shuttle glow [Abreu et al., 1983; Banks et al., 1983; Langhoff et al., 1983; Mende et al., 1983; Slanger, 1983; Yee and Abreu, 1983]. The spectrometer uses a circular variable filter (CVF) to provide a spectral resolving power $(\lambda/\Delta\lambda)$ of 100 and a sensitivity (single scan NESR) of less than 2 x 10 watts/cm sr cm . This is necessary to reach the zodiacal light limit, which is considered the limiting flux source for astronomy in the near infrared. The infrared glow study has been requested by the Hubble Space Telescope (HST) project office because of concern expressed by the astronomical community regarding the impact which a glow from HST might have on the feasibility of infrared observations, and on the choice and design of infrared instruments for HST. It has also been proposed (C. R. O'Dell, private communication) that the infrared glow spectrometer be flown on the HST deployment mission, to determine the magnitude and character of the glow surrounding the telescope after ejection from the shuttle. The glow near the shuttle itself will be studied on this and subsequent missions to help characterize and model the emission so that predictions can be made for various spacecraft and various altitudes. The high sensitivity and moderate resolution specified for this instrument are necessary for a complete characterization of the glow.

Instrument Specifications

Figure 1 shows a conceptual drawing of the SIRGE instrument. Table 1 lists the basic specifications. The spectrometer will be mounted in a liquid nitrogen dewar, and housed in a Getaway Special (GAS) can. The instrument will be mated with the Mitchhiker-G avionics, and mounted on a single GAS beam for ease of manifesting on the space shuttle (Figure 2).

The inner liquid nitrogen container will be supported within the GAS can with a thermally isolated structure, and will be rediatively shielded with multiple-layer-insulation. Fill and vent ports will be provided, along with a pumping port for the dewar vacuum jacket, and these will be accessible from the top of the GAS can. The effluent gas will be routed away from the vicinity of the optical aperture to avoid potential modification of the local glow effects on orbit. A sealed aperture door will open in orbit to expose the instrument to the glow. This door will also provide a radiation (heat) shield for the aperture during the ground hold time. A sun sensor will close the door automatically. The dewar will have a minimum hold time of 15 days, including 5 days pre-launch hold time. The dewar will be filled with a carbonized rayon porous material to prevent phase separation in zero gravity. The dewar will be vented through a pressure regulator, maintaining the temperature of the liquid nitrogen at 65 kelvin (or lower, TBD).

The spectrometer will use entirely reflective optics (except for the CVF) to reduce scattered light and improve throughput (Figure 3). Reflective optics provide several additional advantages, principally related to the absence of dispersion. Thus, all wavelengths are focussed simultaneously at the same point, and the wavelength response can be extended in future by replacing only the detectors and the wavelength-selecting filters. Alignment can be carried out at visual wavelengths, and the parabolic mirrors can be diamond-machined under numerical control, which greatly assists assembly and alignment.

The input aperture will be baffled to minimize scattered light, e.g. from the Sun, Earth, and Moon. Rejection of off-axis stray light will be further enhanced with a Lyot stop in the fore-optics (Figure 3). The field-of-view of the spectrometer will be 4 x 4 square and the collecting aperture will be 0.6 inch diameter. After passing the Lyot stop, the collected radiation is re-focussed onto a circular-variablefilter wheel (CVF) where wavelength selection occurs. The CVF will have three sections, variable in wavelength: 0.9-1.8, 1.5-3.0, and 2.7-5.5 microns. The spectral resolution of the CVF is 1% of the wavelength. All filter components are available commercially. The transmitted radiation is re-focussed onto an infrared detector (InSb), operated at 65 kelyin (or lower) to provide an NESR of less than 2 x 10 in a 5-second scan. The scan time will be as short as is possible (5 seconds) without degrading sensitivity due to bandwidth limitations. The detector will use a trans-impedance amplifier with a load resistor of approximately 2 x 10 ohms. A stimulator (infrared source) will be located in the pre-optics area to provide an internal calibration source. The expected instrument sensitivity is compared with the zodiacal background, with various external calibration objects, and with possible glow intensities in Figure 4.

A second detector will be provided in the pre-optics area to be used in the broadband mode. It will be sampled at the same rate as the narrow-band detector in the focal plane, but will observe the full spectrum at once to monitor rapid changes in the glow flux level (during thruster firing, for instance) and to measure very weak fluxes. The flight electronics will oversample the focal plane detector signal by a

factor of 5-10 and provide a dynamic range of 10⁵. Additional channels will be provided for the broadband detector and several temperature sensors. The output of the electronics will be compatible with the Hitchhiker avionics. The power and instrument control lines, and the data lines, will be routed through the bottom of the GAS can (Figure 1). The power and instrument control will be supplied via the Hitchhiker avionics. Data will be recorded onboard and also downlinked to ground support equipment, providing direct control of the experiment and real-time data inspection during flight.

The entire assembly will be compatible with GAS/shuttle launch and orbit conditions, and will satisfy structural, thermal, and safety requirements for GAS payloads. The entire flight instrument will be contained in a single GAS can, so that the Hitchhiker avionics and instrument GAS canister can be flown on a single GAS beam (Figure 2).

Sensitivity

In So detectors near 1 mm in diameter and having high sensitivity are commercially available, and will be used. The optical throughput (etendue) is then easily calculated from the f/.83 detector focussing mirror to be

$$A\Omega = 1.03 \times 10^{-2} \text{ cm}^2 \text{ sr}$$
 (1)

This etendue is preserved throughout the optical system. The collecting mirror at the entrance aperture has an effective diameter of 3.14 cm and is operated at f/1.6. The field stop is 4 mm x 4 mm, corresponding to a square beam on the sky of 4.5° x 4.5° .

The Noise-Equivalent-Spectral-Radiance (NESR), for an extended source of uniform surface brightness which fills the field-of-view, is given by

NESR =
$$\frac{NEP}{TA\Omega \Delta v / \tau}$$
 watts/cm² sr cm⁻¹ (2)

where

= $(10^{-4} \text{ v})\text{NEP1}$, the detector NEP at frequency v (cm⁻¹), = 1.8 x 10^{-15} W/ $\sqrt{\text{Hz}}$, the NEP at λ = 1 µm wavelength, NEP NEP1 = 0.4, the total transmittance of the optical system. = 1.03×10^{-2} cm sr, the etendue, T AΩ = v/R, the spectral resolution element, Δv = 100, the spectral resolving power, = ti/R, the integration time per spectral element. t = 5 seconds, the integration time required for one complete Ti N = the number of complete scans, and = Nt, the total integration time.

Then,

NESR =
$$\frac{10^{-4} \text{ R}^{3/2} \text{ NEP1}}{\text{TAg } \sqrt{\tau}}$$
 watts/cm² sr cm⁻¹ (3)

or, using the values given above,

NESR =
$$\frac{4.36 \times 10^{-14}}{\sqrt{\tau}}$$
 watts/cm² sr cm⁻¹ (4)

Note that the NESR expressed in equations (3) and (4) is independent of wavelength, if the resolving power is kept constant.

It is also useful to express the MESR in units of Rayleighs/A (the Rayleigh is a unit of surface brightness equivalent to 10° photons cm² sec⁻¹, radiated into 4π sr),

$$NESR = \frac{4\pi \cdot 10^{-18} \text{ vc } \text{R}^{3/2}}{\text{hc TA}_{\Omega} \sqrt{\tau}}$$
 Rayleighs/8 (5)

For the parameters given above, the NESR may be re-written

$$NESR = \frac{2.75}{\lambda \sqrt{\tau}} Reyleighs/R$$
 (6)

where χ is given in μm . The expected NESR is shown in Figure 4 for τ =100 seconds and a resolving power of 100, representing σ 20 co-added spectral scans.

For faint continuum emissions, the spectral resolving power can be degraded in software by \$10-fold (to R = 10), providing an NESR of 1.4 x 10 $^{-10}$ W//Hz for $_{\rm T}$ = 100 seconds. This is compared with the intensity of the zodiacal light towards the ecliptic pole in Figure 4, where it is seen that good signal-to-noise can be obtained on this important astronomical background source. The zodiacal light is typically 2-3 times brighter in the ecliptic plane, at 90 elongation. The apparent mean surface brightness of Mars, Jupiter, and Saturn, diluted to our beam size in August 1986, are also shown. Spectral structure has been omitted for representation purposes.

The strongest emissions of all may be those of the induced glow. For example, if the unresolved continuum level seen in the ISO spectra (\$\sigma50 R/A\$ at 0.6 $_{\mu}$ m, Torr and Torr [1984]) were assumed to be due to OH Meinel band emission, then Langhoff's spectral model could be used to estimate the intensity expected at 1.5 $_{\mu}$ m [Langhoff et al.,1983]. According to this model, it would be \$\sigma30\$ times brighter there. The ratio of signal-to-noise expected using the SIROE spectrometer (single scan, \$\tau=5\$ seconds) would then be \$\sigma1800\$. However, this is probably an over-estimate for the OH intensity. In addition to potential OH emission, other bands may be present such as NO_2 (\$\varphi_1 + \varphi_3\$, and \$\varphi_3\$), H_2O (\$\varphi_1\$ and \$\varphi_3\$), NO (1-0, overtones, and hot bands), N_2O (\$\varphi_3\$), CO (fundamental, overtones, hot bands), and CO_2 (\$\varphi_3\$), to mention only those which have been suggested or which seem particularly likely.

The flux seen by the detector must be $< 2.5 \times 10^{-12}$ watts, for the NEP used, if amplifier saturation is to be avoided. Hence, the beam averaged surface brightness (at 1 μ m) cannot exceed

$$R_{\text{max}} = 2.5 \times 10^{-12} \text{ watts/cm}^2 \text{ sr cm}^{-1}$$
 (7)

Thus, the maximum signal-to-noise ratio achievable in a single scan will be $$\circ$ 125. If the induced glow were to be as bright as indicated in Figure 4, our amplifiers would be saturated, therefore a commandable ranging capability is included in the electronics design.

Test and Calibration

Careful optical calibration and testing will be conducted in the laboratory, with particular emphasis on measurements of the off-axis rejection of stray light, the absolute intensity calibration, the noise performance, and the measurement of linearity. Additional tests (vibration, thermal, EMI) will be carried out, as required.

Particular emphasis will be placed on intensity calibration. Ground calibration of the assembled system will be carried out in the laboratory, before and after flight. However, because of the long time (probably 1 year) between the calibrations, we plan to make in-flight calibration as well. An internal infrared source (stimulator, Figure 3) will provide relative intensity calibration, and external sources (Mars, Jupiter, Saturn, Figure 4) will provide absolute calibration. The external sources can be acquired by pointing the space shuttle, since our large beam size permits source acquisition with only modest pointing accuracy. Terrestrial limb scans will enable intensity, wavelength, and dynamic range calibration from the known OH Meinel airglow itself. Finally, when viewing deep space, the zodical emission provides an automatic signal for calibration of faint glow emissions.

References

Abreu, V. J., W. R. Skinner, P. B. Hays, and J. H. Yee, Optical effects of spacecraft-environment interaction: Spectrometric observations by the DE-B satellite, AIAA-83-2657-CP, presented at Shuttle Environment and Operations Meeting, Washington, D.C., 1983.

Banks, P. M., P. R. Williamson, and W. J. Raitt, Space Shuttle glow observations, Geophys. Res. Lett., 10, 118-121, 1983.

Langhoff, S. R., R. L. Jaffe, J. H. Yee, and A. Dalgarno, The surface glow of the Atmospheric Explorer C and E satellites, Geophys. Res. Lett., 10, 896-899, 1983.

Mende, S. B., O. K. Garriott, and P. M. Banks, Observations of optical emissions on STS-4, Geophys. Res. Lett., 10, 122-125, 1983.

Slanger, T. G., Conjectures on the origin of the surface glow of space vehicles, Geophys. Res. Lett., 10, 130-132, 1983.

Torr, M. R., and D. Torr, Preliminary results of the imaging spectrometric observatory on Spacelab 1, AIAA-84-0044, presented at AIAA 22nd Aerospace Sciences Meeting, Reno, 1984.

Yee, J. H., and V. J. Abreu, Visible glow induced by spacecraft-environment interaction, Geophys. Res. Lett., 10, 126-129, 1983.

TABLE 1. SHUTTLE INFRARED GLOW EXPERIMENT: SPECIFICATIONS AND REQUIREMENTS

Wavelength Coverage	0.9-5.5 microns	
Resolving Power	100	
Detector	InSb	
Sensitivity (single scan NESR)	<2 x 10 ⁻¹⁴ W/cm ² sr cm ⁻¹	
Scan Time	<pre>55 seconds</pre>	
Operating Temperature	<65 K	
Dewar Hold Time (minimum)	5 days pre-flight 10 days in-flight	
Field-of-View	4° x 4°	
Aperture Size	3.14 cm diameter	

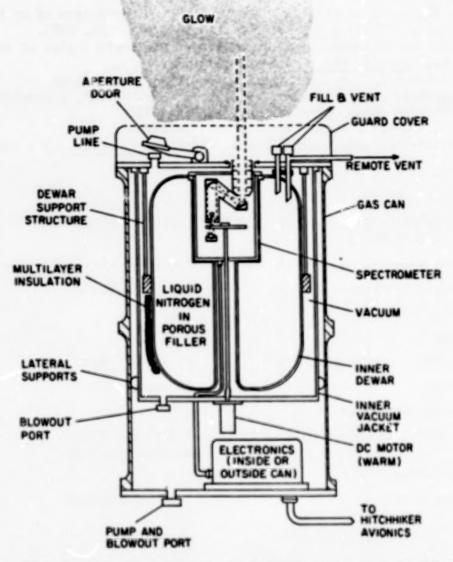


Fig. 1. Conceptual drawing of SIRGE instrument in GAS can.

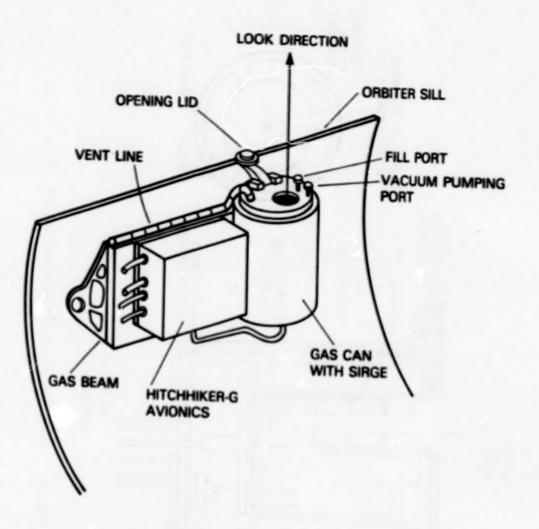


Fig. 2. SIRGE spectrometer Hitchhiker mounting configuration.

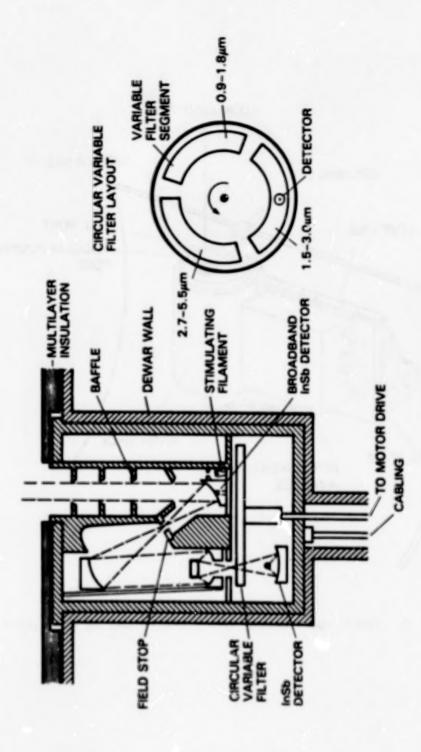


Fig. 3. SIRGE spectrometer optical layout.

. F. W. T. Land State Sect.

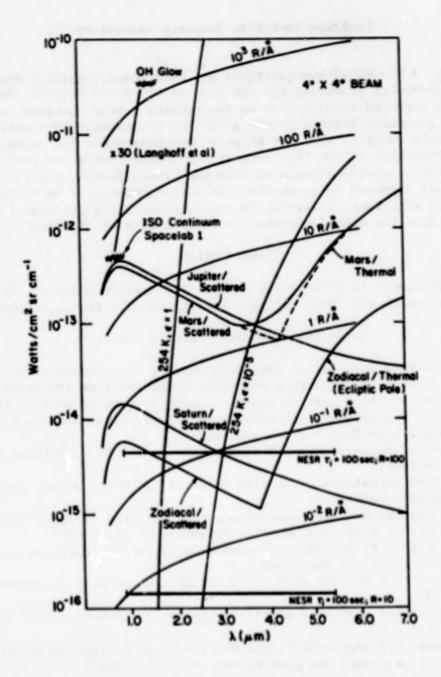


Fig. 4. SIRGE sensitivity limits, calibration sources, and possible glow intensities.

DATA REQUIREMENTS FOR VERIFICATION OF RAM GLOW CHEMISTRY

Gary Swenson and Steve Mende

Lockheed Palo Alto Research Laboratory

Abstract. A set of eleven questions has been posed regarding the surface chemistry producing the ram glow on the space shuttle. The questions surround verification of the chemical cycle involved in the physical processes leading to the glow. The questions, and a matrix of measurements required for most answers, are presented. The measurements include knowledge of the flux composition to and from a ram surface as well as spectroscopic signatures from the UV-visible-IR. A pallet set of experiments proposed to accomplish the measurements will be discussed. An interim experiment involving an available infrared instrument to be operated from the shuttle Orbiter cabin will also be discussed.

Introduction

Several papers in this report address the surface chemistry involved in production of the "red" ram glow associated with the space shuttle.

Questions to Address-Surface Ram Glow

The following is a set of questions that we have assembled which are aimed at further understanding and quantifying the glow processes. This set of questions is a general set that needs answers to further clarify and quantify the physical processes involved. First we address a set of questions for glow from a given material:

- How does NO₂ material exit flux relate to the NO₂ continuum glow on the material?
- How does NO material exit flux relate to NO beta, delta, and/or gamma band emission?
- 3. How does the NO₂ continuum glow extend into the infrared? Does it continue to drop as we observe between 7000 and 8000 A?
- 4. Is the NO₂ "fine structure" superimposed on the continuum as it is in the laboratory spectrum?
- 5. Is there a component of N2 IPG, and if so, how does it extend into the IR?
- 6. How does 1-5 vary with material temperature (between ~250° and 400° K)?
- How does 1-5 vary with NI and OI flux from the atmosphere? (i.e., How can we expect the glow to vary with altitude?)
- 8. How does 1-5 vary with ram angle to the sample surface?
- Does O₂ become a production factor at low altitude as implied by the AE-C data?
- 10. How do different material surfaces influence 1-9 above?
- 11. How does the chemistry become enhanced/quenched with controlled injection of NO and other gases?

This set of questions addresses process verification and quantification for temperature and materials. The experimental approach is outlined below as to how many of these questions can be addressed.

Technical Approach-Experimental Method

The all-up matrix approach with the pallet instruments yields the ultimate in answers to the questions regarding the physical processes, but there are some intermediate experiments that can be assembled quickly which can answer some very important questions.

A portable CVF (Circular Variable Filter) instrument has been fabricated and is available as a candidate instrument to observe the IR component of glow from the Orbiter cabin. The aft flight deck window has reasonable transmission between 1.2 and 2.4 microns (~40%-variable). Figure 1 shows a mechanical configuration of the instrument, and Table 1 is a summary of the optical characteristic.

We herein describe a set of experiments which would answer many of the questions addressed above. This constitutes operating a set of instruments in the space shuttle bay which would monitor the flux of molecules impinging on and emanating from a surface in ram. At the same time, observations of the glow on the surface would be monitored in the UV, visible, and IR wavelengths. A glow mission would require a few orbits of dedicated attitude to perform the glow studies, at low-Earth orbit (~250 km). The instruments would be preprogramed to perform the experiment sequences during the glow attitudes. We have structured a set of instruments which can provide significant information on the processes. Some of the questions posed would require a quality, high-resolution visible spectrometer, as well as a high-resolution cryogenic IR instrument. In the spirit of "a step at a time" and low cost, we have structured an essential set of pallet instruments which can provide many important answers to key processes. A high-resolution visible spectrometer (~1 A resolution) and a cryogenic IR instrument are desirable for follow-up studies as we now understand the chemistry. A basic set of experiments without these refinements is described herein.

The instruments we envision include a sample surface plate (~1 meter x l meter) which would be positioned in the pallet in such a way that the ram atmosphere could be directed towards it. An optical sensing stand would view the plate from nearly edge-on to take advantage of the near surface brightness emanating from the plate surface. The plate would be tipped up, and a mass spectrometer would view the plate from near 45 to plate normal. This set of instruments would constitute the main glow package (see Figure 2).

The plate would be coated with one material and on subsequent mission opportunities, other materials would be studied. The place would ideally have provision for heating electrically so the plate temperature could be elevated to near 400° K. It is possible to make a plate which could rotate to subject two-three different surfaces to ram during a mission, but our initial consideration is to have a single surface. The plate would contain a baffle on the down viewing side of the optical package, such that a black background would be provided to the glow viewing instruments.

The optical package will include three instruments which will document glow from the UV to the IR. The instruments are summarized in Table 2. Instrument 1 will be an automated version of the hand-held

instrument which has flown as a locker experiment in the Orbiter. This instrument will operate in an imaging mode, as well as a spectrometer mode, to clarify the glow in the 4000-8000 A wavelength region. This instrument will document the spatial distributions of the glow and provide the bridge of measurement to the early data set. Instrument 2 will be the UV instrument to clarify NO band emission (as well as any presently unknown UV emissions). Filters for the known NO band emissions between 2000 and 4000 A will be included. The instrument will consist of a UV imager bore-sighted with an f5, 1/8th meter spectrometer. The spectrometer would scan from 2000-4000 A while the imager documents the spatial distributions of the UV glow. Instrument 3 will consist of a thermal, electrically cooled PbS detector to cover the IR wavelengths between 1 and 3+ microns. The IR shape of the NO₂ continuum and possibly other glowing candidates would be measured with this instrument.

A mass spectrometer of the type which is designed to examine the entrance and exit flux of NI, OI, NO, and NO, from the surface plate will be located separately from the optical instruments. This instrument is essential to document the constituent phenomena associated with the chemical processes. The instrument herein is one very different from the AE instrument in that the requirement is to make the measurement of ambient NO and NO2 emanating from the plate. In order to accomplish this, the instrument must be of a type where the molecules are ionized external to an instrument orifice before any wall collisions have occurred. Next, this produced beam would be focused and mass-analyzed as in a conventional mass spectrometer. The instrument would be an orifice-pumped instrument with a mechanical flag in the orifice. The pumping is necessary to minimize orifice collisions in the high-density shuttle environment. The mechanical flag allows a degree of direction control of the sampling beam. The flag would alternately direct molecules from a surface sample plate and from the atmosphere to be sampled by the instrument.

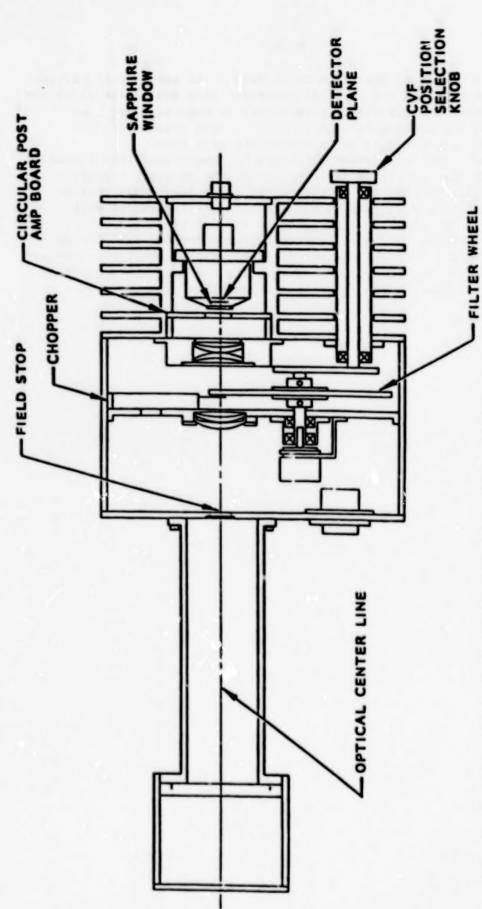
The above surface plate, optical cannister, and mass spectrometer are all essential to a basic pallet payload. A matrix of problems versus instruments has been produced (see Table 3). For most of the questions at hand, several instruments are desired. Model atmospheres can be used with some reliability for the atmospheric flux to the spacecraft, but the measurement with the mass spectrometer is best. Only the mass spectrometer can resolve what is coming off the plate in the way of mass species.

We are also giving consideration to gas release cannisters which, when released, would be located such that the drift cloud would pass over the plate. It has been noted that the thruster effluent acts to enhance the stand-off ram glow significantly for several seconds when impinging on a ram Orbiter surface. The thruster gas consists of significant amounts of NO, which we believe adds to the surface monolayer of NO. This additional source of NO seems to deplete in less than 1 minute in ram. Gas cannisters with NO and other gases which in fact would act to quench the process would be considered. The gas cannisters could be relatively small in size and of the single release type.

We suggest that the "shuttle hitchhiker" concept be a candidate facility within which experiments could be structured. The "hitchhiker" offers a simple interface and minimal delivery time before mission execution. At the same time, it appears to offer command and data handling capabilities which are adequate for the required measurements.

Summary

There are a number of questions which need to be answered to further understand the physical and chemical processes involved in ram glow. The basic questions are scientifically important to understanding the interaction of the atmosphere with the fast moving spacecraft. The questions are well suited to be explored with well known, state-of-the-art instrumentation which can be implemented into a shuttle pallet payload for experiment implementation. the exciting results will be scientifically interesting in themselves since low-energy neutral beams of 5-10 eV are difficult to implement in the laboratory with significant flux levels. The experiments will also yield useful information regarding potential background contamination for planned and future experiments. Through understanding the physical processes, we can understand how to engineer our instrumentation and plan our operations of space optical instrumentation with minimal signal degradation.



A cross section of the Circular Variable Filter (CVF) instrument for infrared detection of the spacecraft glow. The instrument contains a five-element lens set defining a 2 degree FOV. The circular variable filter scans from 1.3 to 3.2 microns. The detector is a PbS material, 4 mm sq., thermal electrically cooled to 1930 K. Detector and window temperatures are recorded as well as detector signal and wavelength position during instrument's operation.

PALLET GLOW INSTRUMENTS (TOP VIEW)

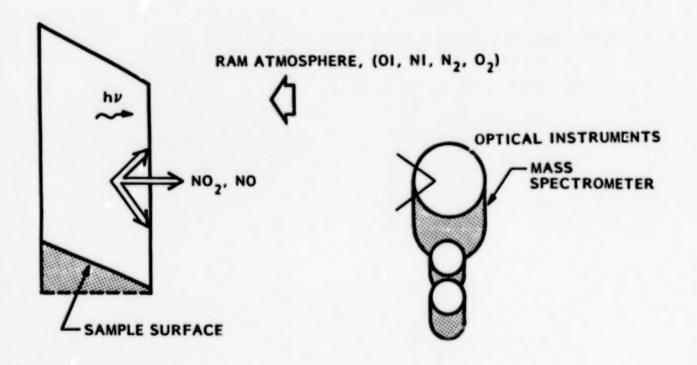


Fig. 2. A schematic representing the pallet-based instruments viewing molecules and glow emanating from a sample surface.

TABLE 1. OPTICAL CHARACTERISTICS OF THE CVF SPECTROPHOTOMETER

PORTABLE INFRARED SPECTROPHOTOMETER [CVF]

- * FIELD-OF-VIEW 2 degress (full)
- * WAVELENGTH RESOLUTION Bandwidth <3% tuned wavelength
- * SPECTRAL RANGE 1.3 to 3.2 microns per scan + shutter
 [reasonable aft window transmission 1.2-2.4 microns]
 - Broadband mode use SC window as filter
- * SENSITIVITY 80 Rayleighs/Angstrom for 1-second integration [detector = 4 x 4 mm, PbS, TE cooled to <200 kelvin]
- * POWER ~17 watts (measured)
- * VOLUME Optical system: L = 35 cm, Width = 12.5 cm Electronics: L = 20 cm, Width = 20 cm, Ht. = 20 cm
- * DATA AND CONTROL TRS 80 + recorder

TABLE 2. A SUMMARY OF A CANDIDATE SET OF PALLET INSTRUMENTS SUITABLE FOR STUDY OF SPACECRAFT RAM GLOW

PALLET GLOW INSTRUMENTATION

- #1 RED BROADBAND IMAGING SPECTROPHOTOMETER
 - * 20 degree FOV
 - * 4000-8000 Angstroms
 - * Resolution 30 Angstroms
 - * Imaging or spectrometer mode
- #2 UV BROADBAND IMAGING SPECTROPHOTOMETER
 - * 20 degree FOV
 - * 2000-4000 Angstroms
 - * Resolution 30 Angstroms
 - * Imaging and spectrometer mode
- #3 IR CVF SPECTROPHOTOMETER
 - * 2 degrees FOV
 - * Spectral range 0.8-3.0 microns
 - * Resolution 3%
- #4 MASS SPECTROMETER (OPEN SOURCE)
 - * 2 degrees FOV
 - * Flag directed beam (10 degree deflection) (monitor source flux and background)
 - * Pumped orifice

TABLE 3. A MATRIX OF QUESTIONS VERSUS INSTRUMENTS REQUIRED TO PROVIDE ANSWERS TO THE QUESTIONS IN A GLOW EXPERIMENT SCENARIO MATIX OF CURRENT PROBLEMS VS. PROPOSED INSTRUMENT

.

	Instrument #	1 1 2 2 2 2	7 2 Z	3	Mann Spect	S (Future
	Problem		40		0000	Dependent
1:	NO ₂ flux versus NO ₂ glow?	×		•	×	
2.	NO flux versus NO glow?		×		×	
3	NO ₂ extend to IR?	•		×		
4	NO ₂ fine structure?	•				
5	N ₂ 1PG superimposed?	•		×		
.9	1-5 vary with temperature?	×	×	×	×	
7.	1-5 vary with NI and OI flux?	×	×	×	×	
	1-5 vary with ram angle?	×	×	×	×	
.6	02 at low altitude?	×	×	•	•	
10.	10. Other materials response?	×	×	×	×	
::	11. Constituent enhance/quenching?	×	*	*	•	×

X - Major instrument * - Contributing instrument

A POSSIBLE GLOW EXPERIMENT FOR THE BOM 1-2 MISSION

Marsha R. Torr

Department of Physics Utah State University Logan, Utah

Abstract

At this time, information on the surface glows and the spatial extent of these glows is very limited. Several fundamental aspects of the glow have yet to be measured, and this situation is not likely to change in the near future because of the limited flight opportunities for such studies. Thus, opportunities to gather the much needed data on this subject using investigations already planned are most valuable.

A possible opportunity for such a study exists during the EOM 1-2 mission scheduled for launch on September 3, 1986. An experiment during this mission could provide the VUV-VIS-NIR spectral characteristics of the glow at approximately 5 Å spectral resolution. However, the EOM 1-2 mission has a very full schedule that already places great demands on the mission planners and investigators. At this time it is not clear whether the natural concerns associated with inserting or substituting a new experiment, however nominal, can be satisfactorily overcome. Therefore, the concept outlined below is at present a concept only.

The EOM 1-2 payload includes spectroscopic and photometric instruments which operate in wavelength regions of great interest to the glow assessment activity. However, as in the case of many remote sensing instruments, these are located in the payload bay in such a way as to avoid viewing any shuttle or payload surfaces. If these instruments are to measure the spectral characteristics of surfaces, it is necessary for such surfaces to be positioned in the field of view of these instruments for the duration of the particular measurement sequence. It is possible that the shuttle on which the EOM 1-2 payload flies will have an RMS in place. An assessment has shown that it is indeed feasible to place a four-sided "cuff" around the end of the RMS. The four sides, each coated with a different material, can then be positioned in turn above the instruments, and in such a way that the surface is alternately pointed into the ram and into the wake.

The implementation of such a measurement sequence is still being evaluated at this time.

SPACE SHUTTLE MECHANISTIC STUDIES TO CHARACTERIZE ATOMIC OXYGEN INTERACTIONS WITH SURFACES

Lubert J. Leger and James T. Visentine

NASA/Lyndon B. Johnson Space Center

Abstract. A materials interaction experiment has been approved to study atomic oxygen interaction mechanisms and develop coatings for Space Station elements requiring long-lived operation in the LEO environment. A brief summary of this experiment is presented and the required exposure conditions are reviewed.

Introduction

An understanding of the surface chemistry which gives rise to atom/ surface interactions within the orbital environment is crucial to establishing a reliable materials interaction data base for Space Station and verifying the operational capability of ground-based neutral beam facilities which simulate the space environment. One of the more important effects of these interactions is oxidation of material surfaces by atomic oxygen, a major constituent of the low-Earth orbital environment. Material interaction studies conducted during flights STS-5 and STS-8 have provided most of the current information regarding the reactivity of spacecraft materials to atomic oxygen, and the results of these studies indicate many materials such as organic films, polymers, and many composites react readily with atomic oxygen and have reactivities in the range 2.5 x 10⁻²⁴ to 3.0 x 10⁻²⁴ cubic centimeters per atom.

The data base provided by these, as well as those to be obtained on LDEF, will be limited in its application, however, because no information will be available which adequately explains the basic mechanisms responsible for atom/surface interactions. Another more serious limitation to this data base is that the total integrated atomic oxygen flux (fluence), derived for these flights and used to determine material interaction rates, must be estimated using thermospheric models to predict atomic oxygen number densities within the orbital environment. Typically, errors of ±25% or greater can be expected for these density estimations, and since they are used to compute fluence, these errors also appear in the surface recession rates for Space Station materials.

Experiment Description

To reslove many of these uncertainties in the data base, a flight experiment has been proposed for the space shuttle that utilizes an ion-neutral mass spectrometer to obtain in situ ambient density measurements and identify reaction products from modeled polymers exposed to the atomic oxygen environment. Using the ambient density measurements from the mass spectrometer along with material recession measurements obtained during the same exposure, accurate reaction rate data will be provided for future spacecraft performance assessment and design.

The mass spectrometer which will be provided by the Air Force Geophysical Laboratory (AFGL) and a mounting arrangement used to expose surfaces to ambient impingement will be mounted in the payload bay on an appropriate structure as shown in Figure 1. For the required exposure the Orbiter will be oriented with the -Z axis pointed into the velocity vector (payload bay in ram). This orientation will provide normal impingement on the exposed surfaces and, with the mass spectrometer entrance port aligned with the Z-axis, will provide for optimal ambient density measurements. A total exposure of 40 hours will be requested to provide significant recession and insure assessment of bulk material reactivity. Several ambient density measurements will be made during the 40-hour exposure.

In addition to the ambient density measurements, the mass spectrometer will also be used to measure products of reaction from atmospheric interaction with surfaces. For these measurements the mass spectrometer will rotate 90° relative to the Z-axis to sample gases evolved from several surfaces being exposed on a carrousel arrangement as shown in Pigure 2. The carrousel will hold five surfaces which will be used to study the interaction mechanism and will be selected on the basis of information provided in that regard. One of the five surfaces may be a material which is known to produce glow such as Z-306 black paint.

To aid in providing the best ambient density and reaction product evolution measurements, the AFGL mass spectrometer will be calibrated using an atomic beam currently being developed at the Los Alamos National Laboratories. This beam generation concept is based on a laser heated plasma concept described in another paper of this meeting (see J. Cross, those proceedings) and should provide kinetic energies of up to 5 eV. Since the beam facility vacuum chamber is large, the flight mass spectrometer can be calibrated in situ and should allow a good understanding of transient processes inside the ion source. Furthermore, the beam facility will be used to characterize reaction products generated on the specific surfaces selected for inclusion on the flight experiment. This product distribution will be comparable with reaction products produced during flight to verify simulation fidelity and study reaction mechanisms.

This latter data should be of interest in glow mechanism studies, in that major constituents produced by ambient impingement will be identified and thereby provide a base of chemical species to consider for light production mechanisms.

Hardware development for the flight experiment is underway, and a late 1986 or early 1987 flight date will be requested from the STS. Funding for experiment development is being provided by Space Station and the Office of Aeronautics and Space Technology/NASA Headquarters.

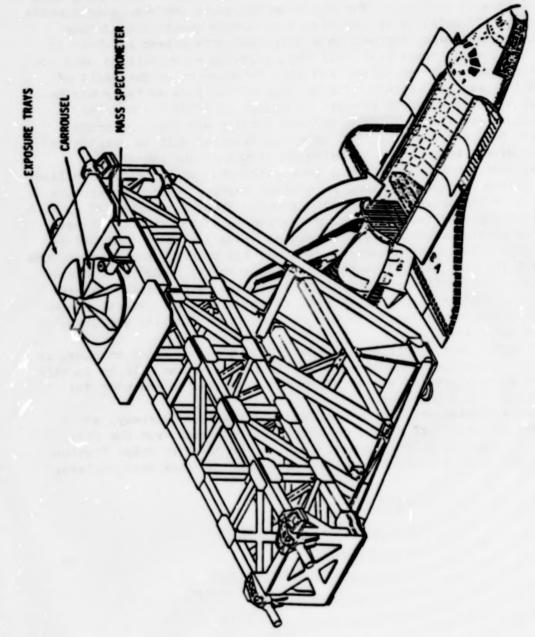
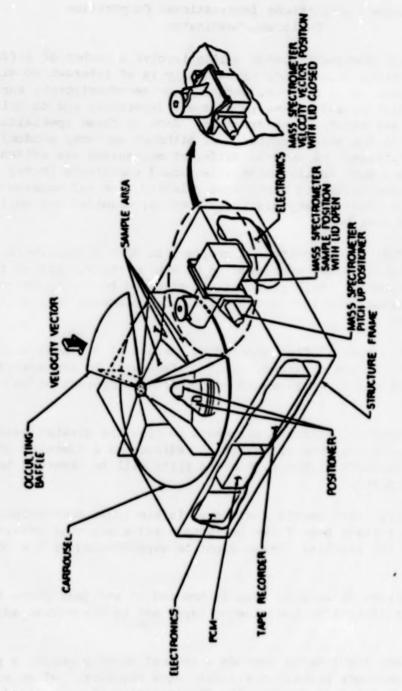


Fig. 1. Atomic oxygen experiment mounted on MPESS structure.



ig. 2. Details of mass spectrometer carrousel arrangement.

THE SHUTTLE GLOW: A PROGRAM TO STUDY THE RAM-INDUCED PHENOMENA

Hugh R. Anderson

Science Applications International Corporation Bellevue, Washington

The ram-induced phenomena almost surely involve a number of different physical interactions whose study historically is of interest to different disciplines. At a minimum, aeronomy (or aerochemistry), surface physics and chemistry, and plasma physics are important, and to this one should probably add rarefied gas dynamics. Each of these specialties was represented at the second conference, although aeronomy predominated. The significance of several different mechanisms was evident to some investigators much earlier than this second conference in May 1985. Papadopoulos published hypotheses relating glow and observed plasma effects in 1983; Kofsky discussed both aerochemical and surface chemistry in the same year.

In January 1984, SAIC submitted a proposal to NASA Headquarters entitled "The Shuttle Glow: A Program to Determine the Physics of the Ram Induced Phenomena." This proposal was prepared by Papadopoulos, Kofsky, and Anderson, and included the following elements in a shuttle-based experiment:

- e The use of a special flat generating surface >1 x 3 m on which the glow can be produced and observed. This surface will be maneuvered to vary the orientation of ram flow and of projected component of geomagnetic field.
- Remotely mounted optical instruments to view the glowing layer on the plate. By scanning, the variation of radiance as a function of wavelength and standoff distance from the plate will be observed looking parallel to the plate.
- The optical instruments include a visible light photographic camera that has already been flown on shuttle and a scanning grating spectrometer in the visible. These might be supplemented by the Orbiter video system.
- In situ plasma diagnostic sensors mounted on and just above the plate to measure effects in the glowing layer and in the medium adjacent to it.
- The plasma instruments include a neutral density gauge, a plasma density and temperature probe, an electric wave receiver, and an energetic electron detector to measure the flux striking the plate and moving in the volume just above it.
- Three near-infrared photometers were included in this set of sensors looking normally outward from the plate.

• The preferred location of the generating plate and in situ diagnostics is on the end of the Remote Manipulator System (RMS) arm. We suggested that a three- or four-sided structure be used, carrying a different surface material on each side; aluminum, kapton, tiles, and other organics were suggested. Only one side would carry the in situ diagnostic suite. Portions of this one side could be electrically biased to alter plasma flow. In this configuration, the optical instruments would be mounted rigidly in the shuttle bay with all motion being accomplished by the RMS.

1 7 3 1

• An alternative consiguration was suggested to avoid dependence on the RMS. The generating plate is hinged at one end to fold up out of the bay so that either of the two sides can be exposed to the ram flow. In this case, the optical instruments will be mounted on a pan-tilt head.

Subsequent to submission of this proposal the desirability of using the MSFC Hitchhiker was pointed out to us by NASA. A preliminary instrument layout was prepared in which the generating plate covers much of the top of the Hitchhiker structure, with the diagnostic sensors above and behind the plate and the optical sensors at the edge. The plate does not hinge, and so the shuttle must be maneuvered to vary ram flow. Increasing knowledge of the phenomena led us to enlarge the set of sensors as follows:

- Four UV photometers were added to cover wavelengths down to 1200 Å, including the O resonance lines that could be excited by electron impact.
- A cryogenic CVF infrared photometer was substituted for the infrared photometers, covering the wavelength range from 0.8 to 14 microns. This instrument will be provided by Carl Rice of the Aerospace Corporation.
- Energetic ion energy spectrometers were added complementing the electron sensors.
- The use of controlled gas releases was suggested as a way of determining the effect of varying the density and constituency of the local gas phase.
- A large carrousel was discussed to afford the capability of presenting four to six different samples to the ram flow.

Our objectives in carrying out this investigation are threefold:

• To observe the full range of ram-induced phenomena, bearing in mind those that are relevant to the Space Telescope and to other large systems. This includes not only photon emission, but the effects of bombarding dielectrics and other materials with energetic charged particles. Not only erosion, but charge implantation and microdischarges can result.

- To understand the full range of physical and chemical effects that result. It is likely that various mechanisms have different importance under different local conditions. For example, the plasma effects clearly occur. In some cases, they may dominate the production of glow. In other cases, they may be unimportant for glow but still significant for production of electrical noise, etc.
- To develop a predictive capability so that the magnitude of glow and the related effects can be calculated for any conditions. As a corollary, means to ameliorate the effects might be developed.

No formal response to our proposal has been received from NASA. Many of the experimental concepts that we suggested are now in general circulation. Their use is being planned in conjunction with existing NASA instrumentation. No dedicated instrument suite is being planned as yet. Now that NASA recognizes the interest and potential problem of the ram-induced phenomena, we look forward to participating in these investigations.

SURVEY OF ULTRAVIOLET SHUTTLE GLOW

Kerry A. Spear, Gregory J. Ucker, and Kent Tobiska

Laboratory for Atmospheric and Space Physics University of Colorado

The University of Colorado Get Away Special (GAS) project (G-285) utilizes the efforts of over 100 students for the purpose of placing four experiments on the shuttle. The undergraduate and graduate students have designed and are constructing each experiment, as well as the engineering support subsystems.

The objective of one experiment, the shuttle glow study, is to conduct a general survey of emissions in the ultraviolet near vehicle surfaces. An approximate wavelength range of 1900-3000 Å will be scanned to observe predominant features. Special emphasis will be placed on studying the band structure of NO near 2000 Å and the Mg+ line at 2800 Å.

The spectrometer, of Ebert-Faste 1/8-meter design, will perform the experiment during spacecraft night. It will be oriented such that the optical axis points to the cargo bay zenith. In order to direct the field-of-view of the instrument onto the shuttle vertical stabilizer (tail), a mirror assembly is employed. The mirror system has been designed to rotate through 7.5 degrees of arc using 10 positions resulting in a spatial resolution of 30 x 3 cm, with the larger dimension corresponding to the horizontal direction. Such a configuration can be attained from the forwardmost position in the cargo bay. Each spatial position will be subjected to a full spectral scan with a resolution on the order of 10 Å.

Detection of shuttle glow in the ultraviolet is anticipated, particularly at lower flight altitudes. The intensity will likely remain below a few tens of rayleighs/angstrom at a distance up to 10 meters from the tail. Spatial scans up to 3 meters from the tail surface should exhibit an intensity which is dependent on the direction of the velocity vector. Results will be published by the University of Colorado students following post-flight data analysis.

AGENDA

SECOND WORKSHOP ON SPACECRAFT GLOW SPACE SCIENCE LABORATORY NASA MARSHALL SPACE FLIGHT CENTER HUNTSVILLE, ALABAMA

MAY 6-7, 1985

Monday - Ma	ay 6, 1985	
8:30 a.m.	Welcome - E. A. T	andberg-Hanssen
8:35 a.m.	Preconference Sun	nmary, Goals - M. R. Torr
Time	Author(s)	Topie
8:50 a.m.	J. Clarke	Space Telescope Implications
9:20 a.m.	S. Mende G. Swenson	Space Shuttle Glow: The Characteristics of the Glow
9:50 a.m.	M. Engebretson	AE and DE Mass Spectrometer Observations Relevant to the Shuttle Glow
10:20 a.m.	G. Swenson S. Mende K. Clifton	Space Shuttle Ram Glow: Implication of NO ₂ Recombination Continuum
10:50 a.m.	A. Dalgarno J. Yee M. LeCompte	The Atmosphere Explorer and the Shuttle Glow
11:30 a.m.	P. Peters	A Model for Explaining Some Features of Shuttle Glow
LUNCH		
1:00 p.m.	D. Kendall S. Mende E. Llewellyn	Orbital Glow Observations at High Spectral Resolution
1:30 p.m.	E. Llewellyn I. McDade	Conjectures on the Nature of the Shuttle Glow
2:00 p.m.	I. Kofsky J. Barrett	Surface-Catalyzed Recombination into Excited Electronic, Vibrational, Rotational, and Kinetic Energy States: A Review
2:30 p.m.	J. Barrett I. Kofsky	The NO-NO ₂ System at Laboratory Surfaces

Monday - May 6, 1985 (Concluded)

Time	Author(s)	<u>Topie</u>
3:00 p.m.	N. Tolk R. Albridge R. Haglund M. Mendenhall J. Tully	Neutral-Particle Erosion and Optical Radiation Processes Produced by Particle and Photon Beams or Surfaces
3:30 p.m.	L. Leger	Effects of Atomic Oxygen on Surfaces: A Flight Experiment
4:00 p.m.	J. Cross	Activated Recombination Desorption: A Potential Component in Mechanisms of Spacecraft Glow
4:30 p.m.	I. Kofsky	Infrared Emission from Desorbed NO2 and NO
5:00 p.m.	G. Carignan E. Miller	Mass Spectrometric Measurements of the Shuttle Environment
5:30 p.m.	W. Langer S. Cohen D. Manos D. McNeill R. Motley M. Ono S. Paul	A Ground-Based Facility for Studying the Mechanism of Spacecraft Glow
5:50 p.m.	G. Arnold D. Peplinski	A Facility for Investigating Interactions of Energetic Atomic Oxygen with Solids
DINNER		
8:00 p.m.	O. Garriot	The STS-9 Shuttle Glow Experience
Tuesday - Ma	ay 7, 1985	
8:30 a.m.	S. Chakrabarti	Investigation of Vehicle Glow in the Far Ultraviolet
8:55 a.m.	B. Green W. Marinelli W. Rawlins	Spectral Identification/Elimination of Molecular Species in Spacecraft Glow
9:20 a.m.	D. Torr A. Khoyloo M. Torr	Enhanced N ₂ Emissions in the Shuttle Environment
9:45 a.m.	R. Rantanen R. Swanson D. Torr	A Mechanism for the Local Concentration Enhancement of the Shuttle Atmosphere

Tuesday - May 7, 1985 (Concluded)

Time	Author(s)	Topic
10:15 a.m.	M. Torr	The UV-VIS Optical Environment of the Shuttle
10:40 a.m.	K. Papadopoulos R. Smith	Spacecraft-Induced Plasma Energization and Its Role on Glow Phenomena
11:10 a.m.	F. Brock	Shuttle Fin Flow Field
11:35 a.m.	G. Fazio D. Koch	Infrared Measurements of Spacecraft Glow Planned for Spacelab 2
LUNCH		
1:00 p.m.	M. Torr	Glow Experiments Proposed for EOM-1/2
1:15 p.m.	G. Swenson S. Mende	Data Requirements for Verification of Ram Glow Chemistry
Discussion a	nd Unscheduled Talks	
1:30 p.m.	M. Mumma D. Jennings	Planned Investigation of Infrared Emissions Associated with the Induced Spacecraft Glow: A Shuttle Infrared Glow Experiment
1:45 p.m.	L. Bareiss	Materials Oxidation and Glow Phenomenon Overview
2:00 p.m.	K. Spear G. Ucker K. Tobiska	Survey of Shuttle Glow in the UV
2:15 p.m.	H. Anderson	Proposed Investigation of Glow and Induced Plasma Effects
SUMMARY	- M. Torr	
ADJOURN		

LIST OF ATTENDEES

SECOND WORKSHOP ON SPACECRAFT GLOW SPACE SCIENCE LABORATORY NASA MARSHALL SPACE FLIGHT CENTER HUNTSVILLE, ALABAMA 35812 MAY 6-7, 1985

Hugh R. Anderson Science Applications International Corporation 13400B Horthup Way, Suite 36 Bellevue, WA 98005 (206) 747-7152

Vappu S. Nuotio-Antar UTSI-USRA 12021 Comanche Trail, SE. Huntsville, AL 35803 (205) 883-1911

Graham S. Arnold The Aerospace Corporation M2/271 P.O. Box 92957 Los Angeles, CA 90009 (213) 647-1935

James D. Austin, Mail #T-2 Ball Aerospace Systems Division P.O. Box 1062 Boulder, CO 80306 (303) 939-4435

Lyle Bareiss, M0487 Martin Marietta Aerospace P.O. Box 179 Denver, CO 80201 (303) 977-8713

Pierre Y. Bely The Johns Hopkins University Space Telescope Science Institute 3800 San Martin Drive Belitmore, MD 21218

Dave H. Bouska BMD SCOM-HS P.O. Box 1500 Huntsville, AL 35807 David E. Brinza NASA Jet Propulsion Laboratory Mail Code 67-201 4800 Oak Grove Drive Pasadena, CA 91109 (818) 354-6836

Lyle Broadfoot University of Arizona Lunar and Planetary Laboratory 3625 East Ajo Way Tucson, AZ 85713

Frank J. Brock
Old Dominion University
Research Foundation
17 Research Drive
Hampton, VA 23666

William H. Brune Harvard University ESL 40 Cambridge, MA 02138

Supriya Chakrabarti University of California, Berkeley Space Sciences Laboratory Berkeley, CA 94720 (415) 642-3524

Joseph Chamberlain
Rice University
Space Physics Department
P.O. Box 1892
Houston, TX 77251
(713) 527-8101

John T. Clarke, Code TA02 Universities Space Research Association NASA Marshall Space Flight Center, AL 35812 (205) 453-3206

K. S. Clifton, Code ES63 Space Science Laboratory NASA Marshall Space Flight Center, AL 35812

Jon B. Cross Los Alamos National Laboratory CHM-2, M3 G738 Los Alamos, MM 87545 (505) 667-4646

Alex Dalgarno
Harvard-Smithsonian Center for
Astrophysics
60 Garden Street
Cambridge, MA 02138
(617) 495-4403

Ilmars Dalins, Code EH22 Materials and Processes Laboratory NASA Marshall Space Flight Center, AL 35812 (205) 453-4350

Rudolf Decher, Code ES61 Space Science Laboratory NASA Marshall Space Flight Center, AL 35812 (205) 453-5130

Ralph Earle, MS19 Teledyne Brown Engineering Cummings Research Park 300 Sparkman Drive Huntsville, AL 35807

Richard F. Ellis LPF University of Maryland College Park, MD 20742 (301) 454-7093

Mark J. Engebretson Augsburg College Department of Physics 731 21st Avenue South Minneapolis, MN 55454 (612) 330-1067 Giovanni G. Fazio Smithsonian Astrophysical Observatory 60 Garden Street Cambridge, MA 02138 (617) 495-7458

Paul D. Feldman
The Johns Hopkins University
Department of Physics and Astronomy
Baltimore, ND 21218
(301) 338-7339

Henry Garrett
NASA Jet Propulsion Laboratory
Mail Code 144-218
4800 Oak Grove Drive
Pasadena, CA 91109
(818) 354-2644

Owen K. Garriott, Code PA NASA Johnson Space Center Houston, TX 77058 (713) 483-6581

Tim Gordon Science and Engineering Associates, Inc. 6535 South Dayton Street Englewood, CO 80111 (303) 790-1572

B. David Green
Atmospheric Sciences Group
Physical Sciences Inc.
Dascomb Research Park
P.O. Box 3100
Andover, MA 01810-7100
(617) 475-9030

John C. Gregory University of Alabama-Huntsville Physics Department Huntsville, AL 35899 (205) 895-6028

Joseph E. Huezer
Old Dominion University
Research Foundation
17 Research Drive
Hampton, VA 23666

Donald E. Jennings, Code 693.1 NASA Goddard Space Flight Center Planetary Systems Branch Laboratory for Extraterrestrial Physics Greenbelt, MD 20771 (301) 344-7701

Jeff Jeter MDT SCO Mail Stop 33 P.O. Box 1181 Huntsville, AL 35807

Irving L. Kofsky PhotoMetrics, Inc. 4 Arrow Drive Woburn, MA 01801 (617) 938-0300

John L. Kulandu Lockheed Missiles and Space Company Department 51-07/Building 592 P.O. Box 3504 Sunnyvale, CA 94088-3504

William D. Langer Princeton University Plasma Physics Laboratory P.O. Box 451 Princeton, NJ 08544 (609) 683-2262

John K. Larabee Lockheed Missiles and Space Company Department 51-07/Building 592 P.O. Box 3504 Sunnyvale, CA 94088-3504 (408) 742-7485 M. A. LeCompte
Harvard-Smithsonian Center for
Astrophysics
60 Garden Street
Cambridge, MA 02138
(617) 495-7239

Lubert J. Leger, Code ES53 NASA Johnson Space Center Houston, TX 77058 (713) 483-2059

John Patrick Lestrade Mississippi State University Physics Department Mississippi State, MS 39762 (601) 325-2323

Harold Liemohn Boeing Aerospace Company Mail Stop 37-68 P.O. Box 3999 Seattle, WA 98124 (206) 773-9954

Edward J. Llewellyn University of Saskatchewan Institute of Space and Atmospheric Studies Saskatoon, SK 57N OWO Canada (306) 966-6401

Mike Loudiana Boeing Aerospace Company Mail Stop 87-68 P.O. Box 3999 Seattle, WA 98124 (206) 773-9954

Charles A. Lundquist Director, Research Institute University of Alabama-Huntsville Huntsville, AL 35899 (205) 895-6100

Rita Mahon University of Maryland College Park, MD 20742 (301) 454-7076

Dennis M. Manos Princeton University Plasma Physics Laboratory P.O. Box 451 Princeton, NJ 08544 (609) 683-2018

Stephen B. Mende
Lockheed Palo Alto Research
Laboratory
Department 91-20, Building 255
3251 Hanover Street
Palo Alto, CA 94304
(415) 858-4082

Edgar R. Miller, Code ES61 Space Science Laboratory NASA Marshall Space Flight Center, AL 35812 (205) 453-5130

M. V. Milnes, Mail Code DA-23
Rockwell International
Space Transportation and Systems
Division
12214 Lakewood Boulevard
Downey, CA 90241

Robert A. Motley Princeton University Plasma Physics Laboratory P.O. Box 451 Princeton, NJ 08544 (609) 683-2564

Michael J. Mumma, Code 693

NASA Goddard Space Flight Center

Planetary Systems Branch

Laboratory for Extraterrestrial

Physics

Greenbelt, MD 20771

(301) 344-6994

Edmond Murad Air Force Geophysics Laboratory PHK/3176 Hanscom Air Force Base Bedford, MA 01731 (617) 861-3046

Charles R. O'Dell
Rice University
Space Physics and Astronomy
Department
P.O. Box 1892
Houston, TX 77251
(713) 527-4939

Peter J. Palmadesso Naval Research Laboratory Code 4700.1P Washington, DC 20375 (202) 767-6780

K. Papadopoulos University of Maryland Department of Physics and Astronomy College Park, MD 20742 (301) 454-6810

Charles E. Patty, Jr.
Teledyne Brown Engineering
Cummings Research Park
300 Sparkman Drive
Huntsville, AL 35807

Douglas L. Patz Nichols Research Corporation 4040 South Memorial Parkway Huntsville, AL 35802 (205) 883-1140

Steven Paul Princeton University Plasma Physics Laboratory P.O. Box 451 Princeton, NJ 08544 (608) 683-3781

Walter T. Pease BMD ATC-D P.O. Box 1500 Huntsville, AL 35807

Palmer N. Peters, Code ES63 Space Science Laboratory NASA Marshall Space Flight Center, AL 35812 (205) 453-5134

Charles Pike Air Force Geophysics Laboratory PHK Hanscom Air Force Base Bedford, MA 01731 (617) 861-3177

Harry C. Poehlmann, Jr., Mail #T-2 Ball Aerospace Systems Division P.O. Box 1062 Boulder, CO 80306 (303) 939-4318

Wilson T. Rawlins
Atmospheric Sciences Group
Physical Sciences, Inc.
Dascomb Research Park
P.O. Box 3100
Andover, MA 01810
(617) 475-9030

Ray O. Rantanen
Science and Engineering
Associates, Inc.
6535 South Dayton Street
Englewood, CO 80111
(303) 790-1572

R. D. Rempt
Boeing Aerospace Company
Mail Stop 87-68
P.O. Box 3999
Seattle, WA 98124
(206) 773-9954

Carl J. Rice The Aerospace Corporation M2/266 P.O. Box 92957 Los Angeles, CA 90009 (213) 647-1749 David A. Roalstad, Mail #LT-1
Ball Aerospace Systems Division
P.O. Box 1062
Boulder, CO 80306
(303) 939-4789

Robert Ruggeri Boeing Aerospace Company Mail Stop 87-68 P.O. Box 3999 Seattle, WA 98124 (206) 773-9955

Bill R. Sandel University of Arizona 3625 East Ajo Way Tucson, AZ 85713 (602) 745-6767

John A. Schmidt Princeton University Plasma Physics Laboratory P.O. Box 451 Princeton, NJ 08544 (609) 683-2564

Thomas G. Slanger SRI International Chemical Physics Laboratory 333 Ravenswood Avenue Menlo Park, CA 94025 (415) 859-2764

Kerry A. Spear University of Colorado Laboratory for Atmospheric and Space Physics, Code 392 5525 Central Avenue Boulder, CO 80301 (303) 492-5393

Fred A. Speer, Code DS30 NASA Marshall Space Flight Center, AL 35812 (205) 453-3033

Roy A. Swanson Boeing Aerospace Company Mail Stop 87-68 P.O. Box 3999 Seattle, WA 98124 (206) 773-9955

Gary R. Swenson
Lockheed Palo Alto Research
Laboratory
Department 91-20, Building 255
3251 Hanover St.
Palo Alto, CA 94304
(415) 858-4097

Bruce Tatarchuk Auburn University Department of Chemical Engineering Auburn, AL 36849 (205) 826-4827

Peter D. Tennyson The Johns Hopkins University Department of Physics and Astronomy 3800 San Martin Drive Baltimore, MD 21218 (301) 338-7365

Dieter L. Teuber Teledyne Brown Engineering Cummings Research Park 300 Sparkman Drive Huntsville, AL 35807 (205) 532-1431

James R. Thompson, Jr. Princeton University Plasma Physics Laboratory P.O. Box 451 Princeton, NJ 08544 (609) 683-2207

Kent Tobisha
University of Colorado
Laboratory for Atmospheric and
Space Physics
Boulder, CO 80301
(303) 492-5440

Norman H. Tolk Vanderbilt University Department of Physics and Astronomy P.O. Box 1807-B Nashville, TN 37235 (615) 322-2828

Douglas G. Torr Center for Atmospheric Research Utah State University Department of Physics, UMC 41 Logan, UT 84322 (801) 750-2779

Marsha R. Torr Center for Atmospheric Research Utah State University Department of Physics, UMC 41 Logan, UT 84322 (801) 750-2685

James Tsacoyeanes Perkin-Elmer Corporation Danbury, CT 06810

Gregory J. Ucker
University of Colorado
Laboratory for Atmospheric and
Space Physics
5525 Central Avenue
Boulder, CO 80301
(303) 492-5440

Richard R. Wondrak
Lockheed Palo Alto Research
Laboratory
Department 91-20, Building 255
3251 Hanover St.
Palo Alto, CA 94304
(415) 858-4050

Hunter Waite, Code ES53 Space Science Laboratory NASA Marshall Space Flight Center, AL 35812 (205) 453-3918

LIST OF ATTENDEES (Concluded)

Francis C. Wang Lockheed Missiles and Space Company P.O. Box 1103 Huntsville, AL 35807 (205) 837-1800

Ann F. Whitaker, Code EH11
Materials and Processes Laboratory
NASA Marshall Space Flight
Center, AL 35812
(205) 453-4877

J.-H. Yee Harvard-Smithsonian Center for Astrophysics 60 Garden Street Cambridge, MA 02138 (617) 495-5873

1.	NASA CP-2391	2. GOVERNMENT ACCESSION NO.	3. RECIPIENT'S CATALOG NO.	
4.	TITLE AND SUSTITLE		5. REPORT DATE September 1985	
	Second Workshop on	Spacecraft Glow	6. PERFORMING ORGANIZATION CODE	
7.	J. H. Waite, Jr., an	nd T. W. Moorehead, Editors	8. PERFORMING ORGANIZATION REPORT # ES53/ES01	
9.	PERFORMING ORGANIZATION NAME	AND ADDRESS	10. WORK UNIT, NO. M-502	
	George C. Marshall Marshall Space Flig	Space Flight Center ght Center, Alabama 35812	11. CONTRACT OR GRANT NO.	
			13. TYPE OF REPORT & PERIOD COVERED	
12.	SPONSORING AGENCY NAME AND A	Conference		
ı	National Aeronautics and Space Administration		Publication	
	Washington, DC 205	546	14. SPONSORING AGENCY CODE	
-				

Sponsored, in part, by the Universities Space Research Association, Washington, DC

16. ABSTRACT

This report contains results of a workshop held on May 6-7, 1985, at the Space Science Laboratory of NASA/Marshall Space Flight Center, Huntsville, Alabama. The contents of this report are divided as follows:

- o In Situ Observations
- o Theoretical Calculations o Laboratory Measurements
- o Future Experiments

 Spacecraft Glow Shuttle Glow Atmospheric Science Aeronomy Atmosphere/Vehicle In	nteraction	 fied — Unlimi	ited